

SYNTHETIC AND FLUXIONALITY STUDIES
OF SMALL ORGANOTRANSITION METAL
CLUSTERS

by

© MICHAEL ROBERT MLEKUZ, B.Sc.

A Thesis

Submitted to the Faculty of Graduate Studies

In Partial Fulfilment of the Requirements

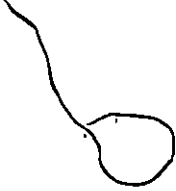
for the Degree

Doctor of Philosophy

McMaster University



May, 1985

ORGANOTRANSITION METAL CLUSTERS



DEDICATION

To my parents and sister,
Marion for their constant
support and encouragement.



DOCTOR OF PHILOSOPHY (1985)

McMaster University
Hamilton, Ontario

TITLE: Synthetic and Fluxionality Studies of Small Organotransition
Metal Clusters

AUTHOR: MICHAEL ROBERT MLEKUZ, B.Sc. (McMaster University)

SUPERVISOR: Dr. M. J. McGlinchey

NUMBER OF PAGES: xii, 173

ABSTRACT

A series of chiral organotransition metal clusters of the type $(\text{PhC}\equiv\text{CCO}_2\text{CHMe}_2)\text{MM}'$ where $\text{M} = \text{CpNi}$ and $\text{M}' = \text{CpMo}(\text{CO})_2$, $\text{Co}(\text{CO})_3$ or CpNi have been treated with $\text{Fe}_2(\text{CO})_9$ to give clusters of the general formula $(\text{RC}\equiv\text{CR})\text{MM}'\text{Fe}(\text{CO})_3$. These clusters are predicted to adopt a square pyramidal geometry and this has been confirmed by X-ray crystallographic studies. In the case of $\text{M}' = \text{CpNi}$ or $\text{Co}(\text{CO})_3$, the $\text{Fe}(\text{CO})_3$ moiety caps the basal plane whereas when $\text{M}' = \text{CpMo}(\text{CO})_2$, it is this moiety which serves as the capping vertex. The former arrangement leads to all the metals obeying the eighteen electron rule while in the latter the Fe and Mo atoms possess electron counts of 17 and 19 respectively.

These trimetallic-alkyne clusters have been shown to exhibit fluxional behaviour. This behaviour has been explained in terms of an alkyne rotation relative to the triangle of metals. When $\text{M}' = \text{CpNi}$, the cluster has been shown to undergo racemisation while when $\text{M}' = \text{CpMo}(\text{CO})_2$ or $\text{Co}(\text{CO})_3$, the clusters exhibit interconversion of diastereomers thus demonstrating the fluxional process to be intramolecular. The mechanism of isomerisation of these M_3C_2 clusters is compared to those predicted by theoretical calculations and also is shown to be related to that of the analogous C_5H_5^+ cation.

A series of synthetic manipulations carried out on the cluster system $\text{Co}_3(\text{CO})_9\text{CR}$ where $\text{R} = \text{CO}_2\text{CHMe}_2$, led to a variety of mixed metal clusters being obtained. Treatment with Cp_2Ni , $[\text{CpNi}(\text{CO})]_2$ or $[\text{CpMo}(\text{CO})_3]_2$ resulted in replacement or modification of one, two or all

three of the original $\text{Co}(\text{CO})_3$ vertices. The problems of employing Cp_2Ni as a reagent in cluster synthesis are also demonstrated. Reaction of these tetrahedral M_3CR clusters with $\text{Fe}_2(\text{CO})_9$ yielded not only the expected square based pyramidal systems but in one case a molecule adopting a close trigonal bipyramidal structure. This latter geometry has been confirmed by X-ray crystallography. The concept of isolobality has been used to compare the structure of this molecule with the previously known Fe_4CR clusters of similar geometry. Qualitative molecular orbital arguments are presented to rationalise the substitution and addition reactions of metal vertices to the tetrahedral clusters.

The geometry of the acylium cation $\text{Co}_3(\text{CO})_9\text{CCO}^+$ has been examined by ^{13}C NMR and evidence is outlined for a tilted configuration of the CCO ligand. A stable hexafluorophosphate salt of $\text{CpMoCo}_2(\text{CO})_8\text{CCO}^+$ has been obtained by the addition of HPF_6 to a solution of $\text{CpMoCo}_2(\text{CO})_8\text{CCO}_2\text{CHMe}_2$ in propionic anhydride. The presence of the acylium cation has been confirmed by its treatment with various nucleophiles resulting in formation of the appropriate derivatives.

ACKNOWLEDGEMENTS

I am deeply indebted for the direction provided by my research supervisor, Dr. M. J. McGlinchey. Dr. McGlinchey's patience in the early stages of this project, his constant encouragement, expert advice and our many stimulating non-professional discussions have played major roles in my development as both a person and a researcher.

I also wish to thank the members of my research committee, Drs. R. A. Bell and G. J. Schrobilgen for useful discussions. I am grateful to Dr. G. Jaouen and his co-workers for supplying some of the compounds in this study. The work of Dr. J.-Y. Saillard, Dr. C. J. L. Lock and R. Faggiani in the area of X-ray crystallography is also appreciated.

With the exception of my research supervisor, the greatest thanks are reserved for Dr. Peter Bougeard. His assistance in the first three years of this project was invaluable, but more importantly his friendship was a source of inspiration during the frustrating moments. I also wish to thank Dr. Doug Bickley for his friendship and as a source of inspiration in continuing my academic pursuits. The help of Dr. Joe Kolis in the ^{13}C O enrichment processes and valuable discussions on cluster chemistry with him are also appreciated.

Special thanks are owed to Mr. Brian Sayer not only for obtaining excellent quality NMR spectra but also for his valuable assistance with other NMR problems.

To the people who have passed through Dr. McGlinchey's lab during my stay, Peter, Doug, Hao, Mary, Bob, Clement, Shane, Roger, Norman, Karen, Mike, Richard, Reg and Debbie. I express my gratitude for the many academic and especially the non-academic activities and discussions we participated in.

I would also like to thank Mrs. Carol Dada for typing this thesis with professional skill and patience.

The financial assistance of the Department of Chemistry of McMaster University and NSERC is gratefully acknowledged.

Finally, I would like to thank the many other new friends I have made these past four years, especially Gary, John, Rob, Carl, Toad, Joan and Maria for all their help. These new friendships have also made me that more appreciative of the support given to me these past years by my long time friends, Art, Frank, Pete and Louie.

TABLE OF CONTENTS

	<u>PAGE</u>
CHAPTER 1: INTRODUCTION	1
1.1 General	1
1.2 Synthetic Routes to Metal Carbonyl Clusters	3
1.3 Bonding in Metal Clusters	7
1.4 The Bridge between Inorganic and Organic Chemistry - Isolobality	25
1.5 Applications of Transition Metal Clusters	32
1.6 Statement of Problem	34
CHAPTER 2: SYNTHESSES AND STRUCTURES OF TRIMETALLIC ALKYNE CLUSTERS	36
2.1 Introduction	36
2.2 Synthesis of Heterotrimetallic Alkyne Clusters	40
2.3 Structures of Trimetallic Alkyne Clusters	50
CHAPTER 3: FLUXIONALITY STUDIES ON TRIMETALLIC ALKYNE CLUSTERS	58
3.1 Introduction	58
3.2 Fluxionality in Homometallic M_3C_2 Clusters	64
3.3 Fluxionality in Heterometallic M_3C_2 Clusters	68
3.4 Mechanistic Implications	74

	<u>PAGE</u>
CHAPTER 4: SYNTHETIC MANIPULATIONS OF THE	81
$\text{Co}_3(\text{CO})_9\text{CCO}_2\text{CHMe}_2$ CLUSTER	
4.1 Introduction	81
4.2 Bis(Cyclopentadienyl)Nickel as a Cluster	85
Reagent	
4.3 Syntheses of Mixed Metal Alkylidyne Clusters	89
4.4 Close Clusters	96
4.5 The Isolobal Nature of CpRh and $\text{Fe}(\text{CO})_3$	104
Fragments	
CHAPTER 5: INVESTIGATIONS OF TRIMETALLIC ACYLIUM	111
CATION CLUSTERS	
5.1 Introduction	111
5.2 Dynamic NMR Studies of $\text{Co}_3(\text{CO})_9\text{CCO}^+$	113
5.3 A Novel Route to $[\text{Co}_3(\text{CO})_9\text{C}]_2$	119
5.4 Synthesis and Characterization of a Mixed	124
Metal Acylium Cation	
5.5 Proposals for Future Work	126
CHAPTER 6: EXPERIMENTAL	129
6.1 General Spectroscopic Techniques	129
6.2 General Procedures	129
6.3 Experimental Procedures for Chapter 2	129
6.4 Experimental Procedures for Chapter 4	132
6.5 Experimental Procedures for Chapter 5	146
APPENDIX	149
REFERENCES	158

LIST OF TABLES

	<u>PAGE</u>
1. Number of Skeletal Bonding Electrons Contributed by Various Metal Cluster Vertices	20
2. Electron Counting in Clusters	21
3. Bonding Capabilities in Metal Clusters	22
4. Summary of Basic Isolobal Relationships	32
5. Selected Bond Distances and Bond Angles for $\text{Cp}_2\text{Ni}_2\text{Fe}(\text{CO})_3(\text{PhC}_2\text{CO}_2\text{CMe}_2\text{H})$, 16	57b
6. Selected Bond Distances and Bond Angles for $\text{CpNiCoFe}(\text{CO})_6(\text{PhC}_2\text{CO}_2\text{CMe}_2\text{H})$, 17	57c
7. Selected Bond Distances and Bond Angles for $\text{Cp}_2\text{NiMoFe}(\text{CO})_5(\text{PhC}_2\text{CO}_2\text{CMe}_2\text{H})$, 18	57d
8. Comparison of ΔG^\ddagger Values for Alkyne Rotation	80
9. Selected Interatomic Distances (Å) and Angles (deg.) for $\text{Cp}_3\text{Co}_2\text{MoFe}(\text{CO})_5\text{CCO}_2\text{CMe}_2\text{H}$, 33	94b
10. Comparison of ^{13}C Shifts in Ketenylidene Clusters	117
A1. Crystal Data for $\text{Cp}_2\text{Ni}_2\text{Fe}(\text{CO})_3(\text{PhC}_2\text{CO}_2\text{CMe}_2\text{H})$, 16	150
A2. Crystal Data for $\text{CpNiCoFe}(\text{CO})_6(\text{PhC}_2\text{CO}_2\text{CMe}_2\text{H})$, 17	151
A3. Crystal Data for $\text{Cp}_2\text{NiMoFe}(\text{CO})_5(\text{PhC}_2\text{CO}_2\text{CMe}_2\text{H})$, 18	152
A4. Positional Parameters for Non-Hydrogen Atoms of $\text{Cp}_2\text{Ni}_2\text{Fe}(\text{CO})_3(\text{PhC}_2\text{CO}_2\text{CMe}_2\text{H})$, 16	153
A5. Positional Parameters for Non-Hydrogen Atoms of $\text{CpNiCoFe}(\text{CO})_6(\text{PhC}_2\text{CO}_2\text{CMe}_2\text{H})$, 17	154

	<u>PAGE</u>
A6. Positional Parameters for Non-Hydrogen Atoms of CpNiMoFe(CO) ₅ (PhC ₂ CO ₂ CMe ₂ H), 18	155
A7. Crystal Data for Cp ₃ Co ₂ MoFe(CO) ₅ CCO ₂ CMe ₂ H, 33	156
A8. Atomic Positional Coordinates and Temperature Factors (Å ²) for Cp ₃ Co ₂ MoFe(CO) ₅ CCO ₂ CMe ₂ H, 33	157

LIST OF FIGURES

	<u>PAGE</u>
1. Use of the Metal-Carbyne Unit as a Building Block in Cluster Synthesis	8
2. Structures of Various Metal Carbonyls	10
3. The Skeletal Bonding Molecular Orbitals of $B_6H_6^{2-}$	13
4. Symmetry Adapted Linear Combinations of Orbitals Derived from BH and $M(CO)_3$ Fragments	14
5. Polyhedra Corresponding to a Particular Number of Skeletal Electron Pairs	16
6. Examples of Boranes Possessing Seven Skeletal Electron Pairs	17
7. The Isolobal Moieties BH and $Fe(CO)_3$	26
8. Derivation of the $M(CO)_5$, $M(CO)_4$ and $M(CO)_3$ Fragments from an $M(CO)_6$ Complex	30
9. Some Typical Bonding Modes of Alkynes in Clusters	38
10. The Expansion of $M_2C_2R_2$ Tetrahedral Clusters to Square-Based Pyramidal Clusters	47
11. 1H NMR Spectrum of $Cp_2NiMoFe(CO)_5(PhC_2CO_2CMe_2H)$, $\overline{18}$	49
12. ORTEP Diagram of $Cp_2Ni_2Fe(CO)_3(PhC_2CO_2CMe_2H)$, $\overline{16}$	52
13. ORTEP Diagram of $CpNiCoFe(CO)_6(PhC_2CO_2CMe_2H)$, $\overline{17}$	53
14. ORTEP Diagram of $Cp_2NiMoFe(CO)_5(PhC_2CO_2CMe_2H)$, $\overline{18}$	54
15. Experimental 80 MHz and 250 MHz Variable-Temperature 1H NMR Spectra of the Cyclopentadienyl and Methyl Regions of $\overline{16}$	71
16. Acetylene Rotation on One Face of a Cluster Showing Interconversion of Diastereomers but not of Enantiomers	73

	<u>PAGE</u>
17. Experimental and Simulated 250 MHz Variable-Temperature ^1H NMR Spectra of $\overset{18}{\text{C}}$	75
18. Alkyne Migration Mechanisms in Trimetallic Systems	77-78
19. A Rearrangement Mechanism for the $\text{MM}'\text{M}''(\text{RC}\equiv\text{CR}')$ Cluster Analogous to that of the C_5H_5^+ System	79
20. Clusters Obtained from the Reactions of $\text{Co}_3(\text{CO})_9\text{CCO}_2\text{CMe}_2\text{H}$ and Cp_2Ni	87
21. Synthetic Scheme Relating Molecules $\overset{23}{\text{C}}$, $\overset{24}{\text{C}}$ and $\overset{28}{\text{C}}$ through $\overset{35}{\text{C}}$	91
22. ORTEP Diagram of $\text{Cp}_3\text{Co}_2\text{MoFe}(\text{CO})_5\text{CCO}_2\text{CMe}_2\text{H}$, $\overset{33}{\text{C}}$	95
23. Comparison of Core Geometries of $\text{Cp}_3\text{Co}_2\text{MoFe}(\text{CO})_5\text{CCO}_2\text{CMe}_2\text{H}$, $\overset{33}{\text{C}}$ and $\text{Fe}_4(\text{CO})_{12}\text{CCO}_2\text{CH}_3^-$	99
24. Qualitative Molecular Orbital Diagram Rationalising Substitution Reactions on Tetrahedral Clusters	102
25. Synthetic Scheme Involving Cluster Reactions with $\text{C}_5\text{Me}_5\text{Rh}(\text{CO})_2$ and $\text{C}_9\text{H}_7\text{Rh}(\text{C}_2\text{H}_4)_2$	110
26. Proposed Structures for the $\text{Co}_3(\text{CO})_9\text{CCO}^+$ Complex	114
27. Experimental 125 MHz Variable-Temperature ^{13}C NMR Spectra of $\text{Co}_3(\text{CO})_9\text{CCO}^+$	118
28. ORTEP Diagram of $[\text{Co}_3(\text{CO})_9\text{C}]_2$	121
29. Proposed Mechanism for $[\text{Co}_3(\text{CO})_9\text{C}]_2$ Formation	123

CHAPTER I

INTRODUCTION

1.1 General

Transition metal cluster chemistry has been one of the most widely studied areas of inorganic chemistry for the past ten years. This considerable attention is perhaps exemplified in the large number of review articles which have appeared on the subject recently.¹⁻¹¹ These reviews have covered the areas of synthesis, structure and reactivity of metal clusters. The interest in clusters is not restricted only to academics; industrialists have explored their possible use as catalysts.

The concept of polynuclear metallic species is not a novel one. Werner in fact was the first to propose their existence. He viewed these complexes as ones not containing metal-metal bonds but as mononuclear species joined together by sharing one or more ligands. It was with the employment of X-ray crystallography that the existence of the first metal cluster containing metal-metal bonds was confirmed. Brosset in 1946 showed the structure $\text{Mo}_6\text{Cl}_8^{4+}$ to be an octahedron of Mo atoms, with Mo-Mo distances indicative of direct bonding. This report and a similar one on $\text{Ta}_6\text{Cl}_{14} \cdot 7\text{H}_2\text{O}$ still did not stimulate great interest in this area of chemistry. It was not until the early 1960s with the discovery of the $\text{Re}_3\text{Cl}_{12}^{3-}$ cluster that the field of metal cluster chemistry began to be explored in earnest. Now metal clusters containing three to six metal atoms are quite common and larger clusters containing up to 38 metal atoms

have been characterized.^{12,13}

Cotton has defined metal clusters as a group of two or more metal atoms in which there are substantial and direct bonds between the metal atoms.¹² Alternatively, a cluster has been called a discrete molecular species in which three or more metal atoms interact (bond) to form triangular or polyhedral arrays.¹⁴ Atoms other than metals may be contained within the cluster framework. They include oxygen, phosphorus, sulfur, carbon and nitrogen. In some cases they may not only be contained within the cluster framework but may become encapsulated within it.

Two basic types of transition metal clusters exist. There are those derived from transition metal carbonyls and those of the transition metal halide type. The two types are not really related to each other. Those belonging to the former group include not only those based on the formula $M_x(CO)_y^n$ (x = 2 through 38) but clusters containing ligands such as hydrides, alkyls, olefins, acetylenes and phosphines. It is this type of cluster which contains interstitial atoms such as H, C, P. In metal carbonyl clusters the metals possess formal oxidation states of zero or negative values. Bonding in these systems utilizes all nine valence orbitals on the metal, i.e., (1 x s, 3 x p, 5 x d). In terms of reactivity, metal carbonyl clusters seem to undergo more reactions than those of the metal halide type. A great majority of the metal carbonyl clusters are formed by Group VIII metals.

Metal halide clusters consist mainly of second and third row transition metals found in Groups Va, VIa and VIIa. Initially they were studied to a greater extent, possibly due to their relationship with

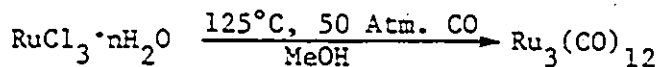
metal-metal triple and quadruple bond complexes. In contrast to metal carbonyl clusters, the metals in halide type clusters are found in the +2 and +3 oxidation state. Examples of clusters include $\text{Mo}_6\text{Cl}_8^{4+}$, $\text{W}_6\text{Cl}_8^{4+}$, $\text{Nb}_6\text{Cl}_{12}^{2+}$, $\text{Ta}_6\text{Br}_{12}^{2+}$ and $\text{Re}_3\text{Cl}_{12}^{3-}$. In the first two clusters, the halide ions bridge the faces of the octahedron of metals, while in the next two the halide bridges the edges of the octahedron. Bonding in metal halide clusters primarily involves the nd orbitals with small contributions from the s and p orbitals. This differs from metal carbonyl clusters. The reason for the difference is that when a metal is ionized the energy difference between the d orbitals and the outer s and p orbitals increases. Perhaps the only similarity between the two cluster types is the prevalence of clusters containing the heavier metal atoms. This may be explained by the greater tendency for metal-metal bonding which is necessary for cluster formation, for the heavier elements.

There are other types of metal clusters which are known but these two types seem to be the longest known and best studied. In both cases presented above, the core of metal atoms is enveloped by a set of ligands which play some part in stabilizing the cluster. An interesting group of metal clusters are the so called naked clusters which include species such as Sn_9^{4-} and Bi_9^{5+} ^{15,16}. Of the transition metals only the Group IIIa metals and Zr and Hf are not found in clusters. The Group Ib metals exist as clusters but not of the carbonyl or halide type. They are stabilized by donor ligands coordinated through N, P or S.

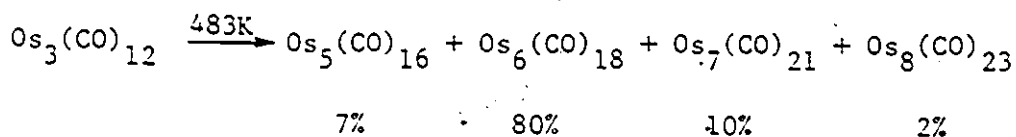
1.2 Synthetic Routes to Metal Carbonyl Clusters

One of the major goals of laboratories investigating metal cluster chemistry has been the development of logical, controlled methods

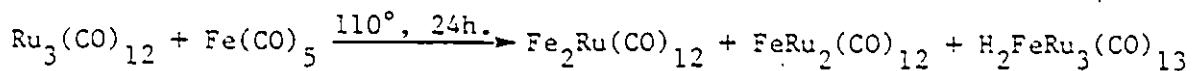
of synthesis. Primarily, this has involved mixed metal clusters, as routes to the small homometallic carbonyl clusters are already well established. The latter usually involve heating a solution of the metal salt under a high pressure CO atmosphere.¹⁷



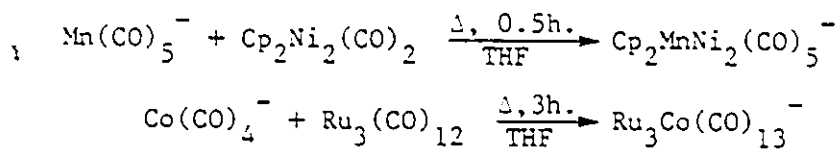
Routes to higher nuclearity homometallic clusters simply involve the pyrolysis of lower nuclearity metal carbonyls. The best known example of this type of synthetic technique is one employing $\text{Os}_3(\text{CO})_{12}$ as the starting material.¹⁸

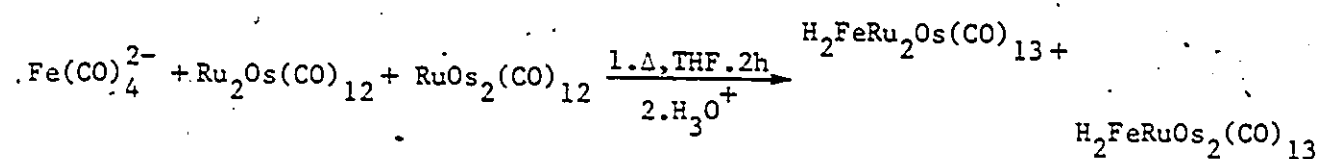


Early mixed cluster syntheses were no more imaginative. They involved placing together a couple of different metal carbonyl species, allowing them to react via thermolysis or photolysis and finally separating the mixture of products which had been formed. This type of route was plagued with many problems, such as low yields, poor reproducibility and difficulties in product separation. Photolysis or thermolysis most probably results in the formation of coordinatively unsaturated species. These species, which are generated by loss of CO or metal-metal bond cleavage from the starting materials, then react with the starting material to yield products. An example of this type of reaction is the following:^{19,20}

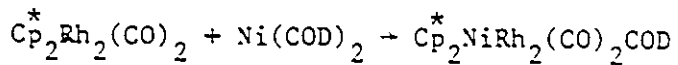
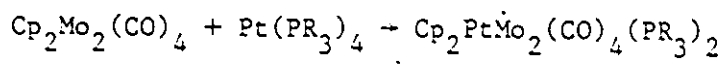
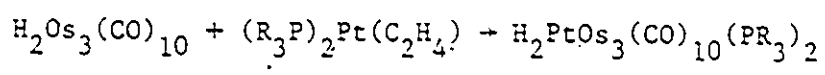


Two of the more successful routes to mixed metal clusters have their origins in organic chemistry. The first involves attack of a metal carbonyl anion on a di- or polynuclear carbonyl complex accompanied by subsequent loss of carbonyl ligands. In this regard the reaction resembles a nucleophilic displacement. Examples also exist where the metal carbonyl anions react with metal halide complexes with displacement of halide, however these lead mostly to binuclear complexes. The first known mixed metal cluster $\text{FeCo}_3(\text{CO})_{12}^-$ was prepared by Chini and his co-workers employing metal carbonyl anions.²¹ A major advantage of this route is, since the reaction products in most cases are anions, they may be precipitated out of solution by addition of salts containing large cations such as bis(triphenylphosphoranylidene)ammonium (PPN^+) and tetraphenylarsonium (Ph_4As^+). These usually give crystals which are suitable for X-ray diffraction purposes. Problems arise in this technique if the metal carbonyl anion is a strong reducing agent or if the neutral carbonyl complex is easily reduced. Therefore, a redox reaction rather than a condensation of the two fragments occurs. Another drawback is that the reactions proceed much better with mononuclear than with polynuclear carbonyl anions. This occurs because polynuclear anions can be considered softer nucleophiles as the negative charge is more delocalised. Examples of clusters obtained from the treatment of readily available simple metal carbonyls with metal carbonyl anions are shown below:²²⁻²⁴





A common reaction in organic chemistry to synthesize cyclopropane rings involves addition of a carbene to an alkene. The other major route to mixed clusters resembles this reaction greatly. It involves addition of a metal complex to a coordinatively-unsaturated di- or polynuclear complex. The metal complex is coordinatively unsaturated due to the presence of metal-metal multiple bonds. The metal-metal multiple bond may be found in an isolable molecule or can be generated in situ by elimination of carbonyl ligands. Advantages of this route include mildness of reaction conditions and good yields of products. Chemical reactions below indicate a few of the mixed clusters that have been prepared via this synthetic pathway.²⁵⁻²⁷



In a similar vein, it has long been realised by organic chemists that the dimerisation of acetylenes might yield tetrahedrane.²⁸ They have investigated the reaction of $\text{Co}_2(\text{CO})_8$ with alkynes and found it to yield tetrahedral clusters of the type $\text{R}_2\text{C}_2\text{Co}_2(\text{CO})_6$.²⁹ It was later realised that additions of alkynes to other well characterised metal-metal triple bonded species provides an excellent route to a variety of tetrahedral systems.^{30,31} Closely related to this reaction is the work of Stone and his co-workers employing metal carbyne complexes $\text{L}_n\text{M}\equiv\text{CR}$.^{10,11} These carbyne complexes were found to behave very similarly to alkynes

and this has led to a tremendous variety of mixed clusters being characterised. Some of these results are seen in Figure 1.

Other methods of mixed metal cluster synthesis are known, these include condensation and metal exchange reactions. The former involves two species reacting together to form a metal-metal bond with concomitant elimination of a small molecule such as H_2 or CH_4 . These usually involve the reaction of two metal hydrides or a metal hydride and metal alkyl. In metal exchange reactions, a known polynuclear metal complex is reacted with a mononuclear metal complex. The hoped for result is replacement of a metal fragment on the original polynuclear complex by the reactant mononuclear metal complex.

One can therefore see the steady progression in the area of cluster syntheses. It has advanced from the age of serendipity into the era of logical, controlled methods with some degree of mechanistic understanding.

1.3 Bonding in Metal Clusters

In cluster chemistry, as with both organic and inorganic chemistry, the number of electrons associated with a group of atoms determines how these atoms arrange themselves in space. Valence Shell Electron Pair Repulsion (VSEPR) theory allows for the prediction of molecular geometries in main group molecules based on the number of electron pairs associated with the central atom of the molecule.

Organometallic chemistry has long been dominated by the "Effective Atomic Number" (EAN) Rule or the $18e^-$ rule as it is better known.³³ According to this concept, transition metals in low oxidation states can use all nine ($1 \times s$, $3 \times p$, $5 \times d$) valence orbitals for bonding. A

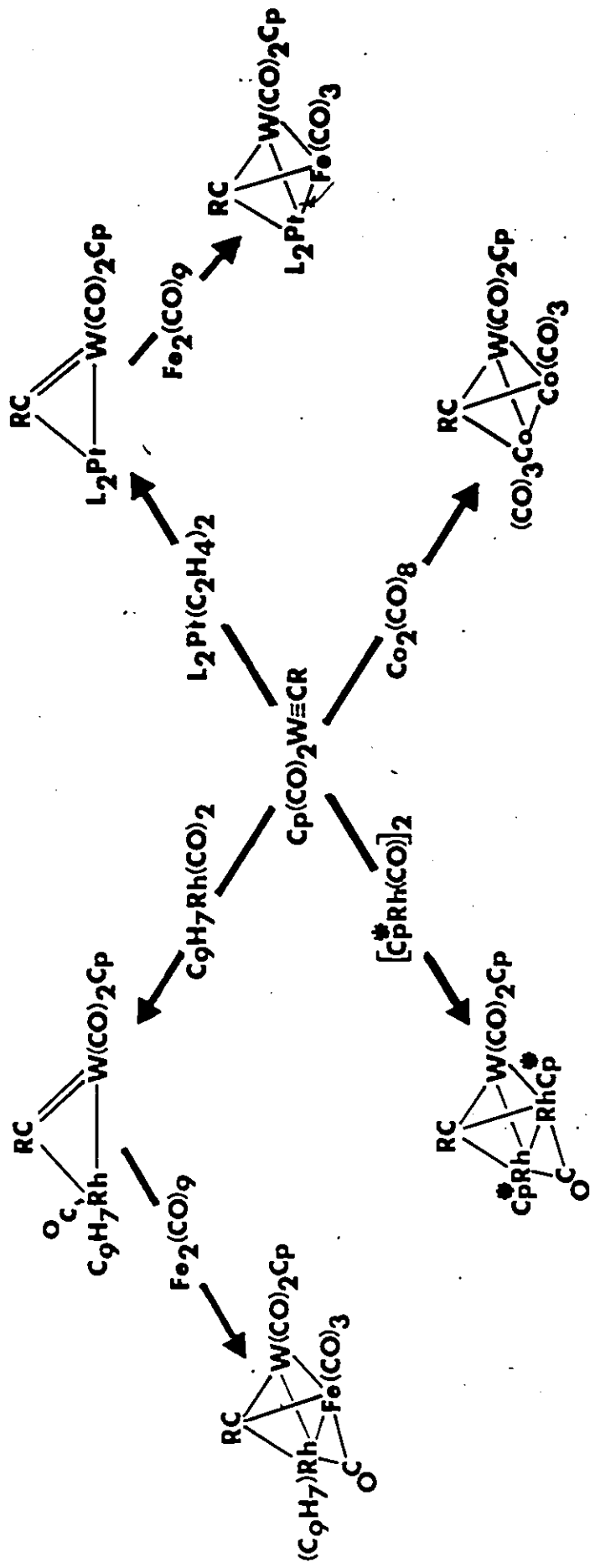


Figure 1:
Use of the Metal-Carbyne Unit as a Building Block in Cluster Synthesis

majority of mononuclear organometallic compounds conform to this rule. Exceptions are found in the early transition metals as well as the two late transition metal groups, the Ni and Cu triads. In these metals the p orbitals are found at higher energy levels which makes them less available for bonding. As a result of this, 16 and 14 \bar{e} configurations are common.

The EAN rule has been quite successful in accounting for the behaviour of many catalytic intermediates and the idea of 16 electron to 18 electron interconversions is quite well established.³⁴ Therefore, organo-transition metal complexes in which the central metal is assigned a 16 electron configuration are regarded as coordinatively unsaturated. In contrast, a metal possessing an 18 electron configuration could not function as a catalytic centre without either losing or migrating a ligand or decreasing the hapticity of a poly-hapto substituent so as to generate a vacant site.³⁵

Following this definition, complexes such as $(RC\equiv CR)Co_2(CO)_6$,¹ whose structure has been shown to be a tetrahedron would be regarded as being coordinatively saturated.³⁶ One could assign eighteen electrons to each metal centre via nine valence electrons for the metal, six electrons from the three carbonyl ligands and three electrons from the metal-metal and metal-carbon bonds. In addition one can see that each carbon atom has achieved the stable octet configuration of the nearest noble gas. However, in spite of this coordinatively saturated configuration, these complexes are highly reactive even under mild conditions. Clearly a different concept is needed to explain this behaviour.

Figure 2 illustrates a series of metal carbonyls. Typically

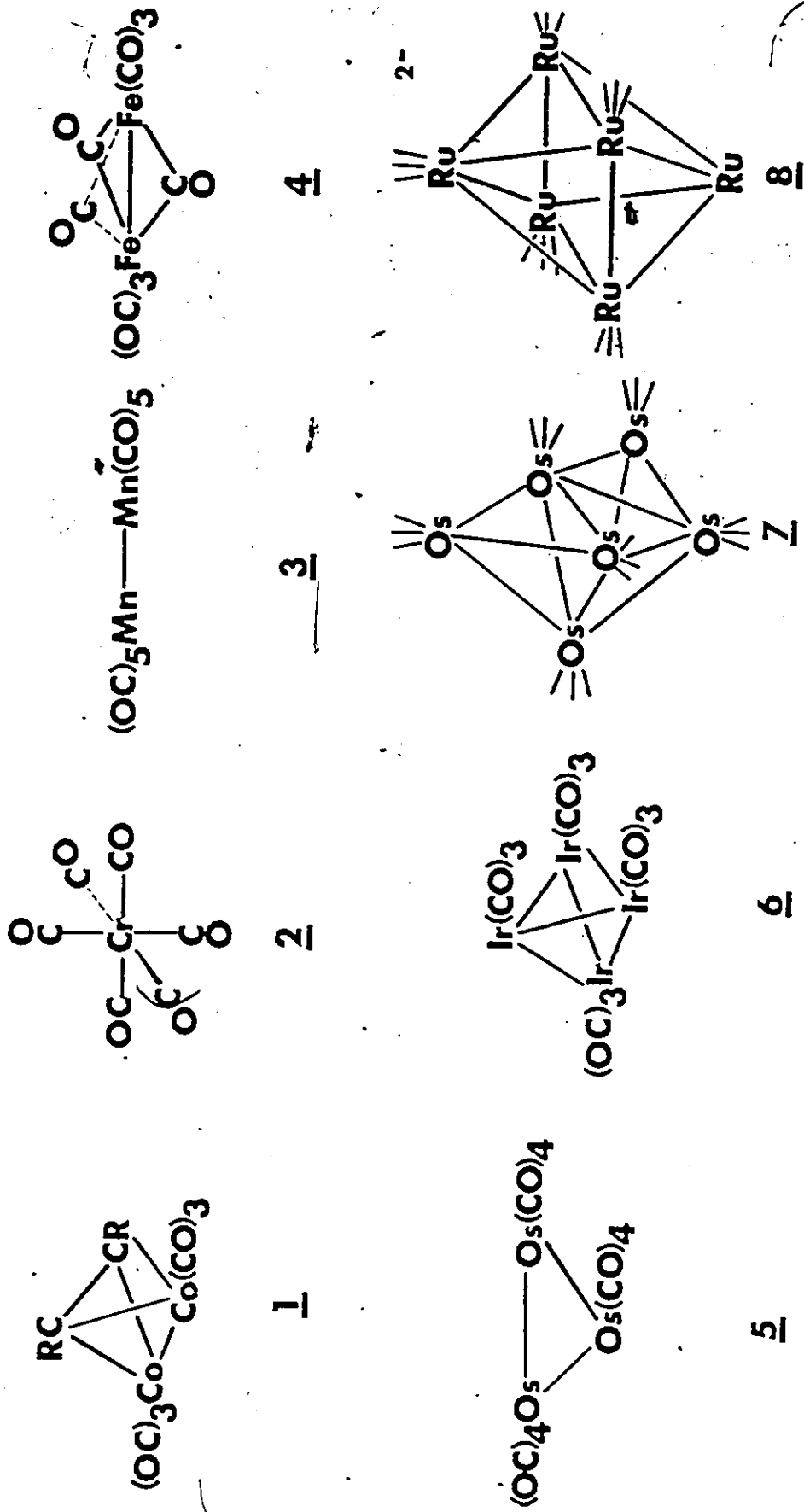


Figure 2:
Structures of Various Metal Carbonyls

for the mono- through tetrametallic complexes χ through ζ one can assign 18 electron configurations for each metal. This type of approach is based on valence bond theory. The skeletal bonding electrons are assigned to localised 2-centre-2 electron metal-metal bonds. However, as one moves to higher nuclearity clusters the localised bonding model becomes inadequate. This is exemplified by the hexanuclear clusters $\text{Os}_6(\text{CO})_{18}^{\eta}$ and $\text{Ru}_6(\text{CO})_{18}^{2-}$. One would expect an octahedral cluster to possess 84 electrons, with 24 of them assigned to the 12 metal-metal bonds along the polyhedral edges. $\text{Os}_6(\text{CO})_{18}$ has an electron count of 84. According to the localised bonding approach it should possess an octahedral geometry. It does not; instead the structure it adopts is that of a mono-capped trigonal bipyramid. Using the normal electron counting formalism, one would place $18 \frac{1}{3}$ electrons on each Ru atom in $\text{Ru}_6(\text{CO})_{18}^{2-}$. $\text{Ru}_6(\text{CO})_{18}^{2-}$ has 86 electrons associated with it, two more than that predicted for an octahedral cluster by the localised bonding approach, yet in spite of this apparent excess of electrons it is found to have an octahedral geometry. Similarly, the isolectronic molecule $\text{Rh}_6(\text{CO})_{16}$ is also an octahedron. Therefore, octahedral clusters should have 86 valence electrons rather than 84. In an apparent paradox these seemingly electron rich clusters may have their geometries rationalized by being considered electron deficient.

Most conceptions of bonding in molecules are based on the Lewis theory that all bonded atoms be held together by at least one pair of electrons.³⁷ Electron deficient molecules are those which do not possess enough electrons to form 2-electron bonds between adjacent atoms. An example of such a system is $\text{B}_6\text{H}_6^{2-}$ which has 26 valence electrons

(12 of which are needed to form the six exo-skeletal B-H bonds), leaving only 14 electrons, i.e., 7 electron pairs with which to bond together the six boron atoms in the cluster. Since an octahedron has 12 edges, 12 electron pairs would be required to bond the borons in a Lewis type fashion. Historically, molecules of this type have been termed electron deficient.³⁸ Nevertheless, in molecular orbital terms no such problem exists since, from a basis set of sp , p_x and p_y atomic orbitals (AO) on each boron, one can readily construct an energy level scheme with seven strongly bonded molecular orbitals (MO) as is seen in Figure 3.³⁹

Each skeletal boron contributes three atomic orbitals, a radially oriented sp hybrid and pair of tangentially oriented p orbitals. The remaining sp hybrid is used in formation of the B-H exoskeletal bond. King has proposed these systems be termed globally delocalised as opposed to edge localised.⁴⁰ Hence the octahedral cluster $B_6H_6^{2-}$ has seven skeletal electron pairs and is globally delocalised while the cluster C_8H_8 (cubane) has twelve skeletal electrons and is edge localised. An edge localised structure is possible for cubane because each CH fragment may contribute 3 electrons for skeletal bonding as opposed to 2 electrons for a BH fragment.

Returning to the case of $Ru_6(CO)_{18}^{2-}$,⁸ it has been shown in an important paper by Mingos that a parallelism exists between symmetry-adapted linear combinations of p and sp hybridized orbitals of the boranes and those derivable from d orbitals of metal carbonyl fragments.⁴¹ Some of these are shown in Figure 4 and they provide a solid basis for the electron counting schemes initially proposed by Wade and further

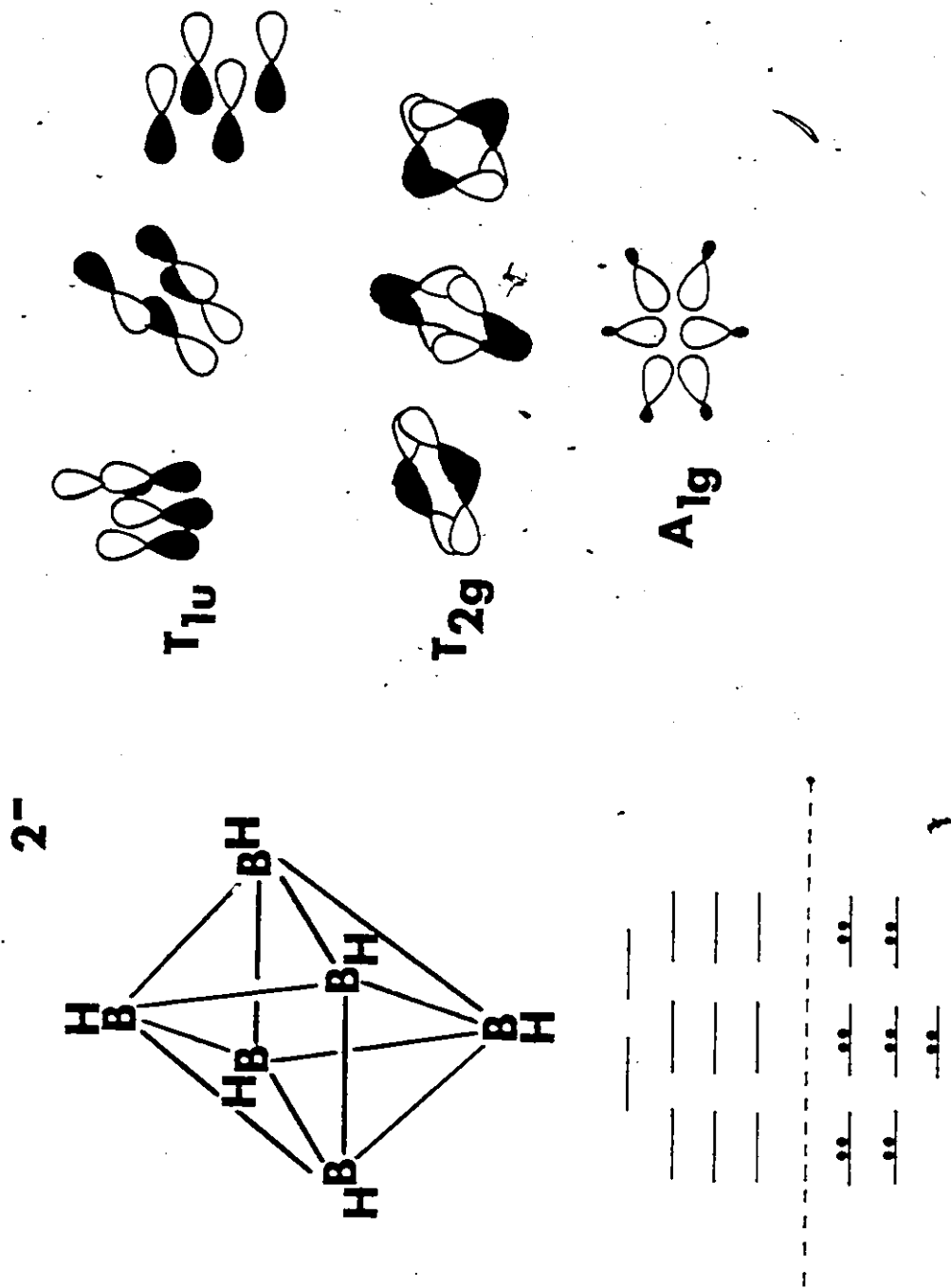


Figure 3:
The Skeletal Bonding Molecular Orbitals of $B_6H_6^{2-}$

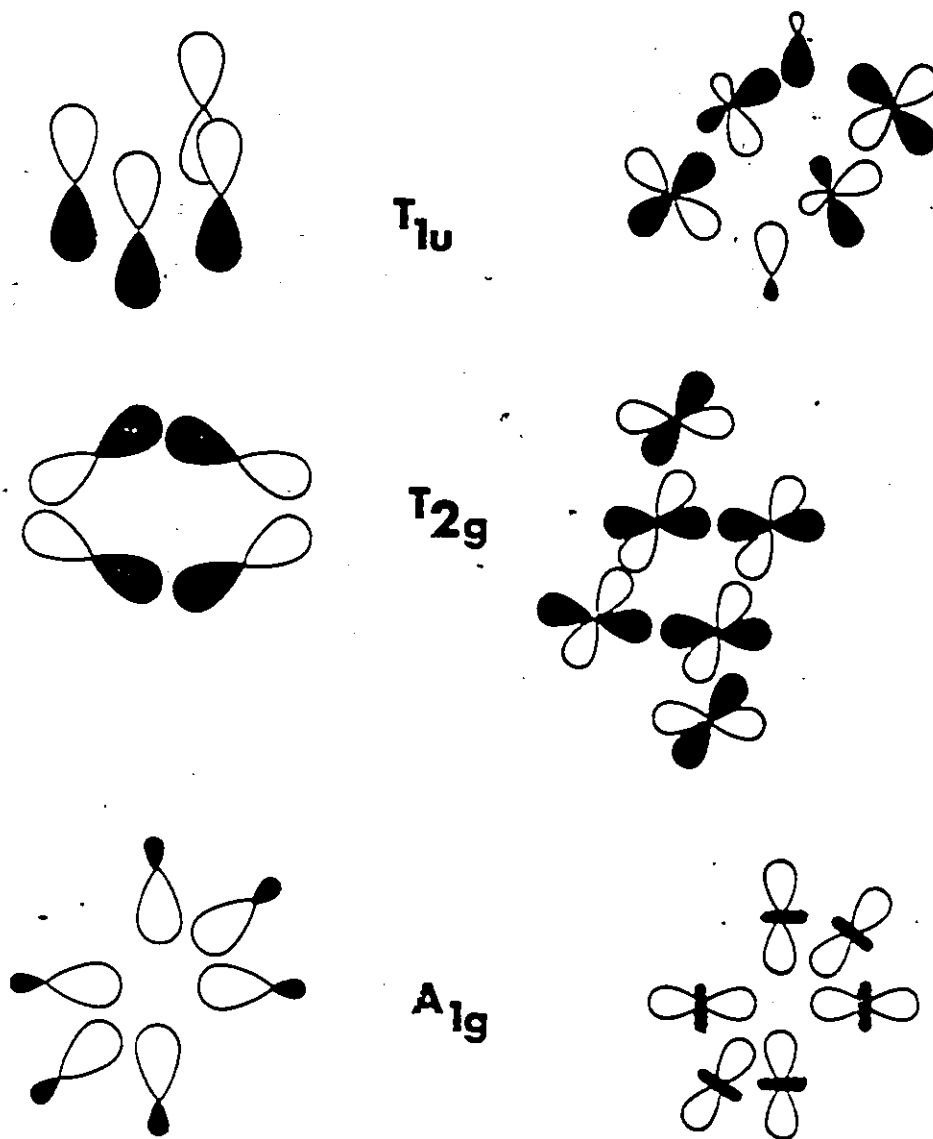


Figure 4:
Symmetry Adapted Linear Combinations of Orbitals Derived from BH and
M(CO)₃ Fragments

developed by Mingos for boranes, carboranes, main group and transition metal clusters.

This electron counting scheme has become better known as the polyhedral skeletal electron pair approach (PSEP).⁴²⁻⁴⁶ It provides a simple method to account for the structures of cluster compounds via correlation between polyhedral shape of a cluster and the total number of skeletal electrons. The general conclusions which have emerged from PSEP have had a profound yet simplifying effect on the view of clusters.

As has been previously indicated, the bonding in the six vertex $B_6H_6^{2-}$ molecule is already visualised as involving seven globally delocalised electron pairs. Indeed it has been shown that each of the $B_nH_n^{2-}$ systems gives rise to n bonding M.O.'s for the BH bonds and $n+1$ skeletal bonding M.O.'s. Therefore $B_nH_n^{2-}$ should be characterised by polyhedral electron counts of $4n+2$. Some typical geometries and the electron counts associated with them are presented in Figure 5.⁴² For transition metal clusters one must take into consideration the filling of the d-orbitals. They will have $10n$ more electrons than the boranes, so they will be characterised by electron counts of $14n+2$. As a corollary, one can invert this reasoning so as to state a given number of skeletal electron pairs associated with a particular molecular geometry. Typically, clusters possessing 14 skeletal electrons are predicted to be based on the octahedron. This is indeed exemplified by the boranes $B_6H_6^{2-}$, B_5H_9 ($\equiv B_5H_5^{4-}$) and B_4H_{10} ($\equiv B_4H_4^{6-}$) shown in Figure 6. These molecules may all be considered to be based on the same deltahedron but with zero, one and two unoccupied vertices. These

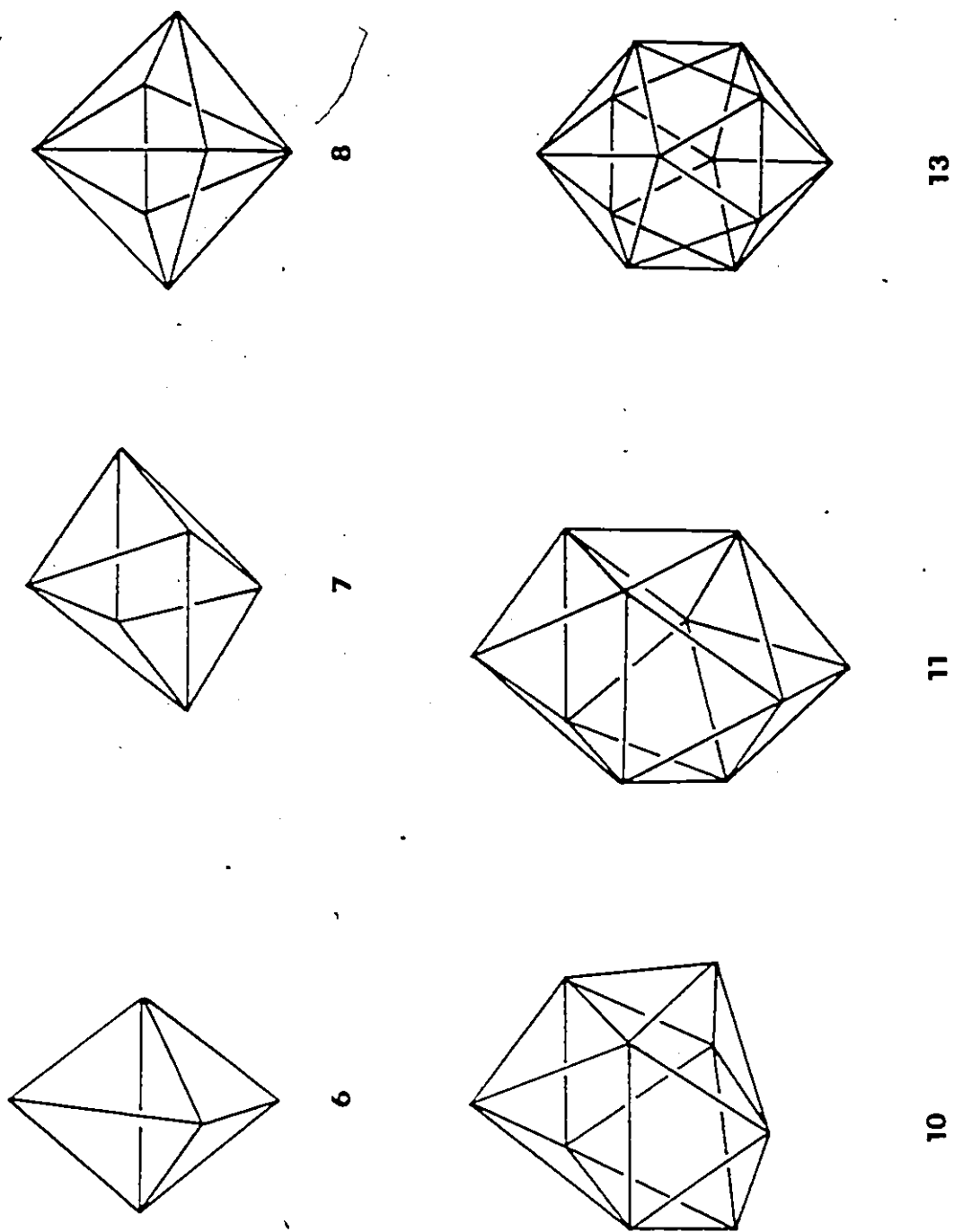
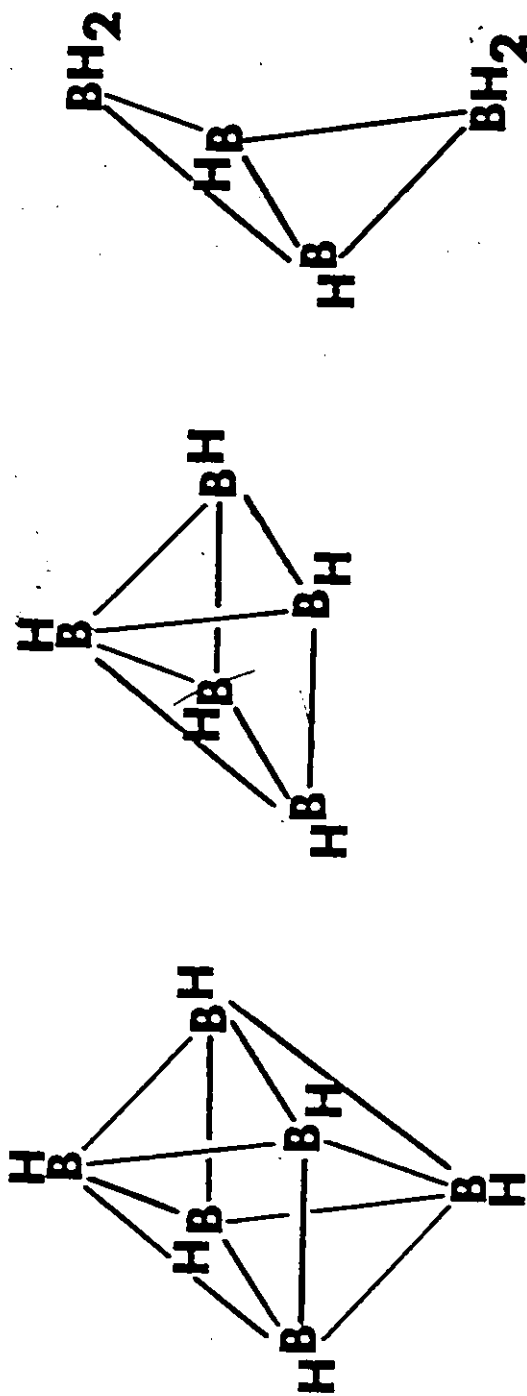


Figure 5:
Polyhedra Corresponding to a Particular Number of Skeletal Electron Pairs



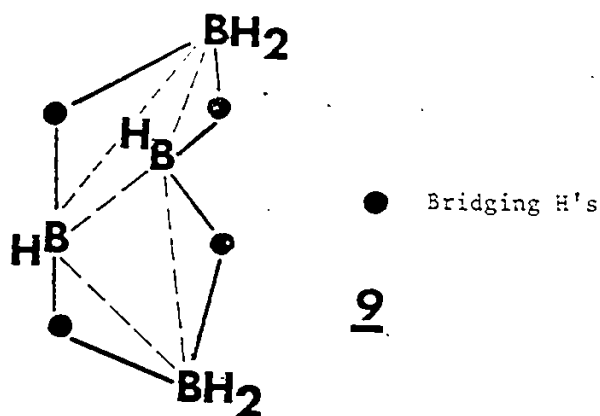
Vertices	
6	closo
5	nido
4	arachno

Figure 6:
Examples of Boranes Possessing Seven Skeletal Electron Pairs

have been termed *closo* (closed cage), *nido* (nest) and *arachno* (cobweb) molecules, respectively. *Nido* molecules are derived from *closo* molecules by removing the BH unit of highest connectivity, while *arachno* result via loss of two adjacent BH vertices from a *closo* molecule.

Boranes adopt deltahedra, rather than the 3 connected polyhedra adopted by alicyclic carbon compounds, because each BH fragment has only two electrons for skeletal bonding. A deltahedron is a convex polyhedron of maximum compactness, i.e., all the faces are triangular. These deltahedral structures maximize the number of nearest neighbour boron atoms, thus encouraging the most effective delocalisation of the boron skeletal electron pairs.

The number of skeletal electron pairs associated with *nido*, $B_n H_n^{4-}$ and *arachno*, $B_n H_n^{6-}$ molecules are $n+2$ and $n+3$ respectively. One would imagine that the more open structures adopted by these molecules would imply that electron density is being positioned in regions of space not proximate to the nuclei.⁴⁷ Such is not really the case since in the neutral boranes the open faces are stitched up by bridging protons as in 9. These extra hydrogens are involved in skeletal bonding



as they lie on the same spherical surface as the skeletal boron atoms. Even though each apical boron atom has 2 terminal hydrogens in B_4H_{10} only one of these is located outside the spherical surface.

An easier method to determine the polyhedral geometry of a cluster other than to count the total number of electrons associated with the cluster is to classify the cluster vertices as being n electron donors to the cluster skeleton.^{48,49} This would simplify electron counting for both mixed metal and larger clusters. In the case of a main group fragment such as CH, which possesses 5 valence electrons, 2 electrons are needed for formation of the exo-skeletal CH bond, thus it contributes 3 electrons for cluster bonding. Similarly, a BH unit would serve as a two electron donor. For both CH and BH units, 3 AO's are supplied for skeletal bonding.

In transition metal clusters the problem is somewhat more complicated. If one takes $Ru_6(CO)_{18}^{2-}$ which possesses 86 valence electrons and assigns 18 electron pairs to the 18 metal-carbon bonds, 36 AO's and 25 electron pairs would remain for skeletal bonding. Applying this reasoning would allocate some electrons into antibonding orbitals, which would cause a destabilization in the cluster framework. Clearly, since no distortion or instability in the structure is observed, another approach is necessary. To simplify the bonding, 3 electron pairs on each metal are assigned to non-bonding orbitals along with the 3 electron pairs necessary for metal carbon bonding. For $Ru_6(CO)_{18}^{2-}$ this leaves 7 electron pairs and 18 AO's to describe the skeletal bonding; with this method all the skeletal electron pairs will be accommodated in bonding MO's. The existence of these three

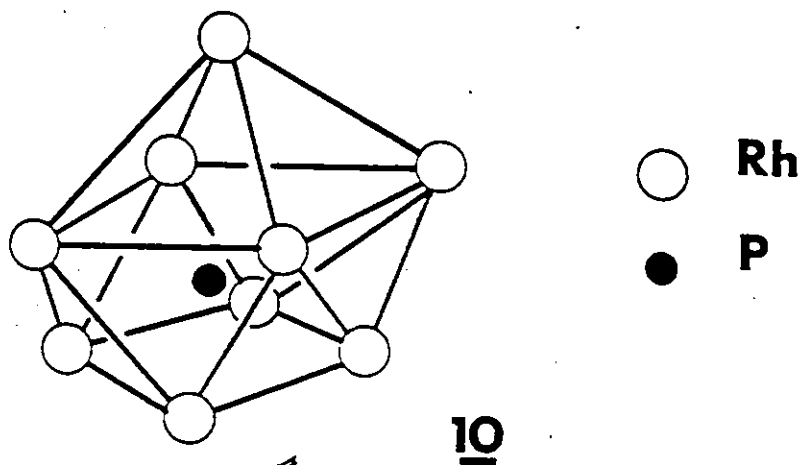
non-bonding pairs are seen in cases where a metal carbonyl group caps the face of a polyhedral cluster, e.g., $\text{Os}_6(\text{CO})_{18}$. In this example the $\text{Os}(\text{CO})_3$ group can use its 3 AO's to interact with a lone pair on each Os of the face it is capping. Therefore, for an organometallic unit, the number of electrons a cluster fragment contributes to skeletal bonding is equal to the number of electrons left in the three AO's required for skeletal bonding, after electrons are assigned to the six valence shell orbitals for ligand bonding. In Table 1 are listed a variety of metal cluster fragments and the number of electrons they donate to the cluster skeleton.

Table 1 - Number of Skeletal Bonding Electrons Contributed
by Various Metal Cluster Vertices

Valence \bar{e}	Transition Metal(M)	$\text{M}(\text{CO})_2$	$\text{M}(\text{CO})_3$	$\text{M}(\text{CO})_4$	CpM	$\text{CpM}(\text{CO})_2$
6	Cr, Mo, W	-2	0	2	-1	3
7	Mn, Tc, Re	-1	1	3	0	4
8	Fe, Ru, Os	0	2	4	1	5
9	Co, Rh, Ir	1	3	5	2	6
10	Ni, Pd, Pt	2	4	6	3	-

In conclusion PSEP accounts very well for the structures of 4 through 7 atom clusters, but inevitably with large clusters the model will tend to break down as the central core becomes more like a close packed metal fragment.⁵⁰ There are, however, examples of larger vertex clusters which still behave according to the concepts of PSEP. The cluster $\text{Rh}_9\text{P}(\text{CO})_{21}^{2-}$ ¹⁰ does not satisfy the E.A.N. rule but is well accounted for by PSEP. It has 130 valence electrons and subtraction

of $9 \times 12 = 108$ electrons for the exo-skeletal ligands leaves 11 electron pairs for cluster bonding. The structure the molecule should adopt is that of a 10 vertex deltahedron, viz. a dicated square antiprism but with a vertex missing. This structural prediction has been confirmed crystallographically.⁵¹



The application of PSEP to various clusters which are then categorized as being closo, nido or arachno molecules is shown in Table 2.

Table 2 - Electron Counting in Clusters

	Total Valence Electrons	Exo-Skeletal Electrons	Cluster Electrons	Shape
$\text{Ru}_6(\text{CO})_{18}^{2-}$	86	6×12	14	closo-octahedron
$\text{Fe}_5(\text{CO})_{15}\text{C}$	74	5×12	14	nido-octahedron
$\text{Fe}_4(\text{CO})_{12}\text{C}^{2-}$	62	4×12	14	arachno-octahedron
$\text{Os}_5(\text{CO})_{15}^{2-}$	72	5×12	12	closo-tbp
$\text{Co}_4(\text{CO})_{12}$	60	4×12	12	nido-tbp

An alternative bonding scheme for metal clusters has been proposed by Lauher.⁵² Through the use of extended-Hückel calculations on bare metal clusters, the bonding capabilities and resulting geometries of clusters can be rationalized via the number of cluster valence molecular orbitals. These calculations reveal that the molecular orbitals of a cluster may be divided into two classes, the highly antibonding orbitals (HLAO) and cluster valence molecular orbitals (CVMO). The latter are of suitable energy to be used for both metal-ligand and metal-metal bonding. Each cluster of a given size and geometry has a particular number of CVMO's associated with it. The predictions are solely for clusters comprised of transition metal fragments; if a cluster contains a main group fragment which has replaced a transition metal fragment this will reduce the requirements for cluster valence electrons along with that for atomic and molecular orbitals by 10 and 5 respectively. A few examples of the bonding capabilities of various metal clusters are shown in Table 3.

Table 3 - Bonding Capabilities in Metal Clusters

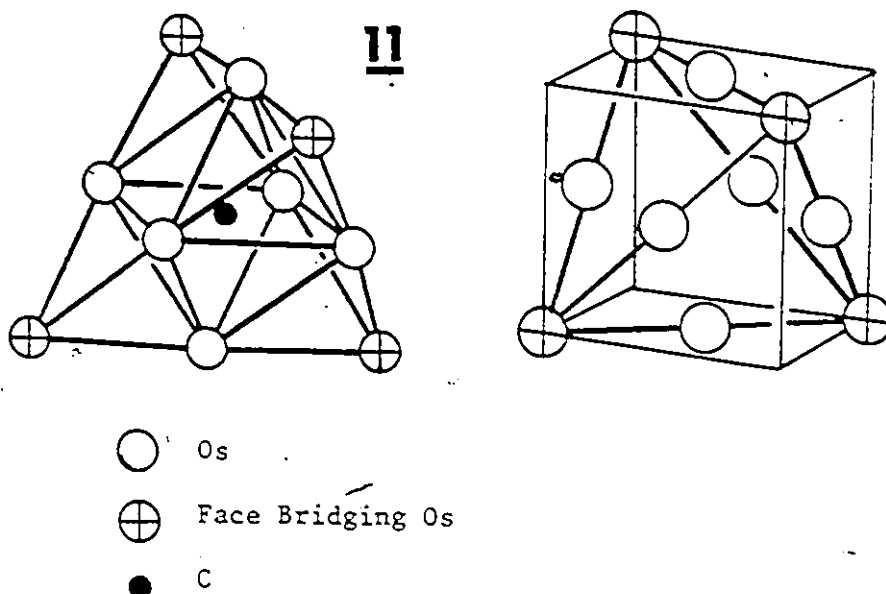
Geometry	N	9N	CVE	CVMO	HLAO	Example
tetrahedron	4	36	60	30	6	$\text{Co}_4(\text{CO})_{12}$
tetrahedron	4	31	50	25	6	$\text{Co}_3(\text{CO})_9\text{CR}$
tetrahedron	4	26	40	20	6	$\text{Co}_2(\text{CO})_6\text{C}_2\text{R}_2$
trigonal bipyramid	5	45	72	36	9	$\text{Os}_5(\text{CO})_{16}$
trigonal bipyramid	5	40	62	31	9	$\text{Fe}_4(\text{CO})_{12}\text{CR}^-$
trigonal bipyramid	5	35	52	26	9	$\text{Fe}_3(\text{CO})_9\text{C}_2\text{R}_2$
square based pyramid	5	45	74	37	8	$\text{Fe}_5(\text{CO})_{15}\text{C}$
square based pyramid	5	40	64	32	8	$\text{CpNiFeCo}_2(\text{CO})_9\text{CR}$
square based pyramid	5	35	54	27	8	$\text{Cp}_2\text{Ni}_2\text{Fe}(\text{CO})_3\text{C}_2\text{R}_2$

There are a few differences between the geometries predicted by Lauher and those of PSEP. For example, for a metal cluster to adopt a closo-pentagonal bipyramid geometry, one would need 100 cluster valence electrons, which would go into 50 CVMO to account for both metal-ligand and metal-metal bonding. Lauher's calculations show that only 49 CVMO are needed. A significant interaction occurs between the 2 atoms occupying the axial positions. This results in one of the orbitals becoming anti-bonding; if an elongation between these two atoms occurs, the CVMO number becomes 50.

Another anomaly between the two rules occurs for the molecule $\text{HFe}_4(\text{CO})_{13}^-$. Via PSEP theory, this molecule (which possesses 60 valence electrons) would be considered a nido-trigonal bipyramid. From Lauher's calculations it possesses 31 CVMO, therefore it would be considered to be an electron deficient butterfly. In order to become electron precise it would have to react with a suitable additional ligand or one of the existing ligands could bind in an unusual fashion. This latter possibility is observed in $\text{HFe}_4(\text{CO})_{13}^-$ as one of the carbonyls is coordinating to another Fe atom via its oxygen. In this manner the CO ligand is behaving as a four electron donor.⁵³

Other methods have been employed to predict the structures of metal clusters. Recently an electron counting theory based on Euler's theorem and the EAN rule has been developed.⁵⁴ The more advanced methods include SCF-X α -SW calculations.⁵⁵ While these methods might provide a better understanding of the electronic structure of the clusters on which they were carried out, both PSEP and Lauher's method have the advantages of being simpler and more widely applicable.

To conclude, the current picture of metal clusters reveals that for a low nuclearity cluster with a high ligand-to-metal ratio the E.A.N. rule applies and one can assign each transition metal 18 electrons in localised bonds. As the ligand-to-metal ratio decreases, one sees a gradual increase in the delocalisation of electron density within the cluster framework; this behaviour parallels that observed in borane, carborane and main group cluster chemistry. Finally, with even larger clusters of transition metal atoms, the regions of delocalised electron density are seen to merge almost into a conventional metallic structure in the centre of the cluster while the ligands merely coat the molecular periphery; the relationship to surface chemistry thus becomes more pronounced. Molecular orbital studies have analysed the changes involved in proceeding gradually from tri-metallic systems to large multi-metallic clusters.⁵⁶ A very nice example of the gradual transition from a cluster to a conventional metal is provided by the tetra-capped closo-octahedral cluster $\text{Os}_{10}\text{C}(\text{CO})_{24}^{2-}$, 11, for which the relationship to the face-centred cubic unit cell is readily apparent.⁵⁷



1.4 The Bridge Between Inorganic and Organic Chemistry - Isolobality

Much of the understanding of cluster chemistry has resulted by drawing analogies between it and other disciplines of chemistry. Most synthetic routes to mixed metal clusters have their origins in classical organic chemistry and the structure of many clusters can be ascertained employing the same principles applied to borane chemistry. It is clear that there must be some similarity between transition metal fragments and BH, CH units etc.

One can draw a parallel between the BH unit, which presents three orbitals and two electrons, and the $\text{Fe}(\text{CO})_3$ moiety which likewise donates three orbitals and two electrons to the cluster. The $\text{Fe}(\text{CO})_3$ unit has a d_{z^2} - sp_3 hybrid pointing along the 3-fold axis away from the CO ligands, which is similar to the radially orientated sp hybrid of the BH unit. In addition the two dp hybrid orbitals on the metal can be considered to be counterparts of the two tangentially oriented p atomic orbitals, (see Figure 7). Of course, the BH unit is in total a four electron system with four orbitals. Two exo-skeletal electrons are contained in one of the orbitals allowing for formation of the BH bond. The $\text{Fe}(\text{CO})_3$ moiety is a 14 electron system which has twelve exo-skeletal electrons to form a σ and π bond between the iron and each of the three carbonyl ligands. Indeed the interchangeability of BH and $\text{Fe}(\text{CO})_3$ units has been demonstrated in work by Fehlner.^{58,59} The series of compounds $\text{B}_n\text{H}_{n+4}[\text{Fe}(\text{CO})_3]_{5-n}$ exists for $n = 5, 4$ and 3 . These $\text{Fe}(\text{CO})_3$ substituted molecules adopt the same square pyramidal geometry of B_5H_9 as typified by $\text{B}_4\text{H}_8\text{Fe}(\text{CO})_3$.⁶⁰

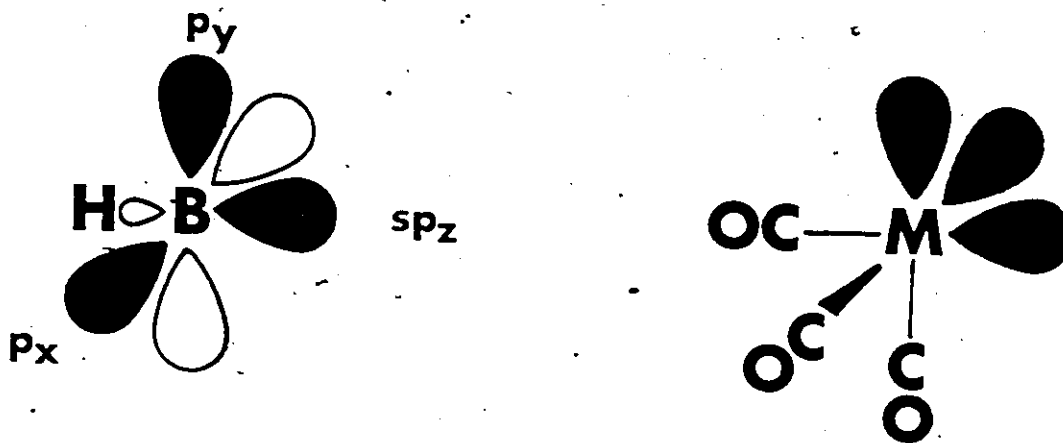
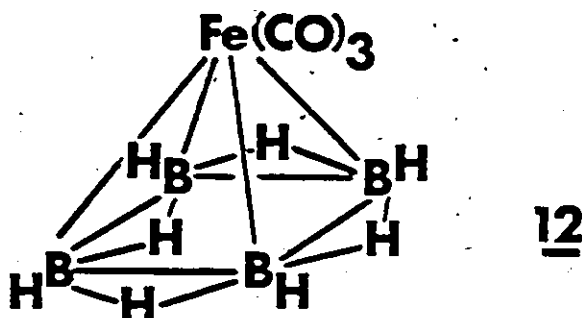


Figure 7:
The Isolobal Moieties BH and $\text{Fe}(\text{CO})_3$



If one replaces the three CO ligands on Fe by a Cp⁻ and keeps the d⁸ configuration but assigns it to Co⁺, you then have CpCo. One could also classify a CpCo unit as donating 3 orbitals and two electrons to a cluster. Indeed, its interchangeability with BH units has been demonstrated by Grimes and Hawthorne^{61,62} on the closo carborane C₂B₈H₁₀, and the series C₂B_nH_{n+2}(CpCo)_{8-n} for n = 8, 7, 6, 5 exists. One sees that the interchangeability of BH units applies to closo as well as nido systems. There are a large number of boranes and carboranes in which BH or CH units have been substituted by an extensive range of both main group and transition metal units.⁶³

The transition metal units Fe(CO)₃ and CpCo are not strictly isoelectronic with the BH fragment, as the metal orbitals which are donated to the cluster have considerable d character. The term which describes the relationship between the metal and BH fragments is isolobal.

It implies that the number, symmetry properties, extent in space and energies of the frontier orbitals of these units are similar. The isolobal analogy has been skillfully exploited by Hoffmann and his associates⁶⁴⁻⁶⁸ in pointing out the similarities between organometallic chemistry and organic chemistry.

One can see the other isolobal relationships which are possible by regarding the $M(CO)_3$ unit as a fragment derived from an octahedral $M(CO)_6$ species. The orbitals the $M(CO)_3$ unit provides for cluster bonding are directed towards the area in which the missing CO ligands were previously found. Employing this treatment, the $Mn(CO)_5$ unit can be viewed as being isolobal with a methyl radical; they each provide a single orbital containing one electron. Therefore, when $Mn(CO)_5$ dimerizes to form $Mn_2(CO)_{10}$ this could be viewed as the all-organometallic version of ethane. Also the compound combining the two isolobal fragments is also known, i.e., $(CO)_5MnCH_3$.

In addition to drawing parallels between organometallic chemistry and organic chemistry, the isolobality principle can also be useful in understanding bonding in clusters. An example of its utility in this area is the case of the $M(CO)_4$ fragment, when $M = Fe, Ru, Os$. In Table 1 this fragment was predicted by PSEP as donating four electrons for cluster bonding. If one then takes a look at the simplest cluster formed by this fragment; $M_3(CO)_{12}$, one would have a total of nine atomic orbitals and twelve skeletal electrons. It is clear that not all of the electrons could go into bonding orbitals so one would expect some instability or distortion in the $M_3(CO)_{12}$ molecule. However, none is seen, so an alternative approach must be employed. By taking the $M(CO)_4$

unit as being derived by removing 2 cis CO ligands from $M(CO)_6$, one is left with a fragment providing 2 electrons and 2 orbitals. Thus the $Fe(CO)_4$ unit is isolobal with methylene and one can consider $M_3(CO)_{12}$ to be an organometallic cyclopropane.

Likewise a parallel may be drawn between the $Co(CO)_3$ moiety and a CH fragment, they both provide 3 orbitals and 3 electrons to a cluster. The $Co(CO)_3$ fragment is derived by removing 3 facial CO ligands from an octahedral $M(CO)_6$ complex. The similarity of these two fragments is evidenced by the existence of the whole series ranging from organic to inorganic tetrahedrane, i.e., C_4R_4 , $C_3R_3Co(CO)_3$, $C_2R_2Co_2(CO)_6$, $CRCo_3(CO)_9$ and $Co_4(CO)_{12}$.

The derivation of the $M(CO)_5$, $M(CO)_4$ and $M(CO)_3$ fragments from an $M(CO)_6$ complex is shown in Figure 8.

One can extend the isolobal analogy to include many other fragments through a few more simple observations and manipulations of electronic structure. For example, if a $Mn(CO)_5$ fragment is isolobal with a methyl radical, so will be the two congeneric fragments, viz., $Tc(CO)_5$ and $Re(CO)_5$. Also the five ligands need not be carbonyls, they could be phosphines, chlorides, etc. Removal of an electron from the $d^7 ML_5$ fragment makes $Cr(CO)_5$ isolobal with CH_3^+ while addition of an electron results in $Fe(CO)_5$ being isolobal with CH_3^- . It follows then that $Fe(CO)_5^+$ would be isolobal with the methyl radical.

In addition the metal fragments need not be derived from octahedral ML_6 fragments. The other most common geometry adopted by organometallic compounds is square planar. The square planar geometry is related to the octahedral complex by removal to infinity of the two

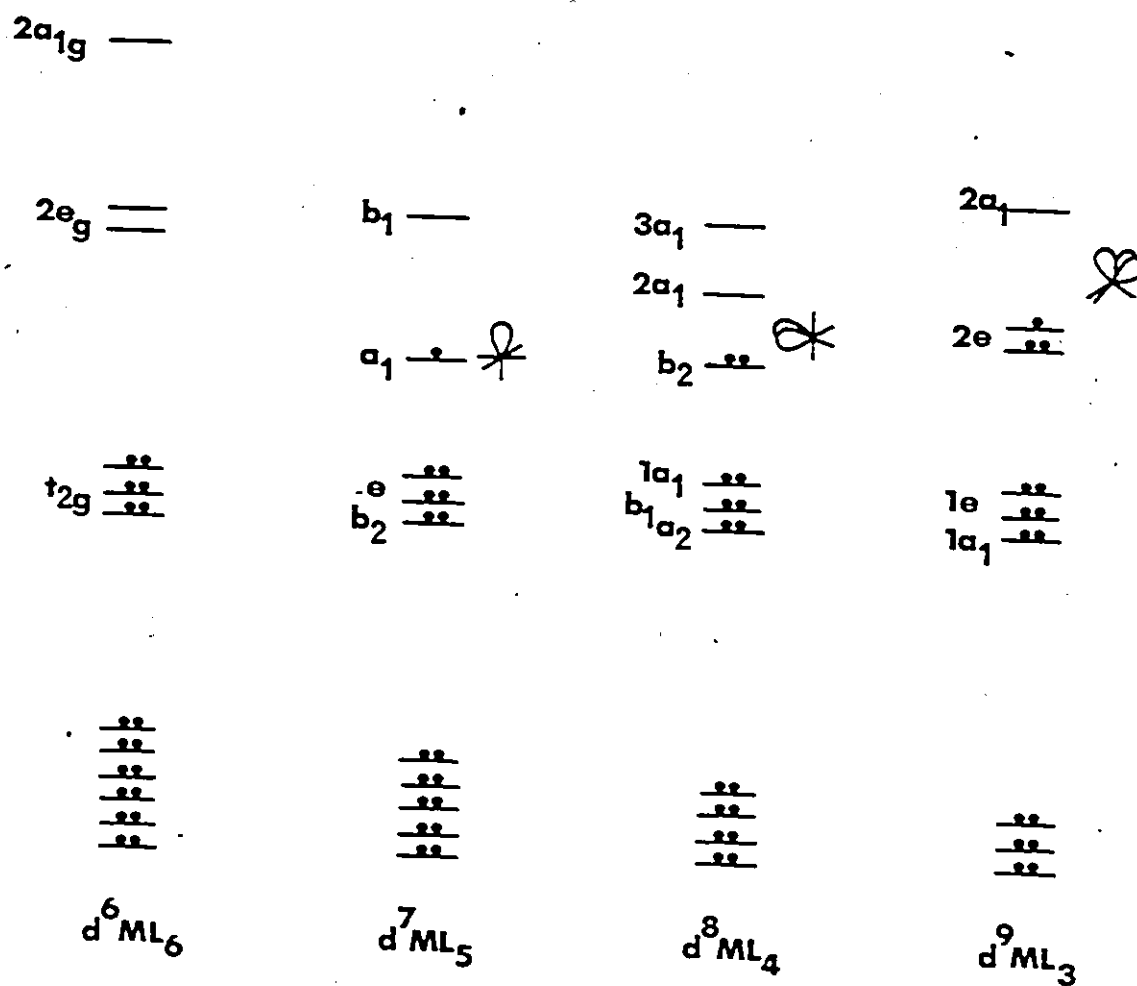


Figure 8:

Derivation of the $M(CO)_5$, $M(CO)_4$ and $M(CO)_3$ Fragments from an $M(CO)_6$ Complex

trans ligands. This affects the electronic structure of the metal so as to lower the metal d_{z^2} atomic orbital in energy to a point where it is of the same energy as the non-bonding metal t_{2g} set in an octahedral complex. One can then see a relationship between the $d^n ML_5$ and T-shaped $d^{n+2} ML_3$ and between the $d^n ML_4$ and the angular shaped $d^{n+2} ML_2$ fragments. This would make $PtCl_3^-$ and $(Ph_3P)_2Pt$ isolobal with CH_3^+ and CH_2 respectively.

Not only is $d^9 Co(CO)_3$ isolobal with a CH unit, but so is the $d^5 CpCr(CO)_2$ unit. If one replaces the Cp^- ligand by 3 carbonyl ligands, one is left with $Cr(CO)_5^+$. $Cr(CO)_5$ is isolobal with CH_3^+ , which would make $Cr(CO)_5^+$ isolobal with CH_3^{2+} . Two deprotonations transform CH_3^{2+} to CH and one can see the isolobal relationship between it and $CpCr(CO)_2$. The fact that $CpCr(CO)_2$ is isolobal with CH is somewhat puzzling as it is essentially a ML_5 fragment with only a single frontier orbital available. However two of the non-bonding t_{2g} metal orbitals are of π pseudosymmetry and can therefore act as frontier orbitals.

The isolobal principle is not a one-to-one mapping. Thus far, its primary use in both organometallic and specifically cluster chemistry has been to rationalize the complex structures these molecules adopt in terms of their much simpler organic analogues. To a lesser extent it has been employed in determining possible synthetic routes for clusters. In this vein, it might be possible to construct clusters via a buildup of metal fragments with the target being clusters whose isolobal analogues have precedent in organic chemistry. Through knowing the frontier orbitals, i.e., the highest occupied molecular orbital (HOMO) and lowest unoccupied molecular orbital (LUMO) of a particular fragment, one might be able to predict the possible products of a reaction.

However, there is no guarantee that molecules predicted to exist will be both thermodynamically stable and kinetically inert. A prime example of the frontier orbitals of a fragment being similar exists for ER_2 , where $E = C, Si, Ge, Sn, Pb$. One would expect ethylene analogues to exist for the remaining elements, yet it has only been recently that silaethylenes have been obtained in a stable form.⁶⁹

Examples of some key isolobal relationships are presented in Table 4.


Table 4 - Summary of Basic Isolobal Relationships

	Cr, Mo, W	Mn, Re, Tc	Fe, Ru, Os	Co, Rh, Ir	Ni, Pd, Pt
CH_3	$d^5 CpML_3$	$d^7 ML_5$	$d^7 CpML_2$	$d^9 ML_4$	$d^9 CpML$
CH_2	$d^6 ML_5$	$d^6 CpML_2$	$d^8 ML_4$	$d^8 CpML$	$d^{10} ML_2$
CH	$d^5 CpML_2$	$d^7 ML_4$	$d^7 CpML$	$d^9 ML_3$	$d^9 CpM$
BH			$d^8 ML_3$	$d^8 CpM$	$d^{10} ML_2$

1.5 Applications of Transition Metal Clusters

A major thrust of organometallic chemistry is geared toward the development of novel catalysts. In particular, much activity has been directed towards the search for an efficient homogeneous Fischer-Tropsch catalyst. There are many examples of organometallic complexes employed as catalysts. They include olefin hydrogenations using Wilkinson's catalyst, $(\phi_3P)_3RhCl$, polymerization of ethylene by titanium alkyls, hydroformylations employing $HCo(CO)_4$ and acetic acid synthesis via $I_2Rh(CO)_2^-$.⁷⁰ All these cases represent homogeneous systems; in contrast heterogeneous catalysis is preferred by industry for the reasons of efficiency and ease of product separation. On the

other hand homogeneous catalysis presents some advantages such as milder conditions of temperature and pressure, in some cases a higher degree of selectivity and the reactions can be more easily studied to yield mechanistic information.



Over the past several years a great deal of attention has been focussed on metal clusters which may be viewed as a bridge between the intensively studied homogeneous monometallic systems and the less well understood reactions occurring on surfaces.⁷¹ Catalytic research on metal clusters is still at a developmental stage as more emphasis has been placed on understanding the synthesis, structure and reactivity of metal clusters. The analogy between clusters and metal surfaces has arisen because of the observation that the structure of larger metal clusters is more reminiscent of close packed metals than that of boranes. This had led to the misconception that clusters possess the same properties as metals. In fact clusters do not have metal properties. This is quite evident in the smaller 4 to 6 atom clusters.⁷²

The comparison between a cluster and a metal surface is best made as that of a polyhedral core of metals with ligands coating the molecular periphery versus a metal surface with a similar set of ligands adsorbed at the surface. This comparison is one of the advantages of studying catalysis with clusters. The other benefits are that clusters may be able to generate reactive mononuclear fragments possessing catalytic activity through the scission of metal-metal bonds. Also, they may allow the possibility of unique catalytic transformations to be carried out in which more than one metal atom site participates.⁷³

Metal clusters have been found to catalyze a wide range of reactions, however, due to the complicated nature of the catalytic reaction cycles, it is difficult to prove the catalyst is actually the cluster. Today there is still no real unequivocal example of catalysis by a cluster compound.⁷⁴ Even when the cluster is recovered intact there is no evidence to suggest that the integrity of the cluster has been maintained throughout the reaction. In a majority of the cases the catalytic species is believed to be a highly reactive mononuclear entity generated under the reaction conditions. The current challenge for researchers is the determination of the nuclearity. Ideally, they would be isolable, but spectroscopic detection may have to suffice.

So far the reactions studied by cluster catalysis have not provided increased activity and selectivity compared to mononuclear systems. Perhaps increased activity and enhanced selectivity may be possible by using combinations of different metals. The other possibility is that clusters need to be designed which are coordinatively unsaturated; these should have higher catalytic activity. Another area in which metal clusters may find utility is as stoichiometric reagents in organic synthesis. There are few examples in this relatively virginal field. The best known is the use of a $\text{Co}_2(\text{CO})_6$ moiety to protect an alkyne linkage.⁷⁵

1.6 Statement of Problem

The goal of this research was to develop routes to four- or five-vertex mixed clusters by carrying out synthetic manipulations on existing cluster systems. The theoretical underpinnings upon which these syntheses

are based include Hoffmann's isolobality principle and the polyhedral skeletal electron pair bonding model. In addition to the synthetic work, it was hoped that one could draw correlations between metal clusters and their existing borane analogues in the areas of reactivity, fluxionality and bonding.

CHAPTER II

SYNTHESES AND STRUCTURES OF TRIMETALLIC ALKYNE CLUSTERS

2.1 Introduction

The first known organometallic compound was Zeise's salt $K[Cl_3Pt(C_2H_4)]$. When its structure was finally elucidated, it seemed a natural progression for chemists to move from olefins to alkynes in search of ligands which could be complexed to metal centres. Alkynes are more versatile than olefins as they offer greater bonding possibilities due to the presence of two orthogonal π systems. In mononuclear metal complexes they bond in a similar manner as do olefins, e.g., they serve as two-electron donors. The alkyne can be found either perpendicular to the metal-ligand plane e.g., $Cl_3Pt(RC\equiv CR)^-$ or lying in the metal-ligand plane, e.g., $(Ph_3P)_2Pt(RC\equiv CR)$.⁷⁶ In the former case the alkyne behaves as a π donor while in the latter there is evidence for the bonding to be described in terms of two metal-carbon σ bonds. In cluster chemistry only a few examples exist where an alkyne functions as a simple two electron donor, e.g., $Ru_3(CO)_{11}(RC\equiv CPPH_2)$,⁷⁷ which bonds via P.

The most common bonding mode for acetylenes is bridging two, three or four metal centres employing both of its filled π orbitals. As the two pairs of π orbitals lie perpendicular to each other, this type of bonding interaction is very difficult to achieve in mononuclear metal complexes. In this vein, the alkyne is serving as a four electron donor. The most common alkyne complexes of this type are those resulting from

the reactions with binuclear metal-metal triple bonded species such as $\text{Co}_2(\text{CO})_6$, $\text{Cp}_2\text{Mo}_2(\text{CO})_4$.^{29,30} The position of the two metal atoms is such that it allows for overlap with both π -orbitals of the alkyne.

Structural data on these species however, indicate that some degree of rehybridization occurs.⁷⁸ Thus, the bonding can be viewed as involving an sp^3 hybridization about each carbon atom with strong sigma bonds to the two metal centres. The length of the carbon-carbon bond in the complexed alkyne is consistent with a single bond, yet some degree of unsaturation must still exist as there have been studies in which the alkyne has been protonated.⁷⁹

As one moves to tri- and tetrametallic alkyne complexes the concept of localised bonding begins to break down and a delocalised bonding interpretation is preferred. The common bonding modes of alkynes to di-, tri- and tetrametallic complexes are shown in Figure 9.

If one includes the carbon atoms of the alkyne as cluster vertices, there is a plethora of clusters derived from the addition of alkynes to polymetallic species. Most of these are of the homometallic variety. The field of alkyne-metal clusters has been widely investigated in many laboratories and has recently been the subject of a comprehensive review.⁸ To date the maximum number of metal atoms to which an alkyne can bond and remain intact is four.⁸⁰

Early syntheses usually involved substitution of carbonyls by the alkyne initiated either thermally or photochemically. However, with these techniques it was difficult to stop at simple substitution and instead alkyne oligomerization was normally observed. Recent synthetic routes have involved the displacement of weakly coordinated

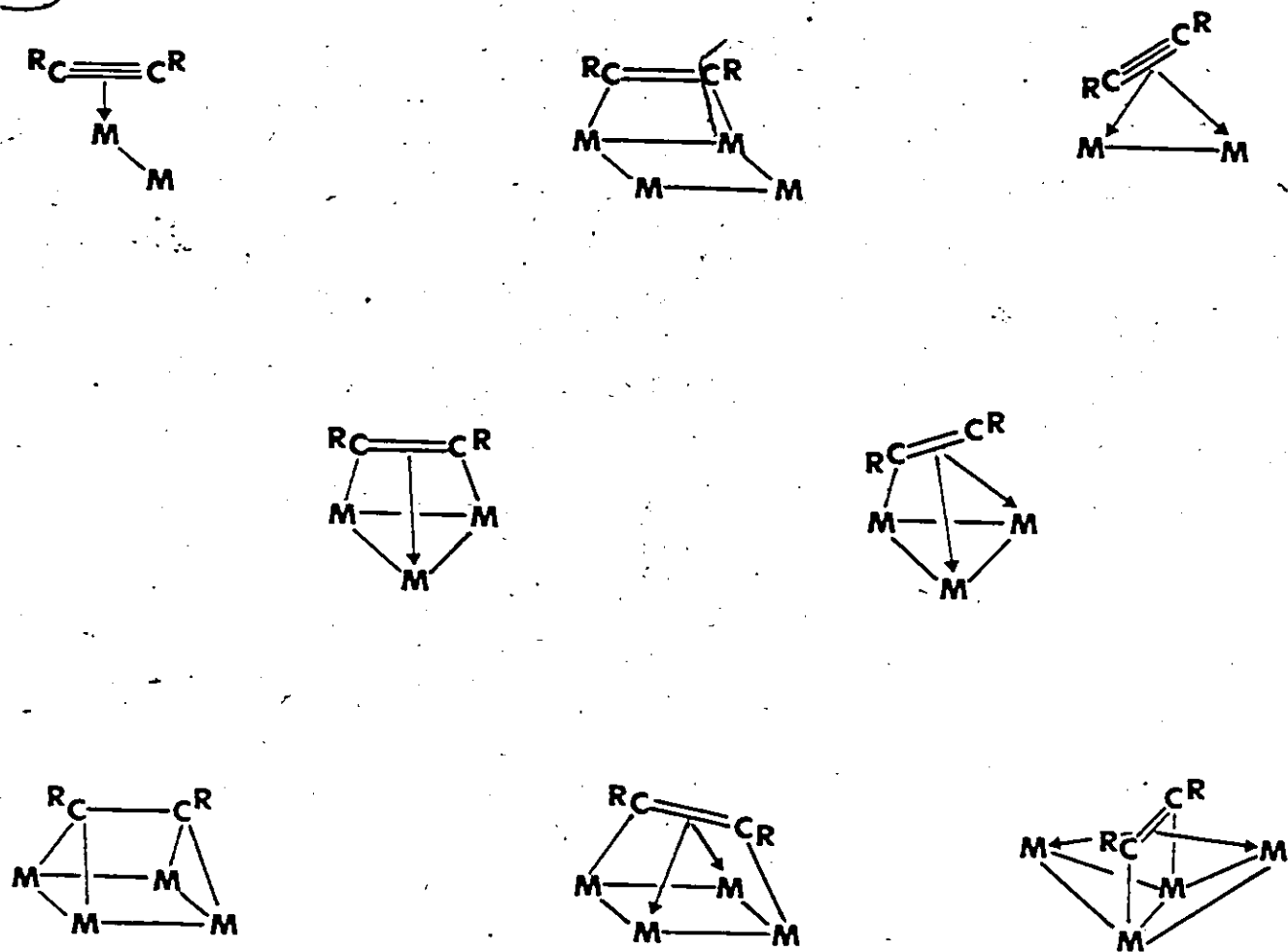


Figure 9:

Some Typical Bonding Modes of Alkynes in Clusters

ligands from clusters or the generation of unsaturated clusters by employing Me_3NO , a reagent known to remove carbonyls by generating CO_2 and Me_3N . The nature of the alkyne dictates the type of complex observed from the reaction with metal clusters. Typically, symmetrical alkynes coordinate without rearrangement, alkyl substituted alkynes coordinate but then isomerize to allyl or allenyl ligands,⁸¹ terminal alkynes split into hydrides and multi-bound acetylides⁸² and phosphido alkynes split into bridging phosphido groups and multi-bound acetylides.⁸³ Naturally, the nature of the product is also dependent upon the identity of the metal carbonyl and on the reaction conditions employed.

The interest in complexing alkynes to metal centres comes from attempts to "activate" the alkyne. By "activation" one means the enhancement of chemical reactivity. In the case of alkynes, one of the measures of activation is the increase in the carbon-carbon bond length. In alkyne complexes, bond order reduction seems to increase as the number of interacting metal atoms is increased. A reaction of considerable importance is the reduction of alkynes by hydrogenation. However, only a few alkyne-metal complexes have turned out to be successful in accomplishing this transformation.

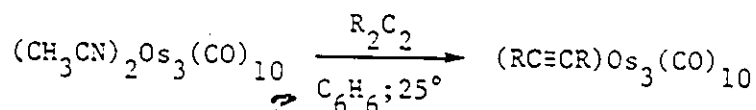
Another reaction which has stimulated investigation of metal-alkyne complexes is the trimerization of alkynes leading to substituted benzenes. In the absence of catalysts this reaction proceeds only at high temperatures and in low yields. The best known catalysts for this reaction are mononuclear complexes such as $\text{CpCo}(\text{CO})_2$ and intermediates in the reaction sequence are believed to be alkyne-metal clusters.⁸⁴ Binuclear metal alkyne complexes are also known to catalyze the

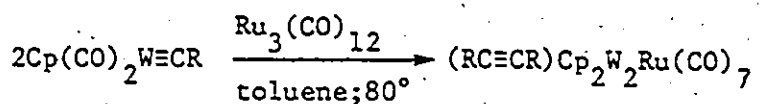
trimerization process. The reaction is believed to proceed by linking of alkyne units on the binuclear metal centres. Binuclear complexes containing more than one alkyne unit have been characterized X-ray crystallographically, thus giving credence to the proposed reaction mechanism.⁸⁵ When this reaction is carried out in the presence of carbon monoxide, a variety of products are obtained including cyclic ketones, quinones and metallocyclic compounds.⁸⁶

This chapter reports the synthesis of chiral heterotrimetallic alkyne clusters via buildup of mononuclear metal fragments. The structure of these clusters have been determined and are compared with known trimetallic alkyne complexes. A model involving a delocalised bonding scheme is used to rationalise not only the synthetic routes but also the structures.

2.2 Synthesis of Heterotrimetallic Alkyne Clusters

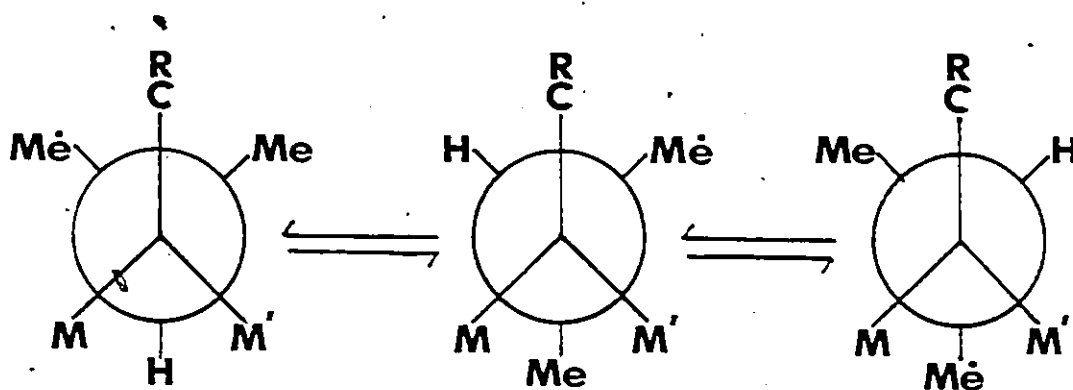
Some trimetallic-alkyne clusters were originally found among the mixtures of products arising from the thermolyses of mononuclear carbonyl derivatives and alkynes.⁸⁷ More recently several rational routes have been developed to this type of cluster. The most obvious one is addition of an alkyne to a metal triangle with concomitant elimination of carbon monoxide, hydrogen or some weakly bound ligand.⁸⁸ A second method involves the coupling of two metal-carbyne fragments in the presence of another metal carbonyl.⁸⁹ Examples of these two routes are indicated below:





The route chosen to be explored in this work involves the expansion of preformed M_2C_2 tetrahedral clusters. Before one can discuss the rationale and chemistry of this route it would be valuable to discuss the syntheses of the tetrahedral precursors.

As mentioned in Section 1.2, tetrahedral precursors of the type M_2C_2 are readily available. However, these compounds are homometallic rather than heterometallic and the latter is a requirement in the eventual goal of producing a chiral cluster. For example, one can reduce the symmetry of $(\text{RC}\equiv\text{CR})\text{M}_2$ (C_{2v}) to C_s by using an unsymmetrical alkyne and then to C_1 by using two different metals $(\text{RC}\equiv\text{CR}')\text{MM}'$. This molecule is now chiral and one needs a probe for chirality. Employing the isopropyl ester of phenylpropionic acid as the alkyne provides a pair of diastereotopic methyl groups which can only be equilibrated via a process which racemizes the cluster.



The first cluster to be synthesized was $(\text{CpNi})_2(\text{PhC}\equiv\text{CCO}_2\text{CHMe}_2)$, ¹³. This is not a heterometallic complex but the particular reasons for the choice of this cluster will be developed later in this section. Binuclear nickel alkyne clusters of this type have been synthesized by many groups.⁹⁰ In this reaction Cp_2Ni and isopropyl phenyl propiolate were refluxed together in toluene. The product is believed to result from generation of a metal-metal triple bond across which the acetylene adds. Other routes to this cluster usually involve the use of $[\text{CpNi}(\text{CO})]_2$, a reagent known to undergo facile decarbonylation to yield the nickel-nickel triple bonded dimer. Cp_2Ni has the advantages of being a less expensive reagent and also that any unreacted Cp_2Ni may be sublimed from the product, which is a dark green oil. The problems of employing Cp_2Ni as a cluster reagent are its poor solubility in organic solvents and the side reactions it undergoes when other metal carbonyls are present. The ¹H NMR spectrum of ¹³ shows a singlet due to the cyclopentadienyl resonance at $\delta 5.31$ and a doublet due to the methyl resonance of the isopropyl group at $\delta 1.24$.

The next cluster synthesized was $\text{Cp}_2\text{NiMo}(\text{CO})_2(\text{PhC}\equiv\text{CCO}_2\text{CHMe}_2)$, ¹⁴, by refluxing Cp_2Ni and $[\text{CpMo}(\text{CO})_3]_2$ in the presence of the alkyne ester in toluene. The reaction is believed to proceed first via rupture of the molybdenum dimer and disproportionation of Cp_2Ni leading to the formation of two organometallic radical species. There is literature precedent for generation of these moieties.⁹¹ Recombination of these species could lead to the mixed metal dimers, many of which are known containing molybdenum.⁹² Continued heating would lead to formation of the mixed metal-metal triple bond to be followed by addition of the

acetylene. Alternatively the product may result from initial formation of the dimolybdenum cluster, $\text{Cp}_2\text{Mo}_2(\text{CO})_4(\text{RC}\equiv\text{R}')$, followed by substitution of a $\text{CpMo}(\text{CO})_2$ vertex with CpNi . The ^1H NMR spectrum of this compound reveals two resonances attributed to cyclopentadienyl groups at $\delta 5.24$ and $\delta 5.14$ respectively. By comparison with other compounds produced in this study, it is believed that the high frequency resonance can be assigned to the cyclopentadienyl group bonded to Ni while the low frequency resonance corresponds to the one bonded to Mo. This molecule is chiral and one does see the expected pair of doublets due to the diastereotopic methyl groups. An interesting feature is observed in the infrared spectrum of the compound. In addition to bands which can be attributed to terminal CO stretches, a strong band is observed at 1857 cm^{-1} . This is indicative of a semi-bridging CO similar to that observed by Cotton in his study on di-molybdenum alkyne complexes.³⁰ The occurrence of the semi-bridging CO may serve to alleviate steric crowding in the cluster.

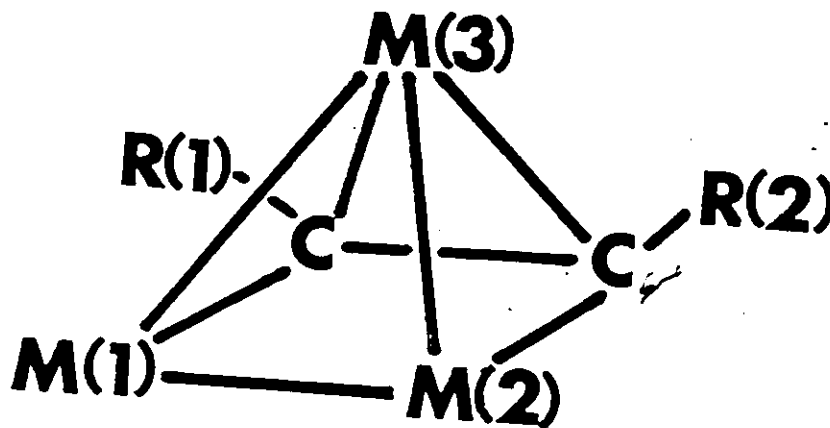
The final cluster, $\text{CpNiCo}(\text{CO})_3(\text{PhC}\equiv\text{CCO}_2\text{CHMe}_2)$, 15, is the major product from the reaction of Cp_2Ni and $\text{Co}_2(\text{CO})_8$ in the presence of the alkyne. Most probably this cluster arises by initial formation of the $\text{Co}_2(\text{CO})_6$ -alkyne adduct, followed by replacement of a $\text{Co}(\text{CO})_3$ unit by a CpNi fragment. There are two other reports in the literature on the synthesis of CoNi -alkyne clusters. The first involves a route similar to the one above except that $[\text{CpNi}(\text{CO})]_2$ is employed as a source of CpNi fragments;³⁶ the second report describes two routes to the cluster; viz., treatment of the dinickel cluster with $\text{Co}_2(\text{CO})_8$ or treatment of the dicobalt cluster with Cp_2Ni .⁹³ This study also reports the X-ray structure of the diphenylacetylene cluster. The ^1H NMR spectrum of 15

exhibits a singlet δ 5.31 due to a cyclopentadienyl group on Ni and a doublet at δ 1.29 for the methyl groups of isopropyl phenylpropiolate. Since $\underline{15}$ is a chiral cluster, one would expect to see a pair of doublets in the Me region in the ^1H NMR spectrum as was observed in $\underline{14}$. However, one must go from a 1.879T field (80 MHz for protons) to a 9.395T field (400 MHz for ^1H) to observe this pattern and even then the doublets overlap. The IR spectrum reveals only bands associated with terminal carbonyl stretches. This is expected if the structure of $\underline{15}$ is similar to that for $\text{CpNiCo}(\text{CO})_3(\text{PhC}\equiv\text{CPh})$ which shows no semi-bridging carbonyl interactions.

The tetrahedral clusters $\underline{13}$ through $\underline{15}$ possess 12 skeletal electrons and their bonding can be viewed in two ways, e.g., employing localised or delocalised models. In the former description one would have an electron pair along each of the six edges of the tetrahedron. Adopting this view, one would regard these molecules as being coordinatively saturated, a point supported by the studies of Muetterties in which $\text{Cp}_2\text{Ni}_2(\text{PhC}\equiv\text{CPh})$ and $\text{Co}_2(\text{CO})_6(\text{PhC}\equiv\text{CPh})$ were examined as possible hydrogenation catalysts.³⁶ However, if one regards the six electron pairs as being delocalised, then according to Wade's Rules, these clusters would be considered to be nido trigonal bipyramids. Photoelectron and nuclear quadrupole resonance data on the isostructural clusters $\text{RCo}_3(\text{CO})_9$, which also possess 12 skeletal electrons, support the idea of electron delocalisation.^{94,95} In addition, the structure of $\text{Fe}_4(\text{CO})_{13}^{2-}$, which can also be regarded as a nido-trigonal bipyramid, reveals a triply bridging carbonyl capping a triangular face of the tetrahedral arrangement of irons.⁹⁶ This could be viewed as serving the same purpose as

bridging hydrogens in nido-boranes. With this vacant site on the surface of the polyhedron, tetrahedral clusters can be thought of as being coordinatively unsaturated. Therefore, one would expect both high reactivity and NMR fluxionality in these tetrahedral clusters. The latter has been observed in previous studies in this laboratory.⁹⁷

In order to test the hypothesis of high reactivity in these systems, clusters 13 through 15 were treated with $\text{Fe}_2(\text{CO})_9$. The anticipated result was the addition of an $\text{Fe}(\text{CO})_3$ unit to the parent cluster leading to chiral trimetallic-alkyne clusters. $\text{Fe}_2(\text{CO})_9$ is a reagent which is known to deliver an $\text{Fe}(\text{CO})_3$ moiety to tetrahedral clusters,^{98,99} bringing about expansion to the square based pyramidal geometry as shown below;



These molecules are chiral if $M(1) \neq M(2)$ or $R(1) \neq R(2)$ or if there is an asymmetrical arrangement of ligands such as a semi-bridging carbonyl; of course, an intrinsically chiral substituent, such as (+)-menthyl; would obviously make the cluster non-superimposable on its mirror image. The interest in chiral clusters is in the hope they may find a use in asymmetric synthesis. Mono-metallic systems with chiral ligands such as DIOP are currently employed in this area.¹⁰⁰

The chiral clusters $\underline{16}$ through $\underline{18}$ were characterised by ^1H NMR spectroscopy, IR spectroscopy, high resolution mass spectrometry and X-ray crystallography. A more detailed discussion of the structure of these molecules is found in Section 2.3. These clusters were obtained from the treatment of the tetrahedral clusters $\underline{13}$ to $\underline{15}$ with $\text{Fe}_2(\text{CO})_9$ in heptane (See Figure 10).

Of the tetrahedral precursors, only $\underline{13}$ was achiral, but upon treatment with $\text{Fe}_2(\text{CO})_9$, the product $\text{Cp}_2\text{Ni}_2\text{Fe}(\text{CO})_3(\text{PhC}\equiv\text{CCO}_2\text{CHMe}_2)$, $\underline{16}$ is chiral. In the ^1H NMR spectrum one observes a pair of singlets at $\delta 5.24$ and $\delta 5.08$ in the cyclopentadienyl region as well as a pair of doublets in the methyl region at $\delta 1.02$ and $\delta 0.93$. There are many clusters containing an FeNi_2 core complexed to an alkyne and indeed, the first of these was synthesized some twenty-five years ago.⁹⁸

$\text{CpNiCoFe}(\text{CO})_6(\text{PhC}\equiv\text{CCO}_2\text{CHMe}_2)$, $\underline{17}$, represents only the second example of an FeCoNi -alkyne cluster. In contrast to its tetrahedral precursor, $\underline{15}$, the chemical shift difference between the two diastereotopic methyl groups is great enough to be observed at 80 MHz. Perhaps the most interesting cluster is $\text{Cp}_2\text{NiMoFe}(\text{CO})_5(\text{PhC}\equiv\text{CCO}_2\text{CHMe}_2)$, $\underline{18}$. The ^1H NMR spectrum reveals two resonances at $\delta 4.78$ and $\delta 5.22$ for the cyclopenta-

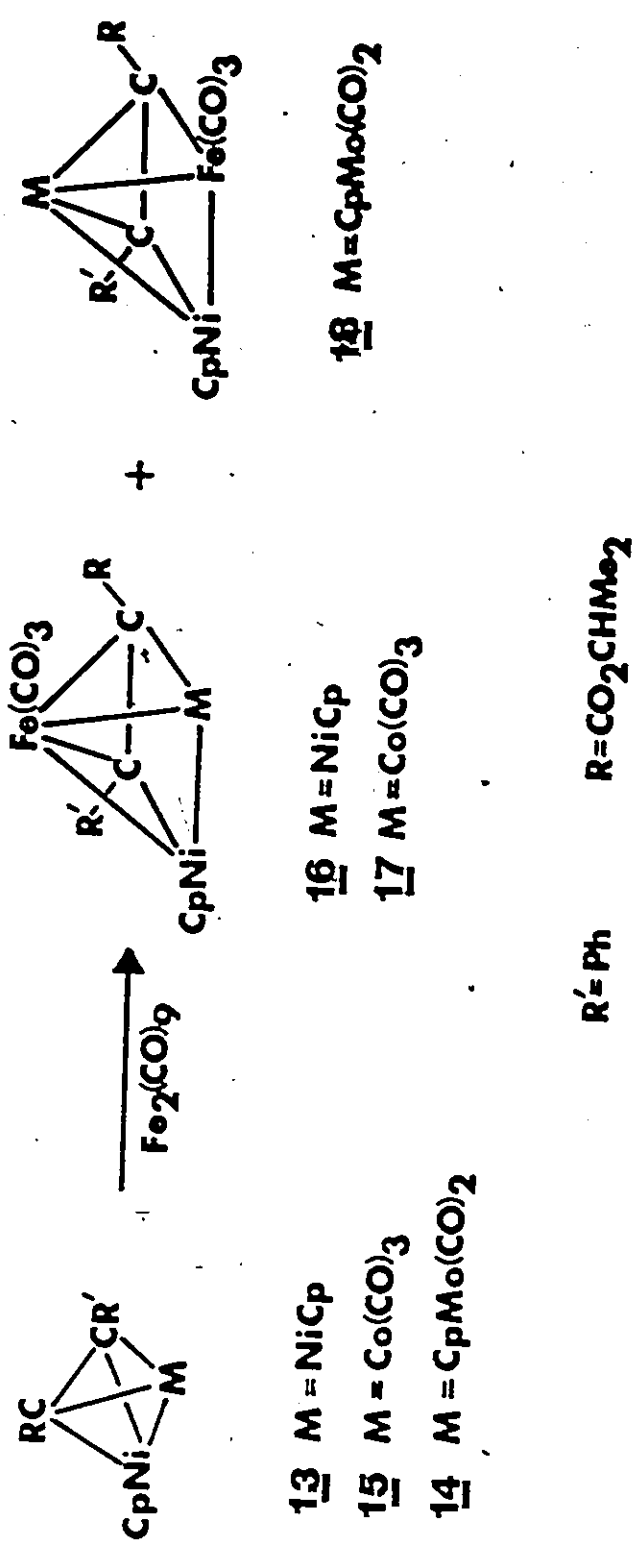


Figure 10:

The Expansion of M₂C₂R₂ Tetrahedral Clusters to Square-Based Pyramidal Clusters

dienyl groups on Mo and Ni respectively. There are also two other resonances in the cyclopentadienyl region at δ 5.42 and δ 5.15 which are one-sixth the intensity of the previous resonances. Furthermore, the methyl region shows three sets of doublets in a ratio of 7:6:1 (See Figure 11). The IR spectrum exhibits weak bands at 1876 and 1830 cm^{-1} suggestive of semi-bridging carbonyl interactions. Both the NMR and IR data are indicative of the presence of at least two structural isomers in solution. The significance of this result will become clearer after the discussion of the structure of $\underline{18}$ in section 2.3.

The synthetic approach outlined above to trimetallic alkyne clusters has the advantages that the conditions are both mild and easily controllable. Subsequent investigations have shown that even milder conditions may be employed when the reactions are performed in tetrahydrofuran (THF). This could be possibly due to the disproportionation of $\text{Fe}_2(\text{CO})_9$ into $\text{Fe}(\text{CO})_5$ and $\text{Fe}(\text{CO})_4\text{-THF}$. The latter is known to be a very reactive species. Separation problems are minimized somewhat when employing THF as one can remove the $\text{Fe}(\text{CO})_5$ produced by volatilization under reduced pressure. In the case of the dinickel cluster it was observed that increased reaction times or more forcing conditions leads to another $\text{Fe}(\text{CO})_3$ moiety being incorporated into the square pyramidal FeNi_2 -alkyne cluster. This latter cluster has been crystallographically characterized by Sappa and his co-workers using C_2Et_2 as the alkyne.¹⁰¹ The structure can be thought of as being derived from a pentagonal bipyramid with $\text{Fe}(\text{CO})_3$ moieties occupying the apical positions but with a basal vertex missing. Successive addition of $\text{Fe}(\text{CO})_3$ moieties has also been observed in the reaction of $\text{Fe}_2(\text{CO})_9$ and $\text{CpMn}(\text{CO})_2(\text{RC}\equiv\text{CR})$.¹⁰²

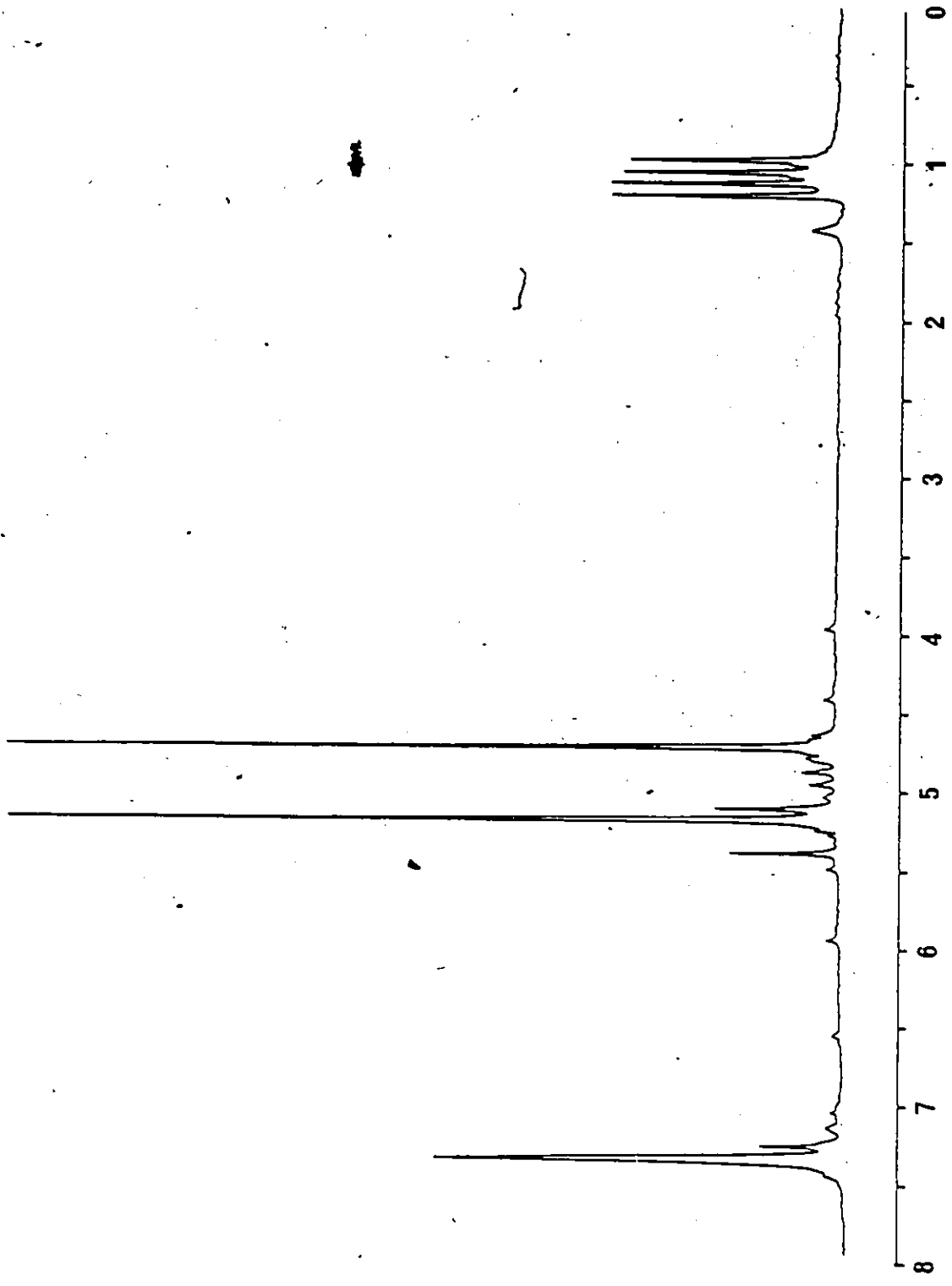
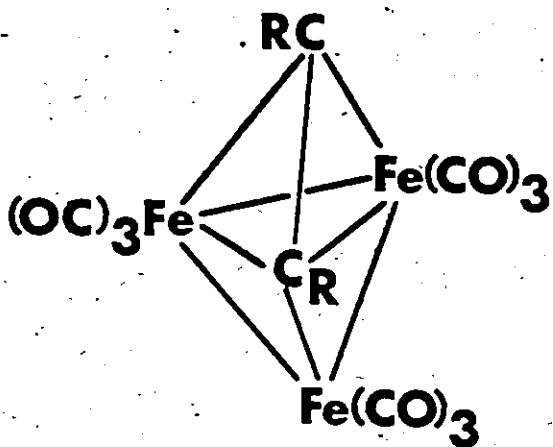
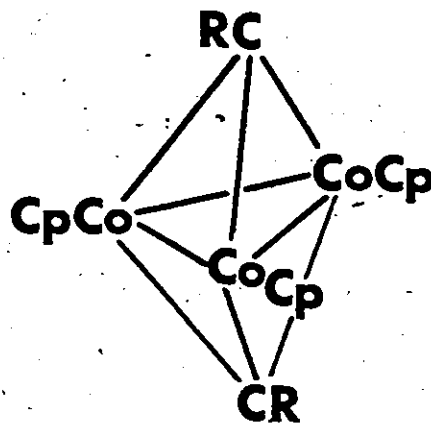


Figure 11:
1H NMR Spectrum of Cp₂NiMoFe(CO)₅(PhC₂O₂CMe₂H)₁₈

The product obtained is a cluster containing a square pyramidal $MnFe_2C_2$ core. This cluster expansion route possesses wider applicability and has proven successful in the reactions of $[CpMo(CO)_2]_2(RC\equiv CR)$ complexes.¹⁰³ Furthermore, it will be shown later that one is not restricted to the addition of $Fe(CO)_3$ units but one can introduce other fragments bearing two skeletal electrons in their three frontier orbitals.

2.3 Structures of Trimetallic Alkyne Clusters

The five vertex trimetallic-dicarbon clusters, M_3C_2 , adopt either a trigonal bipyramidal or a square based pyramidal geometry depending on whether the skeletal electron count is 12 or 14, respectively. These systems can be compared to the closo-carboranes $R_2C_2B_3H_3$ and the nido-borane B_5H_9 respectively.³⁸ Just as one observes 1,2 and 1,5 isomers in the carborane $R_2C_2B_3H_3$, for the trigonal bipyramidal clusters the carbons may be contiguous, as in $Ph_2C_2Fe_3(CO)_9$,^{19, 104} or diaxial as in $R_2C_2Co_3Cp_3$,^{20, 105} There are very few other examples of alkyne-trimetallic clusters possessing the trigonal bipyramidal geometry,^{106, 107} most probably due to the fact no rational routes to clusters of this type have been developed. When the alkyne unit remains intact, it may be oriented perpendicular to the metal triangle as in a trigonal bipyramidal structure; in contrast, in square pyramidal structures the alkyne is parallel to a metal-metal bond of the triangle. In the perpendicular conformation, the alkyne may be seen as forming a σ bond to one metal centre and π bonds to the remaining two. In the parallel arrangement, the alkyne forms σ bonds to two metal centres and a π bond to the third. It has been suggested that the orientation of the alkyne ligand can be related to the nature of the frontier orbitals of the metal triangle.¹⁰⁸

1920

A great many trimetallic-alkyne clusters possessing 14 skeletal electrons have been structurally characterized. Employing the principles of PSEP, one would expect these molecules to adopt a nido-octahedral arrangement. This prediction is confirmed as in all cases the square pyramidal geometry is found.¹⁰⁹ Regardless of the nature of the metals or alkyne contained in the cluster, this geometry is always observed. Subsequently, X-ray crystallographic studies on clusters 16 through 18 show them to follow this pattern (see Figures 12-14).

There are many features which are common to all three structures. In all three complexes the alkyne adopts the $2\sigma+\pi$ bonding mode to the triangle of metals. The alkyne unit and the two σ bonded metal atoms all lie in the same plane. From the carbon-carbon bond lengths of 1.363(4), 1.376(8) and 1.38(2)Å, one sees the acetylenic bond has been reduced. It

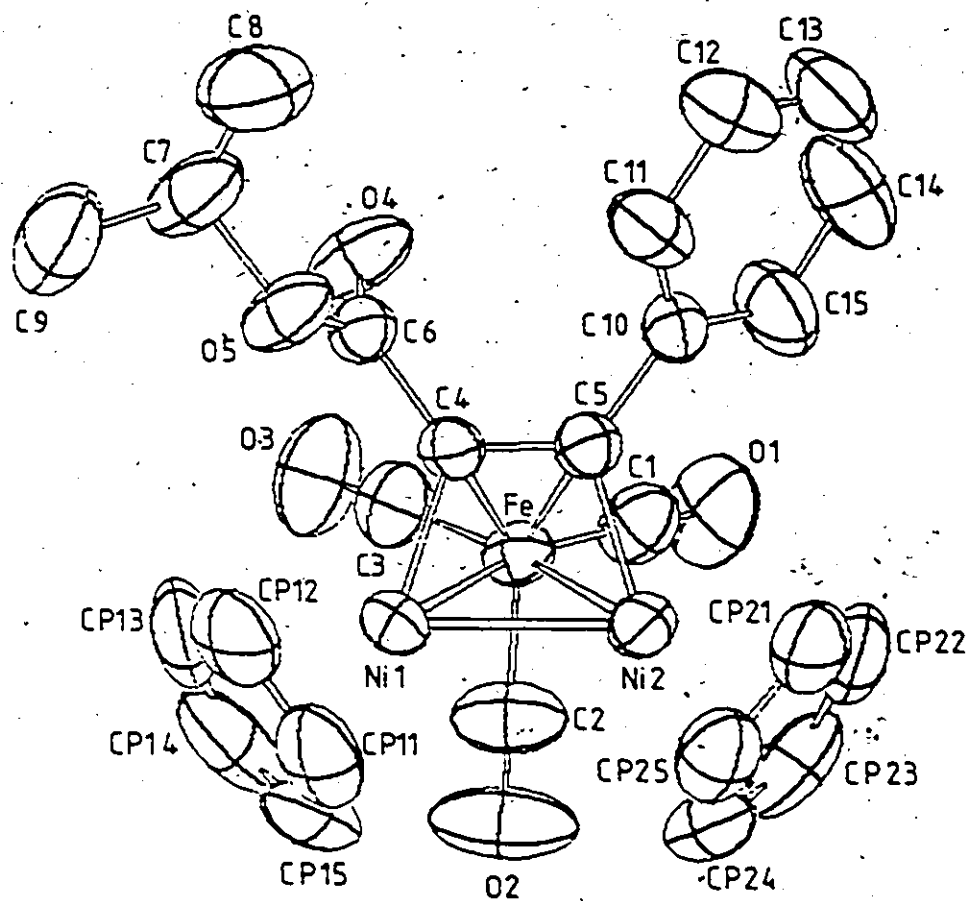


Figure 12:

ORTEP Diagram of $\text{Cp}_2\text{Ni}_2\text{Fe}(\text{CO})_3(\text{PhC}_2\text{CO}_2\text{CMe}_2\text{H})$, 16

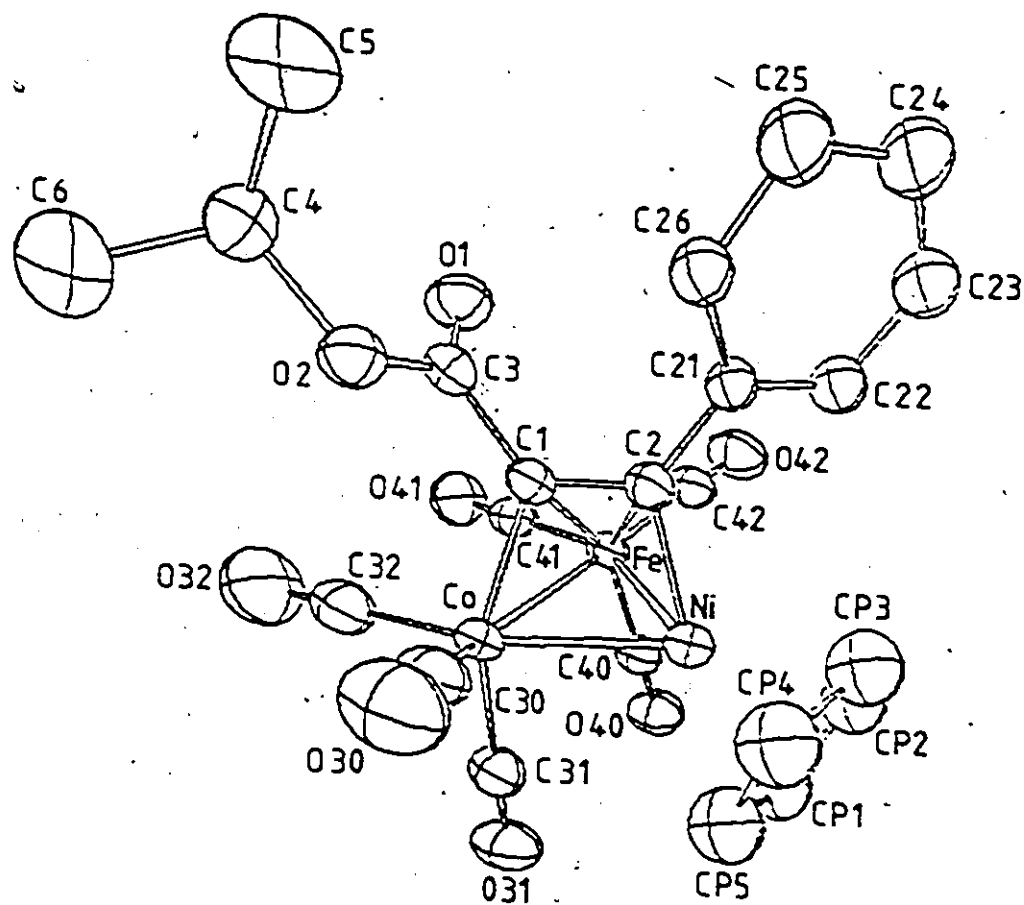


Figure 13:

ORTEP Diagram of $\text{CpNiCoFe}(\text{CO})_6(\text{PhC}_2\text{CO}_2\text{CMe}_2\text{H})$, 17

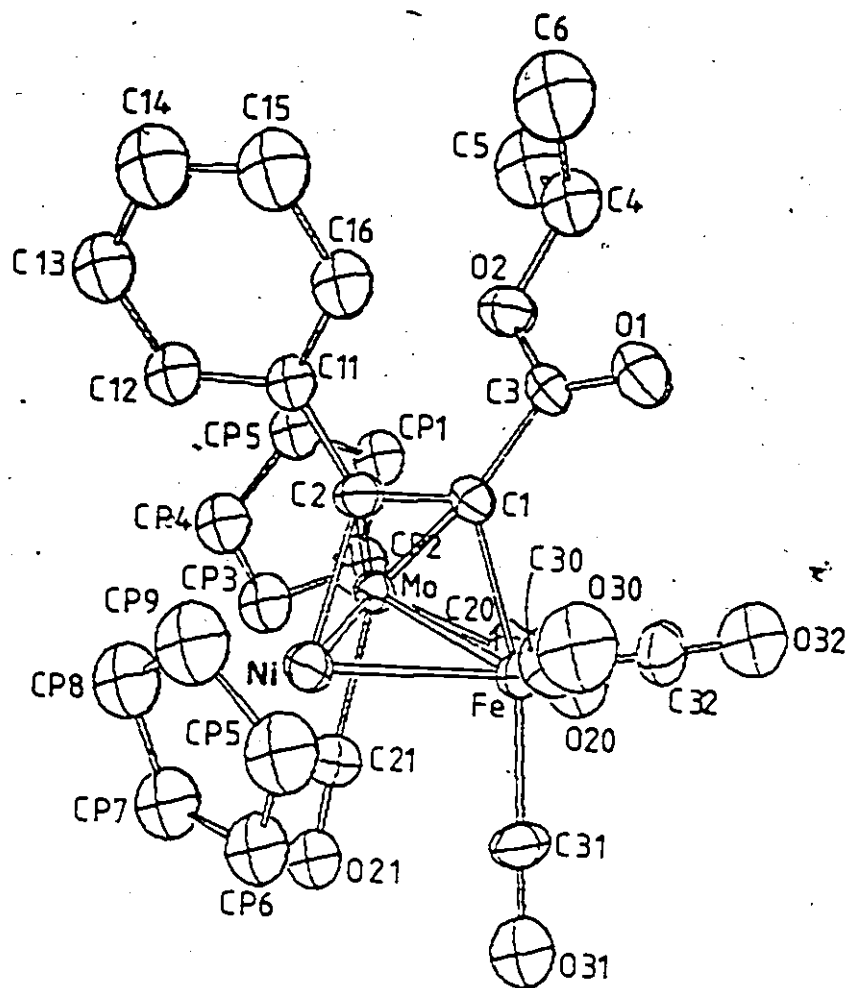


Figure 14:

ORTEP Diagram of $\text{Cp}_2\text{NiMoFe}(\text{CO})_5(\text{PhC}_2\text{CO}_2\text{CMe}_2\text{H})$, 18

has not only lost much of its triple bond character, but is longer than the typical olefinic bond lengths which are of $\sim 1.34\text{\AA}$. The values obtained for the carbon-carbon bond lengths are typical of those obtained in similar alkyne-trimetallic clusters. The reduction of the acetylenic bond is consistent with the alkyne's behaviour as a four-electron donor. In addition, the two substituents on the alkyne are always in a cis arrangement with the carbon containing the phenyl group always σ bonded to a Ni atom. Furthermore, the basal metal-carbon distances are always shorter than the apical metal-carbon distances.

In 16 the three metal atoms form an isosceles triangle ($\text{Ni}(1)\text{-Ni}(2) = 2.442(1)$, $\text{Ni}(1)\text{-Fe} = 2.393(1)$ and $\text{Ni}(2)\text{-Fe} = 2.388(1)\text{\AA}$). This contrasts with that observed in $\text{Cp}_2\text{Ni}_2\text{Fe}(\text{CO})_3(\text{PhC}\equiv\text{CPh})$ where the metal atoms form an equilateral triangle.¹¹⁰ The Ni-Fe bond lengths in this molecule are of the same order of magnitude as those observed in 16, however, the Ni-Ni bond length is somewhat shorter, $2.404(4)\text{\AA}$. For 16, the alkyne lies parallel to the Ni-Ni bond of the metal triangle and with this arrangement each metal atom obeys the E.A.N. rule.

Cluster 17 represents only the second FeCoNi-alkyne cluster to be characterized crystallographically. The alkyne unit lies parallel to the Co-Ni bond of the metal triangle. In the previous study which involved $\text{CpNiCoFe}(\text{CO})_5(\text{Ph}_3\text{P})(\text{PhC}\equiv\text{CPh})$, the alkyne was found to be parallel to the Fe-Ni vector.¹¹¹ With the former orientation, the E.A.N. rule holds for each of the metal atoms. The latter requires a semi-bridging interaction of a carbonyl ligand in order for the E.A.N. rule to be obeyed. The Co-Ni and Co-Fe distances in 17 are $2.442(1)$ and $2.481(1)\text{\AA}$, longer than the corresponding distances in the diphenylacetylene cluster

which were 2.390(4) and 2.467(4) Å respectively. In contrast, the Ni-Fe distances are longer (2.486(4) vs 2.423(1)) in the diphenylacetylene adduct. This could be due to the fact the alkyne is parallel to this vector for $\text{CpNiCoFe}(\text{CO})_5(\text{Ph}_3\text{P})(\text{PhC}\equiv\text{CPh})$. This also is probably responsible for the shorter Co-C bond length of 1.947(6) Å in 17 as compared to 2.04(2) and 2.05(2) Å found in the diphenylacetylene complex.

The crystal structure of 18 shows the alkyne to be parallel to the Fe-Ni vector of the metal triangle. In both 16 and 17, the $\text{Fe}(\text{CO})_3$ unit was found occupying the apex of the square pyramid. In 18 this particular arrangement of the alkyne results in only the Ni atom obeying the E.A.N. rule. The d^8 Fe(0) atom receives six electrons from the three terminal carbonyl groups, viz., one electron from the alkyne, one electron from the Ni atom and one electron from the Mo atom for a total of 17. The d^6 Mo(0) atom receives five electrons from the η^5 -Cp ring, four electrons from the two terminal carbonyl ligands, two electrons from the alkyne, one electron from the Ni atom and one electron from the Fe atom for a total of 19. There are several examples of M_3C_2 clusters in which all of the metal vertices do not obey the E.A.N. rule. They include $\text{Os}_3(\text{CO})_{10}(\text{PhC}\equiv\text{CPh})$,¹¹² $\text{CpNiCoFe}(\text{CO})_5(\text{Ph}_3\text{P})(\text{PhC}\equiv\text{CPh})$,¹¹¹ $\text{RuCo}_2(\text{CO})_9(\text{PhC}\equiv\text{CPh})$,¹¹³ $\text{Cp}_2\text{Ru}_2\text{Ni}(\text{CO})_4(\text{PhC}\equiv\text{CPh})$,¹¹⁴ and $\text{Cp}_3\text{Rh}_3(\text{CO})(\text{PhC}\equiv\text{CPh})$.¹¹⁵ Perhaps even more fascinating is the discovery by two groups independently of the occurrence of both isomers of $\text{Cp}_2\text{W}_2\text{Os}(\text{CO})_7(\text{RC}\equiv\text{CR})$ in the same crystal.^{116,117} This reflects the delicate balance between the isomers possible in M_3C_2 systems. An attempt is made to alleviate the excess electron density on Mo since in 18, a weak semi-bridging interaction between a carbonyl bonded to the molybdenum atom and the iron atom is

observed, (Mo-C(20) = 1.74(2)Å; Fe...C(20) = 2.56(2)Å). The latter distance is much shorter than the sum of the van der Waals radii 3.35Å.¹¹⁸ As indicated earlier, evidence for a semi-bridging carbonyl ligand was observed in the infrared spectrum of 18. In addition, it is possible that the extra signals seen in the cyclopentadienyl region in the ¹H NMR spectrum of 18 can be attributed to the isomer where an Fe(CO)₃ unit occupies the apical position. Comparisons of bond distances in 18 with other trimetallic-alkyne clusters is difficult as no other examples containing a FeMoNi core are known. However, it should be noted that the Fe-Ni distance of 2.504(2)Å is the longest observed in a cluster of this type and the Fe-C(1) distance of 1.95(1)Å is the shortest known.

The relevant bond lengths and bond angles for clusters 16 through 18 are collected in Tables 5 through 7. Crystallographic data for these molecules are found in the appendix.

TABLE 5. Selected Bond Distances (Å) and Angles (deg) for Compound 16.

Ni1 - Ni2	2.442(1)	Ni1-Fe-Ni2	61.4(2)
Ni1 - Fe	2.393(1)	Ni1-Ni2-Fe	59.4(2)
Ni2 - Fe	2.388(1)	Ni2-Ni1-Fe	59.2(2)
Ni1 - C4	1.883(3)	Ni1-C4-C5	108.8(2)
Ni2 - C5	1.906(3)	Ni2-C5-C4	104.3(2)
Fe - C4	2.032(3)	C5-C4-C6	125.3(3)
Fe - C5	2.054(3)	C4-C5-C10	127.0(3)
C4 - C5	1.363(4)		
C4 - C6	1.493(4)		
C5 - C10	1.484(5)		

TABLE 6. Selected Bond Distances (Å) and Angles (deg) for Compound 17.

Co - Ni	2.442(1)	Co - Fe - Ni	59.64(3)
Co - Fe	2.481(1)	Co - Ni - Fe	61.48(3)
Ni - Fe	2.423(1)	Ni - Co - Fe	58.88(3)
Co - C1	1.947(6)	Co - C1 - C2	106.1(4)
Ni - C2	1.890(5)	Ni - C2 - C1	106.2(4)
Fe - C1	2.021(5)	C2 - C1 - C3	125.5(5)
Fe - C2	2.026(5)	C1 - C2 - C21	127.8(5)
C1 - C2	1.376(8)		
C1 - C3	1.488(9)		
C2 - C21	1.485(7)		

TABLE 7. Selected Bond Distances (Å) and Angles (deg) for Compound 18.

Fe - Ni	2.504(2)	Ni - Mo - Fe	55.83(6)
Fe - Mo	2.728(2)	Ni - Fe - Mo	59.82(6)
Ni - Mo	2.616(2)	Fe - Ni - Mo	64.36(6)
Fe - C1	1.95(1)		
Ni - C2	1.92(1)	Fe - C1 - C2	105.3(9)
Mo - C1	2.25(1)	Ni - C2 - C1	108.3(9)
Mo - C2	2.20(1)	C2 - C1 - C3	126(1)
C1 - C2	1.38(2)	C1 - C2 - C11	128(1)
C1 - C3	1.48(3)		
C2 - C11	1.49(2)		

CHAPTER III

FLUXIONALITY STUDIES ON TRIMETALLIC ALKYNE CLUSTERS

3.1 Introduction

Chemists have always been fascinated with molecules that possess more than one thermally accessible structure and which, under certain conditions (especially temperatures) of interest, may pass from one to another of these structures fairly rapidly. This phenomenon is known as fluxionality. It has also been termed stereochemical non-rigidity when the rearrangements can be detected by some chemical or physical means. Molecules whose different configurations are chemically equivalent are considered to be fluxional. These should not be confused with molecules that possess configurations which are chemically non-equivalent. The process by which this class of molecules interconverts configurations is called isomerization or tautomerization, e.g., between keto and enol forms of acetone.

When looking at molecules, one has a tendency to think of static structures, especially in clusters. This is evidenced by the increasing importance of X-ray diffraction as an analytical technique in cluster chemistry. The diffraction methods by which molecular structure is determined are termed instantaneous because the interaction between the molecule and the diffracted wave is shorter than the time required for molecular motions (10^{-18} to 10^{-20} sec). Spectroscopic methods such as IR or UV are slower than diffraction methods (10^{-13} to 10^{-15} sec) but are still faster than molecular interconversions. A spectrum employing

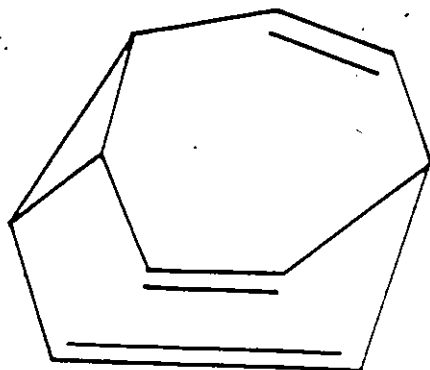
one of these techniques usually is an indication of all molecular configurations present. The most useful spectroscopic method for studying the rearrangements of fluxional molecules is NMR as the time scale of interaction (10^{-1} to 10^{-9} sec) is comparable with the lifetimes of the configurations present.¹¹⁹

The use of variable temperature NMR allows for some degree of control in the rearrangements occurring in a particular molecule. Ideally one would like to freeze a molecule in a particular conformation and then allow it to undergo fluxional behaviour. In most cases this is impossible. Instead one has to settle for slowing down the rearrangements, observing signals for each configuration at low temperature and making them rapid enough at high temperature so an average signal from all the configurations is observed. The rearrangements between configurations have activation energies associated with them. The temperature range of study for NMR spectrometers ranges from -150°C to $+150^{\circ}\text{C}$ allowing for activation energies between 25 and 100 kJ/mole to be measured.

In addition to determining activation barriers for these rearrangements, NMR is useful in distinguishing whether the process is inter- or intramolecular. In intermolecular processes spin-spin coupling is lost. Intramolecular rearrangements can be placed in two classes, mutual or non-mutual exchange. The difference between the two, is that in the latter an intermediate of appreciable concentration exists. It represents a transition state between the two interconverting configurations. By NMR it is possible to distinguish between these classes.¹²⁰

The earliest examples of fluxional molecules were observed in organic chemistry. One of the most remarkable of these is bullvalene,

²¹ whose ¹H NMR spectrum consists of a sharp singlet at 100°C.¹²¹ In inorganic chemistry fluxionality is best illustrated by molecules adopting a trigonal bipyramidal shape. These rearrange via a process known as a Berry pseudo-rotation.¹²² Many examples of fluxional molecules are found in organometallic chemistry, the best known involve cyclic pi systems.¹²³ Logical synthetic routes to clusters and the availability of modern high field NMR spectrometers have made feasible the study of fluxional processes in clusters. In clusters these processes refer to either the movement of ligands bonded to the metal framework of the cluster or a structural reorganization within the metal framework.



21

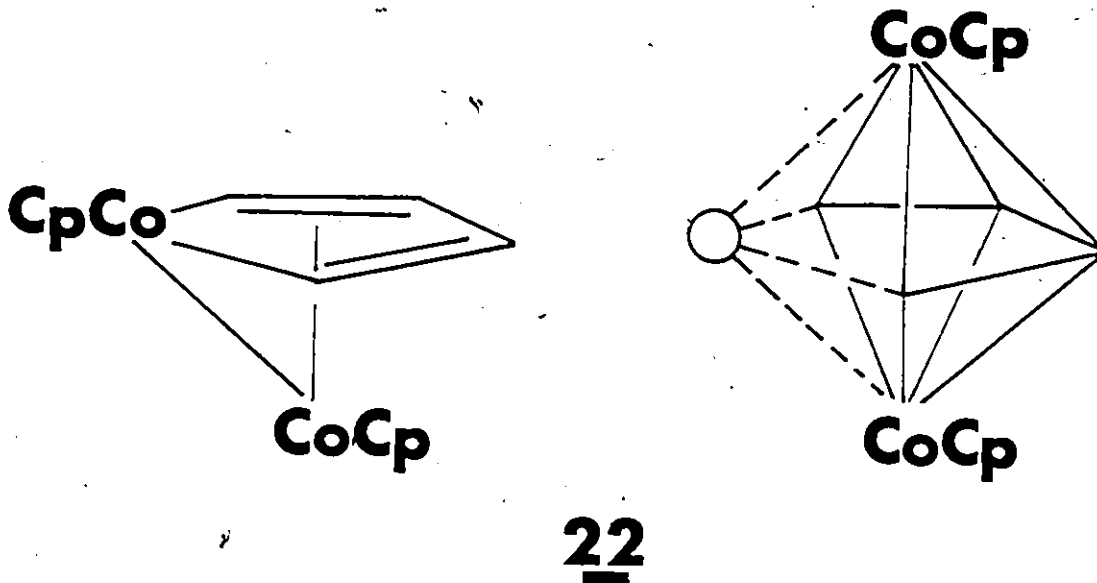
Ligands which are known to migrate include carbonyls, hydrides, isocyanides and certain organic ligands such as polyenes. The most heavily studied has been carbonyl migration in $M_3(CO)_{12}$, $M_4(CO)_{12}$ and

related clusters.¹²⁴⁻¹²⁶ There are two types of carbonyl exchange, localised and delocalised. In the first, ligand rearrangement occurs about one metal atom while the second involves migration from one metal atom to another. The mobility of ligands like carbonyls is believed to be related to their ability to bridge edges and faces of the cluster. Anionic and phosphine substituted clusters have lower energy barriers to carbonyl migrations than their parent clusters. It seems the increased electron density has a tendency to shift carbonyls from terminal to bridging positions making migration easier.

In contrast to the fluxionality of peripheral ligands, the phenomenon of fluxionality of vertices is gradually gaining credence as more examples emerge. One would expect to observe more metal skeletal rearrangements in the future since clusters readily undergo structural changes as the total ligand electron counts change. Also, in some cases metal-metal bonds appear to be weaker than metal-carbonyl bonds. The first example of metal vertex fluxionality was found in $\text{Pt}_9(\text{CO})_{18}^{2-}$. The structure of this molecule consists of three stacked Pt_3 triangles. From the ^{195}Pt NMR studies it is believed that outer metal triangles are rotating with respect to the inner one.¹²² It has been proposed by Johnson that in molecules such as $\text{Fe}_3(\text{CO})_{12}$, the fluxionality can be rationalised in terms of rotation of the metal triangle within a polyhedron of carbonyl groups.¹²⁸ Solid state ^{13}C NMR studies by Hanson give some support to this proposal.¹²⁹ Fluxionality of metal vertices may be involved in the molecule $\text{Rh}_9\text{P}(\text{CO})_{21}^{2-}$,¹⁰ It has been shown by variable temperature ^{103}Rh NMR that the molecule exhibits a 4:4:1 pattern of rhodium environments at low temperature but only a single line at room temper-

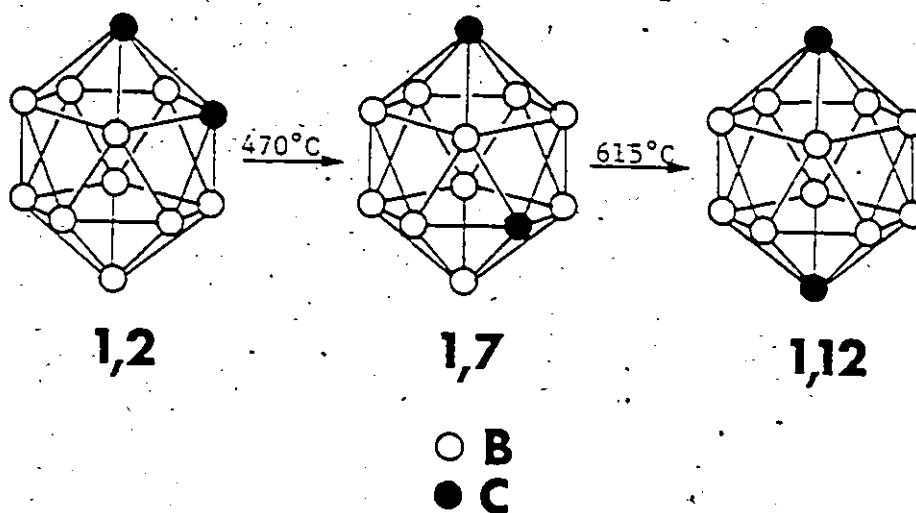
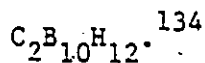
ature.¹³⁰ Very recent studies have demonstrated that interconversion between the capped tetrahedral and butterfly isomers of $\text{HFe}_4(\text{CO})_{13}$ occurs in solution.¹³¹

If one reexamines the fluxional behaviour of certain systems, they can be explained via the fluxionality of vertices. In the molecule $(\text{CpCo}_2)\text{C}_4\text{H}_4$,²² the two CpCo groups are equilibrated at high temperature.¹³² This molecule can be classified as a nido-pentagonal bipyramid (eight skeletal electron pairs); its NMR fluxionality is now readily explicable - perhaps via the alternative nido-structure shown below. Analogous reasoning can be applied to the facile racemisation of Whiting's isostructural ferro-ferradiene.¹³³



Molecules such as $(\text{CpCo})_2\text{C}_4\text{H}_4$ and $\text{Rh}_9\text{P}(\text{CO})_{21}^{2-}$ possess nido structures with a vacant site on the polyhedral surface and thus are expected to be fluxional. On the other hand, rearrangements of closo-

clusters require much higher activation energies than those of nido-clusters. This is exemplified in the icosahedral carborane series,



Geoffroy has shown that a closo-transition metal cluster can rearrange but only on the slow chemical time scale rather than the much faster NMR time scale.⁸⁰ This same behaviour has been exhibited by metalloboranes.¹³⁵

This chapter reports studies on the fluxionality of heterometallic alkyne clusters of the general formula M_3C_2 and shows the mechanism of rearrangement in these systems to be related to that of the analogous C_5H_5^+ cation. To this end, fluxional behaviour previously observed in homometallic M_3C_2 systems is first reviewed.

3.2 Fluxionality in Homometallic M_3C_2 Clusters

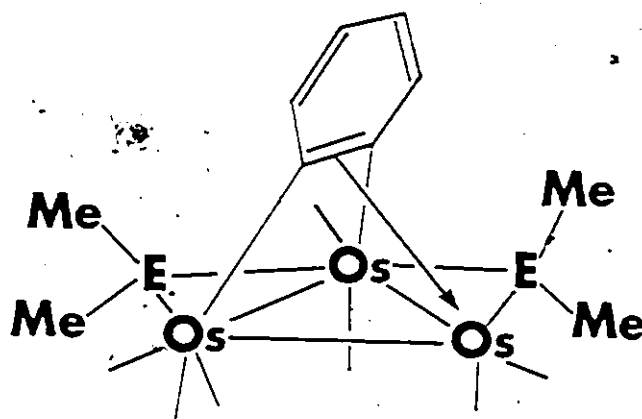
As was seen in Section 2.3, clusters of the formula M_3C_2 which possess 14 skeletal electrons adopt a nido-octahedral geometry. With a vacant site on the polyhedral surface one would expect them to be fluxional. The first reports of NMR fluxionality in molecules of this type were the almost simultaneous publications from the laboratories of Rausch¹³⁶ and Deeming.¹³⁷

Rausch studied the $Cp_3Rh_3(CO)(PhC\equiv CPh)$ system. This was fluxional at room temperature as only one resonance was seen for the cyclopentadienyl protons. Upon cooling to $-88^\circ C$ two signals in a ratio of 2:1 were observed. Enrichment of the cluster with ^{13}CO allowed for observation of the carbonyl resonance by ^{13}C NMR. At room temperature, the resonance appeared as a quartet (i.e., equal coupling to the 3 Rh nuclei) while at $-90^\circ C$, the carbonyl ligand was more strongly coupled to two of the Rh nuclei (triplet) and less strongly coupled to the remaining Rh nucleus (doublet). Rausch's findings were consistent with the X-ray structure of the cluster which showed an unsymmetrical triply bridging configuration for the carbonyl group.¹¹⁵

In order to obtain more details about the rearrangement process, Rausch subsequently employed diphenylacetylene containing a ^{13}C enriched acetylenic carbon.¹³⁸ At room temperature the ^{13}C NMR spectrum revealed the signal due to the enriched acetylene carbon to be a quartet, but at $-87^\circ C$ the signal was an eight line unsymmetrical multiplet. From the dynamic NMR studies the fluxional process proposed was migration of the carbonyl ligand around a quasi-three fold axis on one side of the Rh_3 plane along with concurrent migration of the alkyne about a three fold

axis on the opposite side of the plane.

Deeming observed fluxional behaviour in the complexes $\text{Os}_3(\text{CO})_7(\text{ER}_2)_2(\text{C}_6\text{H}_4)$ where $\text{ER}_2 = \text{PPh}_2, \text{PMe}_2$ or AsMe_2 . These clusters were derived from the reaction of $\text{Os}_3(\text{CO})_{12}$ and EPh_3 or EMe_2Ph at high temperatures. The phenyl group of the arsine or phosphine was found to be transformed into a benzyne ligand bridging the three Os atoms.

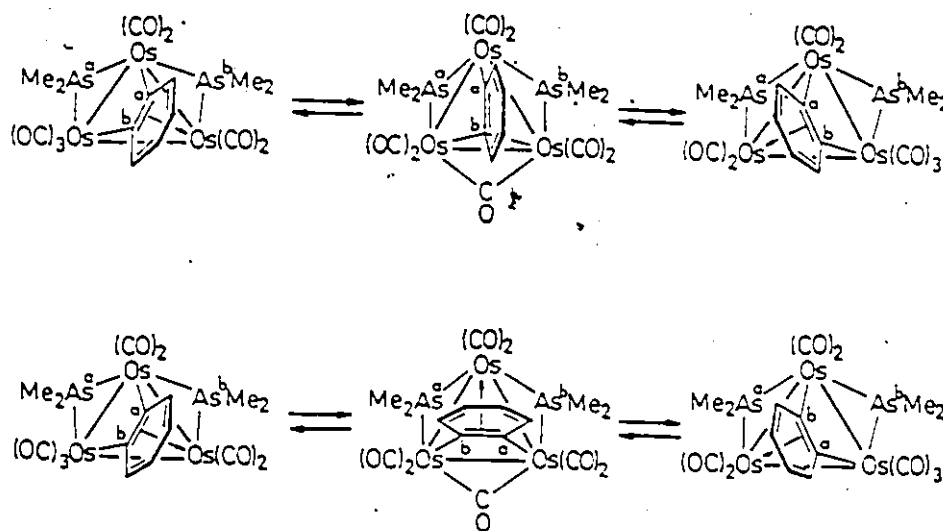


E=As, P

In this study the low temperature ^1H NMR spectrum revealed that the protons of the benzyne exhibited an ABXY pattern while at high temperature an AA'XX' pattern was found. From the structure of the cluster it was expected that four different methyl signals for the 2 EMe_2 groups would be seen. However, only two signals were observed, consistent with equivalent EMe_2 groups but containing non-equivalent methyls on each bridging P or As. In the case PMe_2 groups, the Me group exhibited

triplets in the ^1H NMR spectrum, indicating coupling to two equivalent phosphorus atoms. Attempts to stop the exchange between the two EMe_2 groups proved unsuccessful. The authors suggested the EMe_2 groups might be exchanging at a faster rate than the benzyne protons.

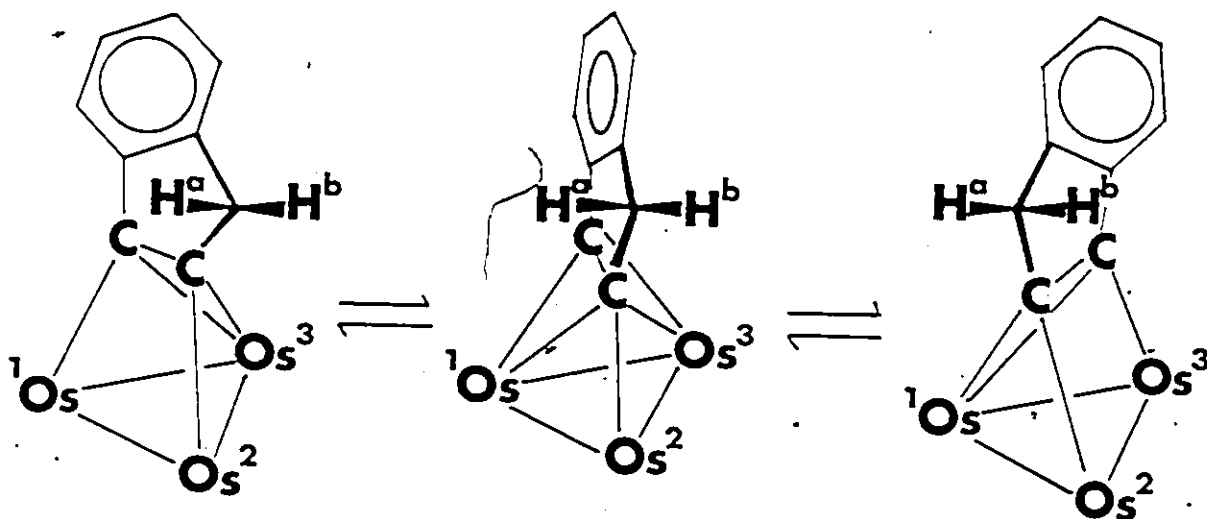
In accord with these observations they proposed the two processes shown below. These both involved rotation of the benzyne moiety relative to the metal triangle. The first allowed for the exchange of the EMe_2 groups without equivalence of the benzyne protons, the second allowed for both. In addition to benzyne rotation the other main feature of the mechanism was carbonyl migration.



Subsequent investigations from Deeming's laboratory confirmed their earlier assumptions.¹³⁹ ^{13}C NMR studies established that carbonyl exchange between the two non-bridged Os atoms did indeed occur. Furthermore, by placing an isopropyl substituent on the benzyne ring, a clearer

understanding of the processes of rearrangement was achieved. In a static configuration the molecule is chiral and a pair of doublets is expected for the diastereotopic methyls of the isopropyl substituent. However, even when the benzyne protons exhibit an ABXY pattern, only a single doublet was observed. They proposed that the process which led to the equilibrations of the EMe_2 groups, also resulted in a time averaged plane of symmetry through the benzyne ring. This leads to only a single doublet being observed.

Deeming's work on $\text{H}_2\text{Os}_3(\text{CO})_9$ (indyne) and related small cycloalkyne complexes also supported his earlier proposals.¹⁴⁰ At low temperatures the methylene hydrogens are different, while at higher temperatures coalescence was observed. This was accounted for by the process indicated below. However, just as in the benzyne case, rotation of the alkyne was not the only mechanism observed, hydride transfer also occurred.



Fluxional processes have also been observed in $H_2Ru_3(CO)_9(C_2R_2)$ where $R = H, Me, Et$ ¹⁴¹ and $HOs_3(CO)_9(SR)(C_6H_4)$ ¹⁴² where $R = Ph, i-Pr$ but only in the former systems was alkyne rotation found to be involved.

3.3 Fluxionality in Heterometallic M_3C_2 Clusters

Initially, the studies of alkyne fluxionality in M_3C_2 clusters were restricted to homometallic systems. The first heterometallic system to be studied was $Cp_2W_2Os(CO)_7(RC\equiv CR)$ where $R = p\text{-tolyl}$, in 1981.¹¹⁶ As was mentioned in Section 2.3, this molecule exists in two isomeric forms. Through dynamic NMR studies, Stone and his co-workers showed each isomer to be chiral thus possessing enantiomers. By monitoring both the proton resonances attributed to the cyclopentadienyl groups bonded to tungsten and the methyl group of the *p*-tolyl substituent, they showed both the isomers and their enantiomers could interconvert. The mechanism proposed to account for this behaviour was a windshield wiper motion of the alkyne about the metal triangle.

The first goal in this study was to observe if the ideas of fluxionality developed for homometallic alkyne clusters could be extended to the heterometallic systems described in Chapter 2. Secondly, it was hoped that finer details of the mechanism of rearrangement could be obtained from the study of these heterometallic clusters. The reason for this was that unlike the homometallic systems previously studied in which alkyne fluxionality was accompanied by carbonyl or hydride migrations, these should not be expected to pose problems in clusters 16 through 18.

To investigate the mechanism of rearrangement in these systems, molecules 16 through 18 were synthesized with several independent probes.

In $\text{Cp}_2\text{Ni}_2\text{Fe}(\text{CO})_3(\text{PhC}\equiv\text{CCO}_2\text{CHMe}_2)$, 16, the molecule was rendered chiral by the use of an unsymmetrical alkyne. This had the secondary effect of making the nickel atoms and their attached cyclopentadienyl ligands non-equivalent. The ^1H NMR spectrum showed this to be true as two resonances of equal intensity were observed in the cyclopentadienyl region. It would have been beneficial to be able to study the rearrangement by observing the metal centre directly rather than sites removed from the metal. In principle, ^{61}Ni NMR is possible but the low natural abundance of the ^{61}Ni isotope (1.19%) made dynamic NMR studies impossible. It was assumed that during the course of the rearrangement process that the cyclopentadienyl ligands did not become detached from their respective nickel atoms. With this caveat it was decided to monitor the ^1H and ^{13}C NMR signals of the rings, so as to obtain information regarding the fluxional process. In addition to the two cyclopentadienyl resonances, the chirality of 16 as a whole is reflected in the diastereotopic nature of the methyl groups in the isopropyl substituent. The 80 MHz ^1H NMR spectrum revealed a pseudo-triplet in the methyl region, but upon going to larger field (250 MHz), the expected pair of doublets was seen.

With these probes it was then possible to test for two different processes. The first involved rotation of the nickel-nickel vector relative to the iron-carbon-carbon triangle. This proposal is not that improbable. Recent data on the fluxional behaviour of the heterometallic complex $\text{MoCoRh}(\mu\text{-CO})_2(\text{CO})_5(\text{C}_5\text{Me}_5)_2$ have been rationalised in terms of rotation of the $\text{CoRh}(\mu\text{-CO})_2(\text{C}_5\text{Me}_5)_2$ fragment about an axis through the Mo and the mid-point of the CoRh vector.¹⁴³ The authors pointed out

that employing the isolobal formalism the dimetal fragment $\text{CoRh}(\mu\text{-CO})_2(\text{C}_5\text{Me}_5)_2$ is analogous to ethylene. Similar arguments could be made for $\underline{16}$, since the CpNi fragment is isolobal with a CH unit, thus making CpNi-CpNi a pseudo-alkyne. The rotation of the nickel-nickel vector would be expected to interconvert the two different cyclopentadienyl environments but would not racemize the molecule, i.e., the diastereotopic character of the isopropyl group would be preserved. In contrast, a formal rotation of the alkyne moiety relative to the metal triangle like that observed in homometallic systems would not only racemize the molecular cluster but would also convert the two CpNi environments. Furthermore, if the alkyne rotation were the only mechanism operating, one would expect the activation energy barriers for the CpNi interconversion and for the methyl coalescence to be identical. The variable temperature ^1H NMR spectra of the cyclopentadienyl and methyl protons of $\underline{16}$ are shown in Figure 15. In order to simplify the spectra of the methyl protons, the CH resonance of the isopropyl group was irradiated, thus instead of a pair of doublets, a pair of singlets is seen at room temperature. The experimental ΔG^\ddagger determined in each case was 63 ± 3 kJ/mole.

There is another possible occurrence which could explain the results obtained from the dynamic ^1H NMR study of $\underline{16}$. It is conceivable that there could have been dissociation of the cluster into non-complexed alkyne and an unsaturated metal triangle (perhaps weakly stabilised by solvent). In Section 2.2 it was pointed out that a major route to homometallic alkyne clusters was displacement of weakly bonded ligands by an alkyne — just the reverse of the proposal above. Such an event would

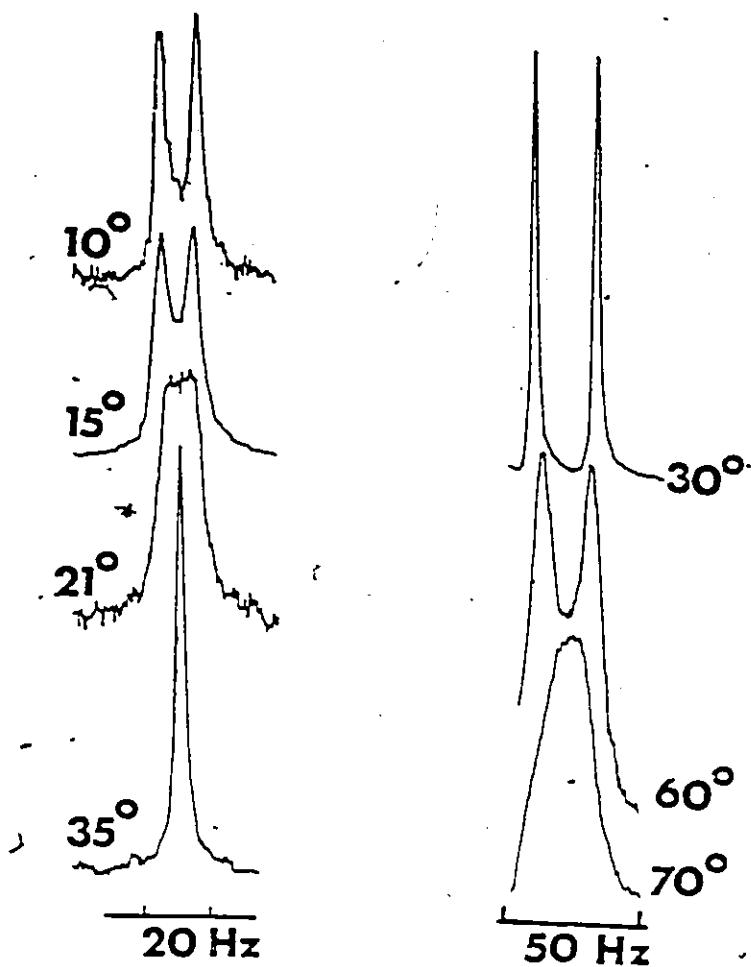
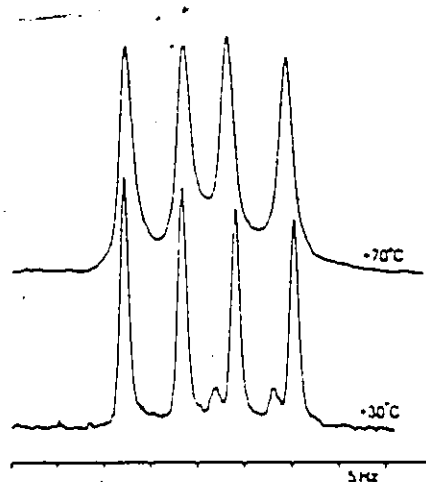


Figure 15:
Experimental 80 MHz and 250 MHz Variable-Temperature ^1H NMR Spectra of
the Cyclopentadienyl and Methyl Regions of $\underline{16}$

simultaneously equilibrate not only the methyls but also the cyclopentadienyl environments. One must therefore, confirm that the process of rearrangement is indeed intramolecular. This experiment was accomplished by carrying out dynamic NMR studies on 17 and 18, in which all three metal atoms are different. As shown in Figure 16 alkyne rotation would not interconvert enantiomers but merely diastereomers. Thus when alkyne rotation is slow on the NMR time scale, each diastereomer should exhibit four peaks in the methyl region - two magnetically non-equivalent methyls, each split into a doublet by the unique isopropyl hydrogen. Now rapid alkyne rotation would equilibrate the diastereomers but cannot interconvert enantiomers without migration of the alkyne from one face of the triangle to the opposite face. This latter process would surely require cluster dissociation.

The low temperature 80 MHz ^1H NMR spectrum of 18 found below showed two sets of four lines (in the ratio of $\sim 6:1$, corresponding to the ratio of the two major diastereomers) but showed just four lines at high temperature indicating that the stereochemical integrity of the cluster was conserved.



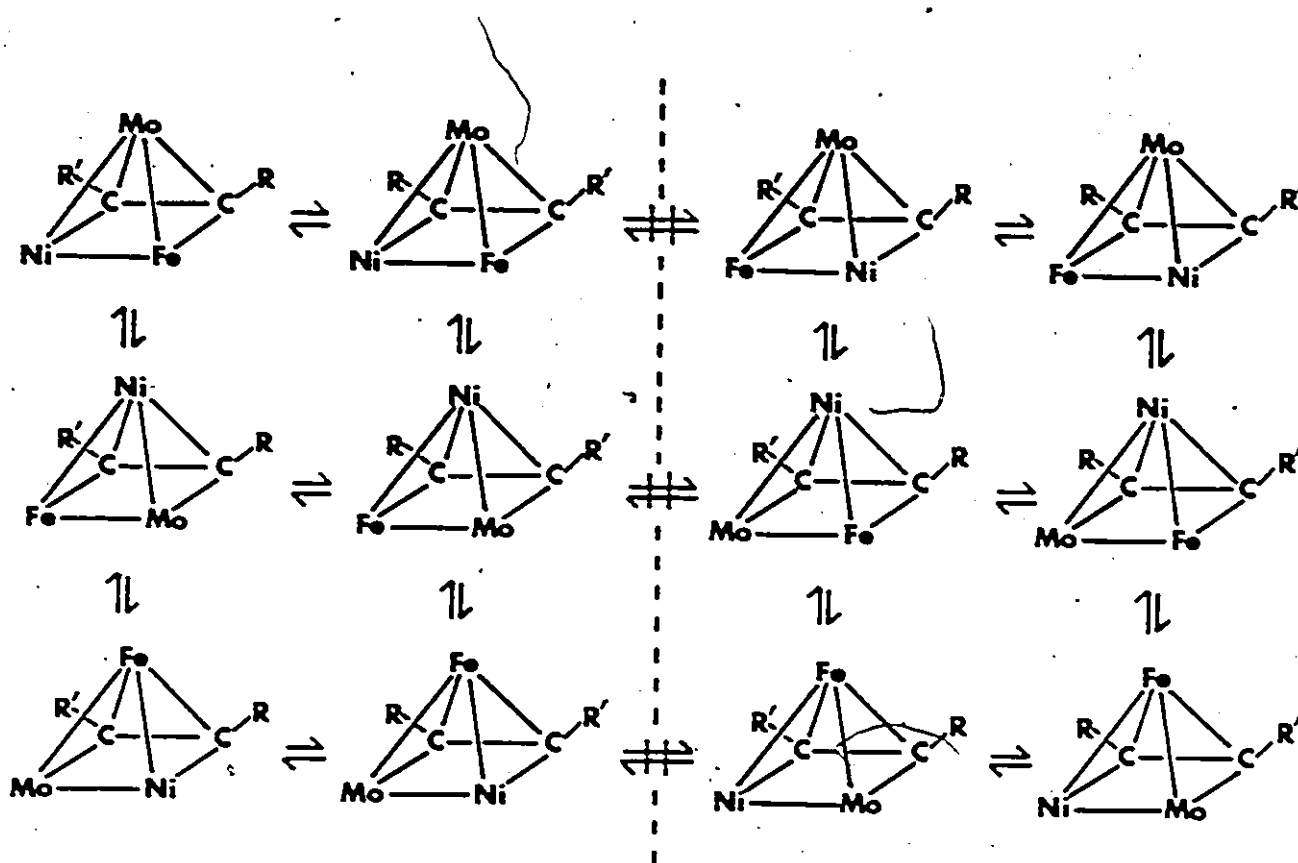


Figure 16:

Acetylene Rotation on One Face of a Cluster Showing Interconversion of Diastereomers but not of Enantiomers

Figure 17 shows the variable-temperature 250 MHz ^1H NMR spectra in the isopropyl methyl region for 18 and the corresponding simulated spectra obtained using the DNMR3 program.¹⁴⁴ Both the 80 MHz and the 250 MHz ^1H NMR spectra of 18 are shown since only in the former case was the rate sufficiently rapid to see complete interconversion of diastereomers. The 250 MHz spectrum exhibited nicely resolved signals but the frequency difference between them was too large to permit coalescence of the peaks. Simulation of the 250 MHz spectrum showed only two equal intensity doublets only when the rate constant exceeded 1000 sec^{-1} , a value corresponding to a temperature inconsistent with maintaining the integrity of the molecule. It is interesting that the only way to obtain a good fit between the experimental and calculated spectra was to invoke exchange between the high field doublet of the minor diastereomer and the low field doublet of the major diastereomer. The experimental ΔG^\ddagger of $69 \pm 4 \text{ kJ/mole}$ for 18 and a value of $67 \pm 3 \text{ kJ/mole}$ found for 17 using similar techniques were close to that obtained for 16. This indicated the same mechanistic pathway is involved in all three molecules.

3.4 Mechanistic Implications

Hoffmann and Schilling have reported a preliminary theoretical analysis of the alkyne rotation process taking $(\text{C}_2\text{H}_2)\text{Fe}_3(\text{CO})_9^{2-}$ as a model compound.¹⁴⁵ Making the assumption of a rigid metal triangle, they calculated the different barriers that a migrating alkyne would have to overcome as it traversed various paths around the metal triangle. Figure 18(a) shows the first of these routes in which the alkyne essentially circumambulates the periphery of the metal triangle, the

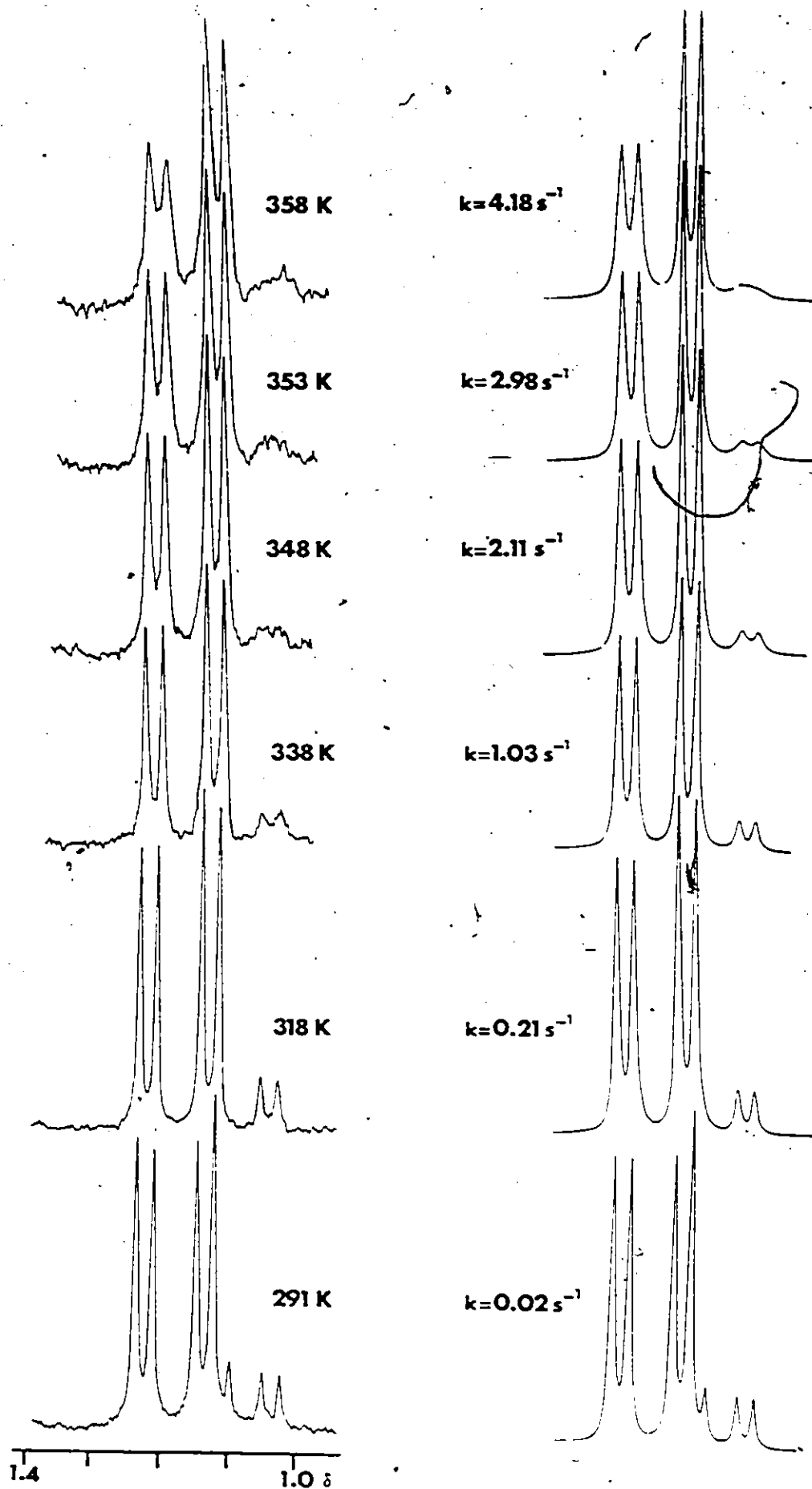


Figure 17:

Experimental and Simulated 250 MHz Variable-Temperature ^1H NMR Spectra of 18

calculated barrier to such a process was 42 kJ/mole. However, such a mechanism would not interconvert the ends of the alkyne, and so if the molecule were chiral because of the asymmetry of the alkyne it would not be racemized. The results obtained from the studies on molecules 16 through 18 as well as Deeming's data¹⁴⁰ on the Os₃-indyne complex militate against such a mechanism.

Hoffmann and Schilling also presented the results of calculations on two other possible pathways of alkyne migration. Both of these allow for racemization but require that the alkyne perform a series of more intricate manoeuvres, one of which is shown in Figure 18(b). These pathways were calculated to have barriers of 38 and 42 kJ/mole respectively. In very naive terms, the alkyne could be visualized as executing a windshield wiper motion across a triangular metal face. Things are not so simple, as in Figure 18 the molecule is viewed in projection. Since the metal triangle defines a plane, the alkyne must also rotate with respect to its own triple bond axis since the substituents are not colinear with the alkyne carbons. This factor must be particularly important for small cycloalkynes where the ring geometry is rigid.¹⁴⁰

It is perhaps useful if the molecules are reduced to their simplest organic analogue, the C₅H₅⁺ system. This has been exhaustively discussed by Stöhrer and Hoffmann.¹⁴⁶ They have pointed out that in the interconversion of the various C_{4v} isomers (which can be recognized as belonging in the nido-B₅H₉ category) the intermediacy of a D_{3h} closo structure is strongly disfavored. Indeed, they proposed the sequence C_{4v} → C_s → C_{2v} → C_s → C_{4v} and in Figure 19 it is shown how this can be

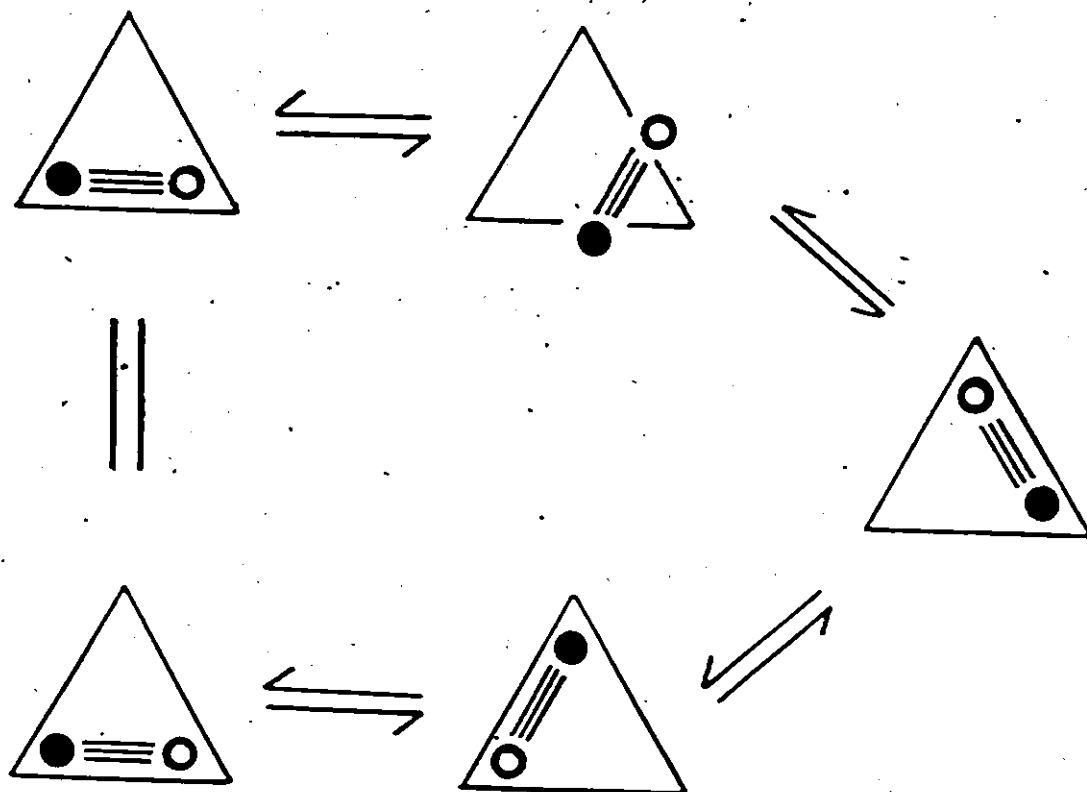


Figure 18 (a):

Migration of an Alkyne about the Molecular Periphery does not Racemise the Cluster

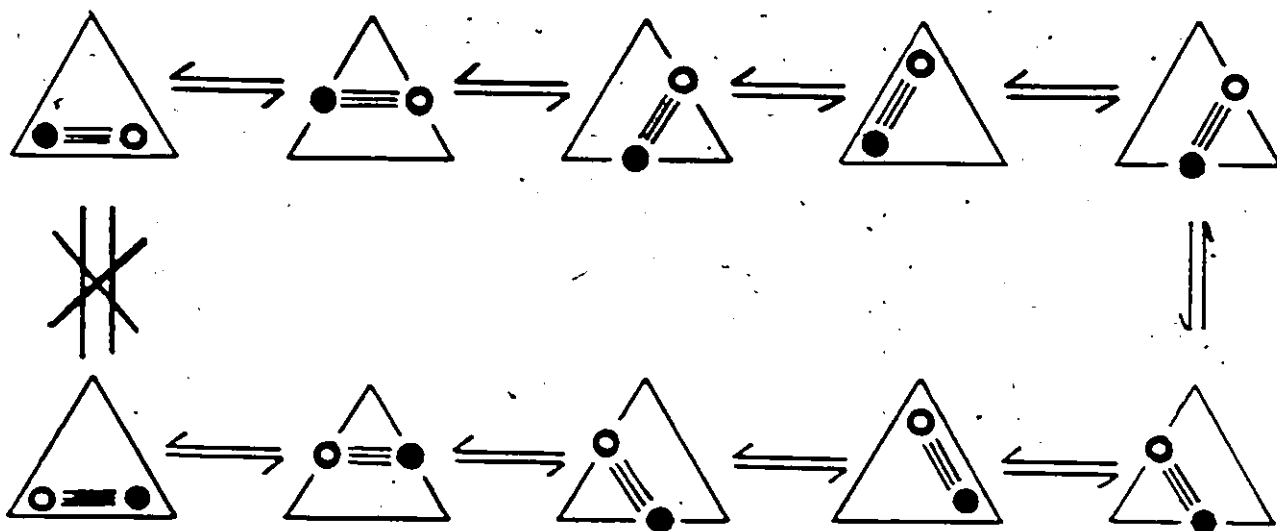


Figure 18 (b):

Windshield wiper motion of an unsymmetrical alkyne leading to racemization of the cluster

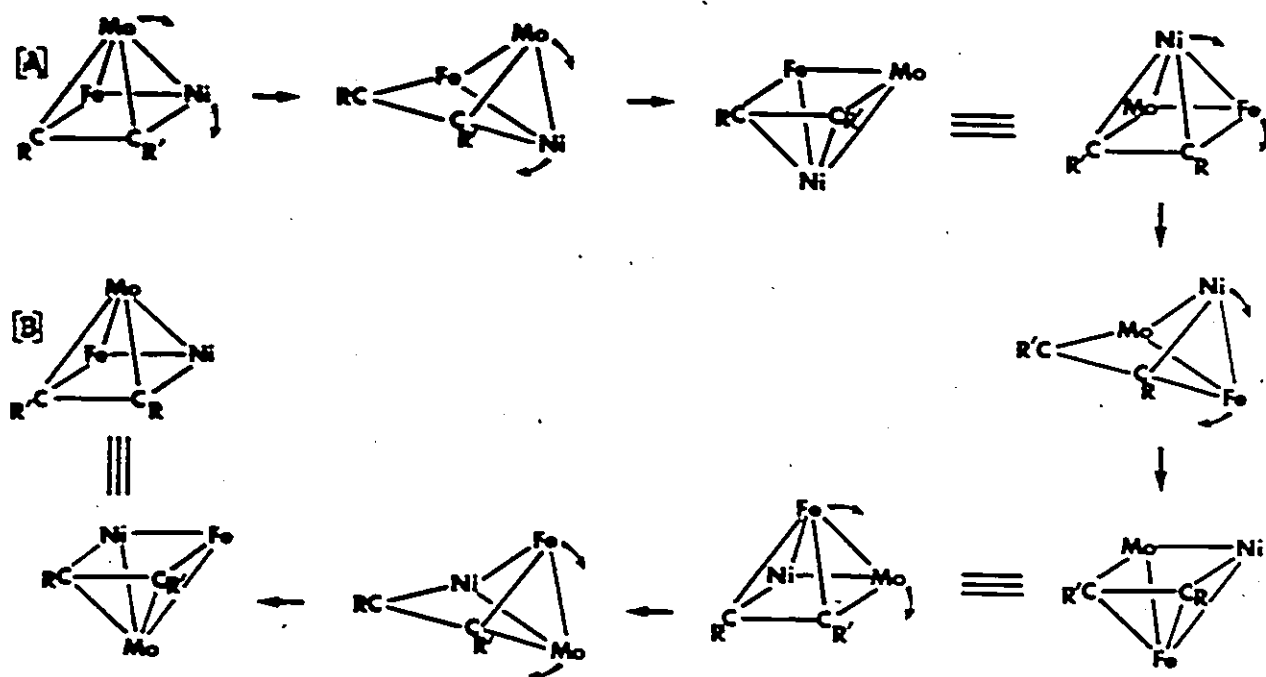


Figure 19:

A Rearrangement Mechanism for the $MM'M''(RC=CR')$ Cluster Analogous to that of the $C_5H_5^+$ System

applied to the M_3C_2 systems. It is clear from Figure 19 that the overall effect of this rearrangement has the same result as does alkyne rotation. Furthermore, the molecules [A] and [B] are seen to be diastereomers rather than enantiomers.

In conclusion the measured barriers to alkyne rotation in heterometallic clusters are very similar to those found in the previously studied homometallic systems (see Table 8). As a result it is a reasonable assumption that the same mechanism of rearrangement is operative in both systems. The theoretically calculated barriers differ from those obtained experimentally in both cases. This may be due to the fact that in the theoretical study the alkyne used as a model was C_2H_2 whereas the experimental studies all employ much larger alkynes.

Table 8 - Comparison of ΔG^\ddagger Values for Alkyne Rotation

Compound	ΔG^\ddagger (kJ/mole)	Reference
$Cp_2Ni_2Fe(CO)_3(PhC\equiv CCO_2CHMe_2)$	63 ± 3	this work
$Cp_2NiMoFe(CO)_5(PhC\equiv CCO_2CHMe_2)$	69 ± 4	this work
$CpNiCoFe(CO)_6(PhC\equiv CCO_2CHMe_2)$	67 ± 3	this work
$Os_3(CO)_7(PMe_2)_2(C_6H_4)$	58.0	137
$Os_3(CO)_7(AsMe_2)_2(C_6H_4)$	51.3	137
$H_2Os_3(CO)_9$ (indyne)	60 ± 2	140
$H_2Os_3(CO)_9$ (cyclooctyne)	67	140
$H_2Ru_3(CO)_9(EtC\equiv CEt)$	52.5	141

CHAPTER IV

SYNTHETIC MANIPULATIONS OF THE $\text{Co}_3(\text{CO})_9\text{CCO}_2\text{CHMe}_2$ CLUSTER

4.1 Introduction

As was mentioned in the first chapter a great deal of effort has been expended in the search for logical high yield routes to mixed metal clusters. It is widely believed that the reactivity of clusters can be fine tuned through the use of different metals; this might allow for behaviour markedly different than that observed in homometallic cluster systems. The most desirable route in the synthesis of mixed metal clusters would involve sequential buildup of clusters from mono- or dinuclear metal fragments.

It is this type of approach that is evident in the pioneering work of Stone's group.^{10,11} They have synthesized numerous tetrahedral clusters composed of three metals and a triply bridging alkylidyne group. These syntheses starting with a metal carbyne synthon have involved successive addition of monometallic fragments leading to a cluster containing three different metal atoms, e.g., $(\text{C}_9\text{H}_7)\text{CpRhWFe}(\text{CO})_5(\mu\text{-CO})-(\mu_3\text{-CR})$.¹⁴⁷ Alternatively, reaction with a dinuclear metal fragment yielded a cluster containing only two different metal species, e.g., $\text{CpWCo}_2(\text{CO})_8(\mu_3\text{-CR})$.¹⁴⁸ Employing these techniques, tetrahedral clusters containing Fe, Mo, Re, Co, Rh, Ni and Pt in addition to W have been synthesized.^{106,149-152}

Until recently it had been very difficult to predict the chemistry of clusters or even rationalise the reactions which they undergo. Many

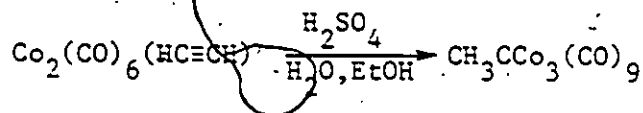
reactions result in cluster breakdown, others cause changes in the structure and/or nuclearity of the cluster. In Stone's work, these problems have been apparently eliminated through the use of the triply bridging alkylidyne moiety. Many studies have shown that in clusters metal ligand bonds are usually much stronger than metal-metal bonds.¹⁵³ Thus, bridging ligands such as the alkylidyne group are important as they allow the cluster to retain its integrity during the course of a reaction. Other atoms or groups such as P, S and NR are also known to bridge metal atoms.⁹

Many examples of homometallic clusters containing a metal triangle bridged by an alkylidyne group exist. There are two basic types: those adopting tetrahedrane and those adopting bicyclobutane core structures. In the former, three metal-metal bonds are found, while in the latter only two are found. The homometallic systems adopting the tetrahedrane geometry include $\text{Co}_3(\text{CO})_9\text{CR}$,¹⁵⁴ $\text{Cp}_3\text{Ni}_3\text{CR}$,^{155,156} $\text{H}_3\text{M}_3(\text{CO})_9\text{CR}$ ($\text{M} = \text{Fe}, \text{Ru}, \text{Os}$)¹⁵⁷⁻¹⁵⁹ and $\text{Cp}_3\text{M}_3(\text{CO})_6\text{CR}$ ($\text{M} = \text{Mo}, \text{W}$).¹⁴⁹ As well as an anionic cluster $\text{Fe}_3(\text{CO})_{10}\text{CH}^-$ ¹⁶⁰ and a cationic system $\text{Cp}_3\text{Rh}_3(\text{CO})_2\text{CH}^+$ ¹⁶¹ are also known. Of all these, the synthesis of the cobalt system seems the most facile.

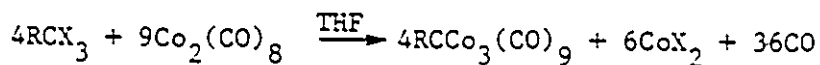
The stability of triangular clusters containing bridging alkylidyne groups offers some interesting possibilities for mixed metal cluster synthesis. It might be possible, with the proper choice of metal fragment, to increase the nuclearity of the parent cluster with minimal structural changes. In addition, one might be able to displace metal fragments on the parent cluster with other metal fragments in a fashion similar to an $\text{S}_{\text{N}}2$ type reaction. Proper choice of the R group might permit one to

monitor the changes the cluster undergoes as the result of these reactions.

The first report on the synthesis of alkylidyne tricobalt nonacarbonyl clusters came in 1958, employing the following method:¹⁶²



This route was restricted to terminal acetylenes only. A more general synthesis utilizing α,α,α -trihalo compounds was developed three years later.¹⁶³ It provided clusters with a wider variety of apical substituents.



The mechanism of reaction in both synthetic routes has yet to be elucidated. In the case of the latter method, speculation has centred on the possible involvement of free radicals. Alternatively, as the final product contains a triply bridging carbyne moiety one could envisage addition of a $\text{Co}_2(\text{CO})_6$ unit across a cobalt carbyne complex, $(\text{CO})_3\text{Co}\equiv\text{CR}$. It is this idea which has been exploited by Stone in his work on mixed metal clusters.

A few review articles covering the study of alkylidyne tricobalt clusters have been published.^{154,164,165} From these studies the general chemical reactivity of the clusters has shown them to be unstable towards attack by oxidizing agents and many bases and nucleophiles. In contrast they have been found stable toward both protonic and Lewis acids. These observations seem to have restricted the investigation into the chemistry of these clusters in that much of the work has been done on the apical carbon substituents. The chemistry of the metal centre has primarily involved the displacement of carbonyl ligands by various Lewis bases such

as phosphines.

In contrast to the studies on the chemistry of the apical carbon substituents, the utility of the alkylidyne tricobalt clusters as precursors in mixed metal cluster synthesis has been relatively unexplored. Vahrenkamp had noted that it was possible to treat the $\text{RCo}_3(\text{CO})_9$ with radicals, $\text{ML}_n(\text{CpCr}(\text{CO})_3, \text{CpMo}(\text{CO})_3, \text{CpW}(\text{CO})_3, \text{CpNi}(\text{CO}))$ generated from the metal dimers, so as to displace a $\text{Co}(\text{CO})_3$ unit and hence incorporate the new moiety in the cluster.¹⁶⁶ In a similar vein, Robinson has synthesized the mixed metal clusters $\text{PhCCo}_2\text{M}(\text{CO})_8\text{Cp}$ ($\text{M} = \text{Cr}, \text{Mo}, \text{W}$) and $\text{PhCCo}_2\text{Fe}(\text{CO})_7\text{Cp}$ employing electron transfer catalysis techniques.¹⁶⁷ The reactions involve attack of a metal carbonylate nucleophile on a cluster radical anion, the latter being generated by addition of a catalytic amount of benzophenone ketyl. Also, treatment of the parent tricobalt cluster with $\text{Fe}(\text{CO})_4^{2-}$ did not yield the hoped-for cluster of higher nuclearity.¹⁶⁸ Instead the major product obtained was $\text{HFeCo}_2(\text{CO})_9\text{CR}$, in which the net result was substitution of a $\text{Co}(\text{CO})_3$ moiety by the $\text{HFe}(\text{CO})_3$ fragment.

This chapter reports a series of synthetic manipulations carried out on the metal fragments of the $\text{Co}_3(\text{CO})_9\text{CR}$ cluster system. These lead to a variety of mixed metal clusters in which replacement or modification of one, two or all three of the original $\text{Co}(\text{CO})_3$ vertices occurs. In addition, some of the resulting tetrahedral clusters have been increased in nuclearity by treatment with appropriate metal fragments. The structure of one of these addition products is presented. Finally, some theoretical arguments are presented to account for the observed experimental results.

4.2 Bis(Cyclopentadienyl)Nickel as a Cluster Reagent

The first step in the investigations of the tricobalt cluster systems involved attempts to displace more than one $\text{Co}(\text{CO})_3$ unit in the parent cluster. In previous studies from other laboratories, this had been achieved only once. Also, all previous examples of metal fragment substitution were carried out on systems where the apical substituent was a stable alkyl or aryl group. It remained to be seen if similar results would be obtained with a more reactive substituent such as the CO_2CHMe_2 group, 23.

The target molecules were $\text{Cp}_2\text{Ni}_2\text{Co}(\text{CO})_3\text{CCO}_2\text{CHMe}_2$ and $\text{Cp}_3\text{Ni}_3\text{CCO}_2\text{CHMe}_2$. Preparations of the trinickel cluster had been previously reported where the apical substituents were PhCH_2 , CMe_3 and SiMe_3 .^{155,156} However, these publications provided no real general route to systems of that type. It was hoped that the synthesis could be achieved via the sequential replacement of $\text{Co}(\text{CO})_3$ units by CpNi moieties. The success of Cp_2Ni in incorporating CpNi fragments into the di- and trimetallic alkyne clusters of Chapter 2, prompted its use rather than $[\text{CpNi}(\text{CO})]_2$ in this work.

At ambient temperature in THF, the treatment of $\text{Co}_3(\text{CO})_9\text{CCO}_2\text{CHMe}_2$ with Cp_2Ni , led to replacement of one $\text{Co}(\text{CO})_3$ unit by CpNi to give 24 in high yield. The only other product obtained from the reaction was $\text{Cp}_2\text{Co}_3(\text{CO})_4\text{CCO}_2\text{CHMe}_2$, 25. However, the yield of 25 was negligible compared to that of 24.

In order to effect multiple substitution, it was clear that more forcing conditions would be required. When an excess of Cp_2Ni was heated under reflux in THF for several hours with the tricobalt cluster, two

major products were isolated.

The first product exhibited a single carbonyl resonance at 1820 cm^{-1} in the infrared, and singlets in the ^1H NMR spectrum at $\delta 4.82(15\text{H})$ and $\delta 9.4(1\text{H})$ in addition to those signals attributed to the isopropyl group. These data, together with the mass spectrometric results allowed its identification as 26 which contains three CpCo moieties, a bridging carbonyl and a hydride. The molecule was, not surprisingly, fluxional and the hydride signal occurred at a similar position to that reported by Geoffroy for the related compound $\text{HFeCo}_2(\text{CO})_9\text{CR}$ where $\text{R} = \text{CH}_3, \text{C}_2\text{H}_5, \text{C}_6\text{H}_5$.¹⁶⁸ The hydride resonance was very broad possibly due to the coupling with the cobalt nuclei which have a quadrupole moment and a nuclear spin of $7/2$. In the structure shown for 26 in Figure 20, the hydride ligand is found in a terminal position so each metal thus satisfies the E.A.N. rule. Previous studies on clusters containing hydrides reveal very few examples of terminal hydride linkages. As a result a more realistic view of the structure of 26 would be one in which the hydride bridges one of the three metal-metal bonds or perhaps even bridges the face of the tetrahedron containing the three metals.

Similarly, the second product showed a bridging carbonyl resonance at 1810 cm^{-1} , two cyclopentadienyl resonances in the ratio of 2:1 but no metal hydride signal. These data, together with the mass spectral fragmentation pattern, are consistent with the formulation as shown in 27 with two CpCo groups and a single CpNi fragment.

The related molecules $\text{Cp}_2\text{Co}_3(\text{CO})_4\text{CCH}_3$ and $(\text{C}_5\text{Me}_5)_2\text{Co}_3(\text{CO})_4\text{CH}_3$ have been prepared by heating the tricobalt cluster under reflux in THF along with C_5H_6 or $\text{C}_5\text{Me}_5\text{H}$ respectively.^{169,170} Structural studies on these two

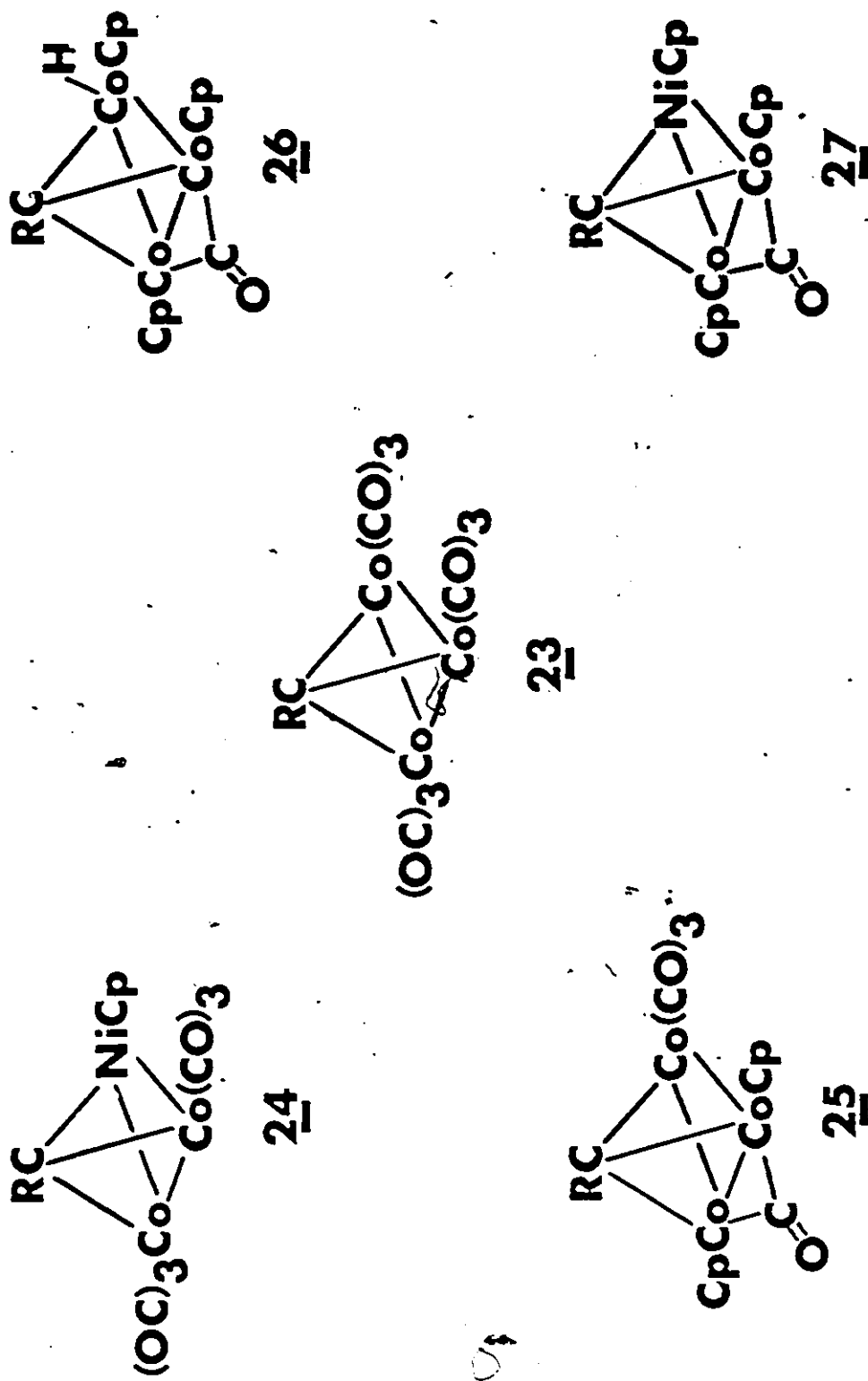


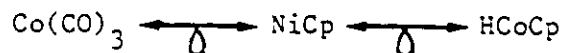
Figure 20:

Clusters Obtained from the Reactions of $\text{Co}_3(\text{CO})_9$, $\text{Co}_2(\text{CMe}_2)_2$ and Cp_2Ni

molecules reveal that both possess a symmetrical bridging carbonyl between the cyclopentadienyl containing Co atoms.

The results obtained from the reaction of $\underline{23}$ with Cp_2Ni demonstrated the propensity of Cp_2Ni to decompose upon thermolysis to release cyclopentadienyl fragments which displace the labile carbonyl ligands on cobalt. This explains the recovery of only small amounts of $\underline{25}$ from the room temperature reaction of Cp_2Ni with $\underline{23}$. Similar behaviour has been observed in the reactions of nickelocene with $\text{Ni}(\text{CO})_4$ and $\text{Fe}(\text{CO})_5$ to produce $\text{Cp}_2\text{Ni}_2(\mu\text{-CO})_2$ and $\text{Cp}_2\text{NiFe}(\text{CO})(\mu\text{-CO})_2$, respectively.^{171,172} The lability of the carbonyls is evident from the reaction of $\underline{23}$ with $\text{Ph}_2\text{PCH}_2\text{CH}_2\text{PPh}_2$ (dppe).¹⁷³ An instantaneous reaction, with noticeable CO evolution, occurs upon dissolving the two compounds in THF, resulting in a quantitative yield of $(\text{dppe})\text{Co}_3(\text{CO})_7\text{CCO}_2\text{CHMe}_2$.

In electron counting terms, the reactions shown in Figure 20 can be explained very simply. Three carbonyls are replaced by one cyclopentadienyl group and a hydrogen, while two cyclopentadienyl groups account for five carbonyl groups. The compounds $\underline{23}$ through $\underline{27}$ provide nice examples of the isolobal relationships;



In conclusion, Cp_2Ni was an excellent reagent for the introduction of a single CpNi fragment under mild conditions, but prolonged heating led to extensive replacement of carbonyl groups by cyclopentadienyl ligands. The complications of employing Cp_2Ni as a reagent in cluster synthesis will also be seen in Section 4.3.

As is evident from the results presented above, the attempt to synthesize a trinickel cluster proved unsuccessful. In the search for a

possible alternate route, the reaction between Cp_2Ni and $\text{Cl}_3\text{CCO}_2\text{CHMe}_2$ was carried out. It was hoped this would proceed in a manner similar to that for the cobalt systems. The proton NMR spectrum of the product isolated showed a single resonance in the cyclopentadienyl region, as well as signals attributed to the isopropyl group. With increased acquisition time these signals began to broaden and eventually all disappeared. Mass spectral evidence while not yielding a parent ion for the expected trinickel cluster did exhibit fragments possessing the correct isotope pattern for three nickels. However, the instability of the product did not allow an unequivocal identification of it as the trinickel cluster.

4.3 Syntheses of Mixed Metal Alkylidyne Clusters

By employing the principles of PSEP, the readily synthesized $\text{RCCo}_3(\text{CO})_9$ clusters possess 12 skeletal electrons. Just as the dimetallic alkyne clusters presented in Chapter 2, the bonding in the tricobalt system may be viewed as either involving six localised bonds along the edges of the tetrahedron or being nido-trigonal bipyramidal molecules using six globally delocalised orbitals. Indeed, as mentioned in Section 2.2, ^{59}Co NQR data⁹⁴ as well as photoelectron spectroscopic results⁹⁵ on the $\text{Co}_3(\text{CO})_9\text{CR}$ systems seem to lend credence to the idea of delocalised bonding.

With the delocalised bonding model, one would expect the behaviour of the $\text{Co}_3(\text{CO})_9\text{CR}$ system to parallel that observed for the analogous dimetallic alkyne complexes. Thus, the tricobalt alkylidyne clusters would be considered to be coordinatively unsaturated (even though conventional electron counting would assign each cobalt 18

electrons). This view would predict high reactivity for the cluster toward electrophiles and might also suggest the possibility of fluxionality of the polyhedral vertices.

In order to investigate the latter two possibilities, a series of mixed metal tetrahedral clusters based on the $\text{Co}_3(\text{CO})_9\text{CR}$ framework were synthesized. Since the consecutive substitution of tricarbonylcobalt moieties by different isolobal fragments would eventually produce a tetrahedral molecule in which the identity of each of the vertices was different, it was recognized that a probe for chirality was essential. Therefore, all syntheses commenced with an alkylidyne tricobalt cluster in which the apical substituent was $\text{R}=\text{CO}_2\text{CHMe}_2$, in order that the potentially diastereotopic methyl groups could be exploited. It was hoped that dynamic NMR studies on a chiral cluster might reveal fluxional behaviour in these systems. In addition, the reactivity of the tetrahedral clusters could be probed by their reactions with $\text{Fe}_2(\text{CO})_9$.

As shown in Figure 21, the replacement of a $\text{Co}(\text{CO})_3$ vertex by either a CpNi unit or a $\text{CpMo}(\text{CO})_2$ fragment, as in 24 or $\text{CpMoCo}_2(\text{CO})_8\text{-CCO}_2\text{CHMe}_2$, 28, respectively proceeded satisfactorily. Indeed, Vahrenkamp had reported similar results but with different substituents on the carbonyl carbon atom.¹⁶⁶ Further reaction of 28 with excess Cp_2Ni gave not only the expected chiral compound $\text{Cp}_2\text{MoNiCo}(\text{CO})_5\text{CCO}_2\text{CHMe}_2$, 29, possessing four different atoms at the polyhedral vertices but also yielded two other compounds, $\text{Cp}_3\text{MoNi}_2(\text{CO})_2\text{CCO}_2\text{CHMe}_2$, 30, and $\text{Cp}_3\text{MoCo}_2(\text{CO})_3\text{CCO}_2\text{CHMe}_2$, 31, from which 29 could not easily be separated chromatographically.

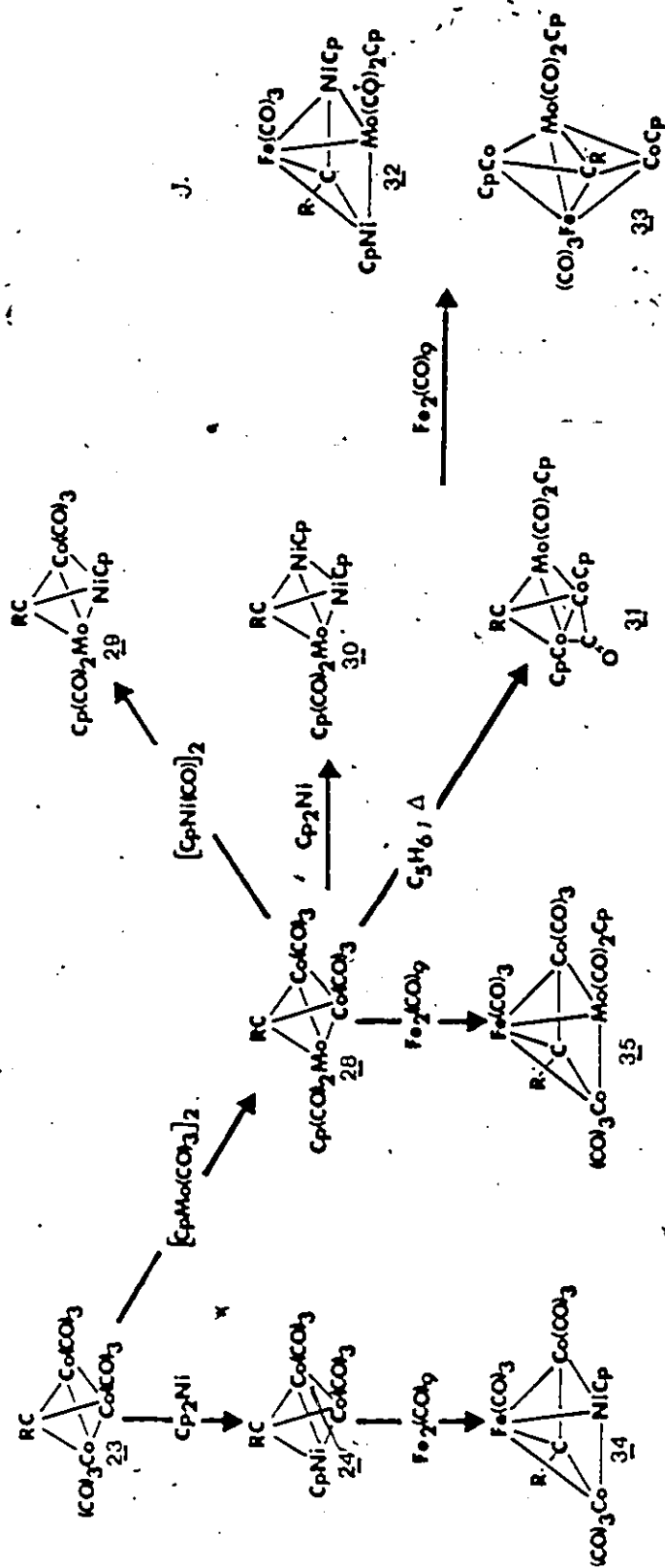


Figure 21:

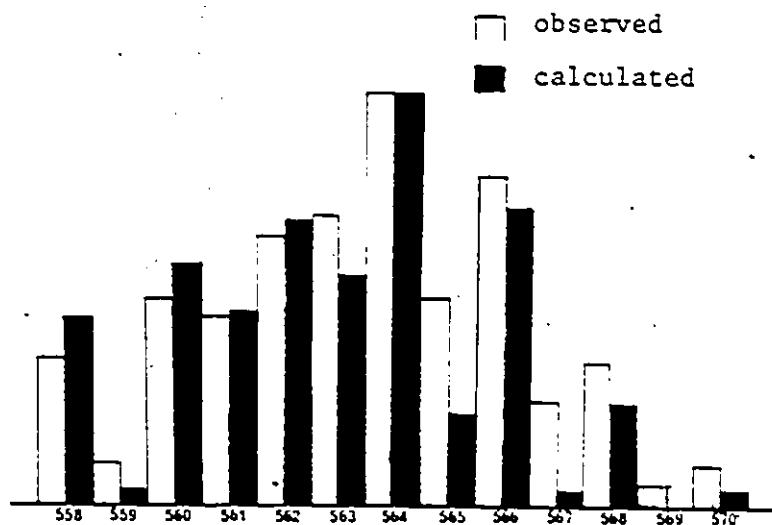
Synthetic Scheme Relating Molecules 23, 24 and 28 through 35

Consequently, this mixture was treated with $\text{Fe}_2(\text{CO})_9$ - a reagent known from the work presented in Chapter 2 on dimetallic alkyne clusters to deliver an $\text{Fe}(\text{CO})_3$ moiety to tetrahedral clusters and bring about expansion to the square based pyramidal geometry. This reaction allowed for the separation of the three cluster species. It was found that only two of the products in the mixture reacted with $\text{Fe}_2(\text{CO})_9$ to yield the five vertex clusters $\text{Cp}_3\text{Ni}_2\text{MoFe}(\text{CO})_5\text{CCO}_2\text{CHMe}_2$, **32**, and $\text{Cp}_3\text{Co}_2\text{MoFe}(\text{CO})_5\text{CCO}_2\text{CHMe}_2$, **33**, leaving the chiral molecule, **29**, unchanged.

The identity of **29** was readily established from mass spectroscopic data. Subsequently, **29** was synthesized independently via the reaction of **28** with $[\text{CpNi}(\text{CO})]_2$. The molecule exhibited two cyclopentadienyl resonances in both the ^1H and ^{13}C NMR spectra. Since the apical carbon was now bonded to three different metal fragments, the isopropyl methyls became diastereotopic and each appeared as a doublet coupled to the unique proton of the isopropyl group. In order to see whether this molecule exhibited similar dynamic behaviour to the related chiral M_2C_2 and M_3C_2 systems of Chapter 2, a variable temperature NMR study was carried out on **29**. It was not possible to coalesce the methyl peaks at 110° . So, if the molecule was fluxional, the barrier was too high for it to be measured by conventional NMR line broadening techniques.

The separation of the products resulting from the treatment of the mixture of **29**, **30** and **31** with $\text{Fe}_2(\text{CO})_9$ not only allowed recovery of the chiral cluster **29** but also yielded two new five vertex clusters, viz., **32** and **33**. The former was isolated in very low yield and was identified mass spectroscopically via its characteristic FeMoNi_2 isotope pattern. Shown below is a comparison of the calculated versus the

observed isotope pattern for $\underline{32}$. This product was clearly derived from an RCMoNi_2 tetrahedral cluster and the incorporation of an $\text{Fe}(\text{CO})_3$ fragment parallels that found in the reaction of $(\text{RC}\equiv\text{CR}')\text{Ni}_2\text{Cp}_2$ with $\text{Fe}_2(\text{CO})_9$ which likewise led to a 14 skeletal electron square-based pyramidal (nido-octahedral) system.



It is interesting to note that the presumed intermediate $\underline{30}$ and the isolated product $\underline{32}$ resulted from replacement of all three of the original tricarbonylcobalt vertices in the starting material. Attempts to synthesize $\underline{30}$ by treatment of $\underline{29}$ with a source of CpNi fragments proved unsuccessful. Only one example of a tetrahedral alkylidyne cluster containing two CpNi units has been reported, $\text{Cp}_3\text{Ni}_2\text{W}(\text{CO})_2\text{CR}$ obtained from the metal carbyne route.¹⁴⁷ It was possible to isolate $\underline{31}$ independently, from the reaction of $\underline{28}$ with an excess of cyclopentadiene in refluxing THF.

This is similar to the approach used to obtain the dicyclopentadienylated derivatives of $\text{Co}_3(\text{CO})_9\text{CMe}$ ^{169,170} and that adopted in the synthesis of $\text{Cp}_3\text{Fe}_3(\text{CO})_3\text{CR}$ from $\text{CpFe}_3(\text{CO})_8\text{CR}$.¹⁷⁴

The results obtained from reacting the mixture of 29 through 31 with $\text{Fe}_2(\text{CO})_9$ prompted further study of its reactivity with other tetrahedral clusters. Probably the most obvious would be the reaction of 23 with $\text{Fe}_2(\text{CO})_9$. However, the reaction only led to decomposition of 23 and no new cluster species was obtained. This result was not surprising as a previous report had indicated the reaction of $(\text{RC}\equiv\text{CR})\text{Co}_2(\text{CO})_6$ complexes with $\text{Fe}_2(\text{CO})_9$ also did not yield any isolable products.⁹⁸ The reaction of $\text{Fe}_2(\text{CO})_9$ with 24 or 28 yielded 34 and 35 respectively. These were identified from mass spectral data. In both cases, there was only one methyl environment in the NMR spectrum suggesting the formation of a molecule with C_s symmetry.

The major product of the reaction of 29, 30 and 31 with di-iron enneacarbonyl was 33. It showed only a single type of methyl signal in the NMR spectrum. This suggested the molecule just like 34 and 35 possessed a plane of symmetry rendering it achiral. Furthermore, it was clear that three cyclopentadienyl groups were present and the chemical shifts indicated that one was bonded to molybdenum while the remaining two were attached to cobalt. The molecular structure of the cluster was determined by X-ray crystallography. Figure 22 shows an ORTEP structure of 33, the relevant bond lengths and bond angles are collected in Table 9. Crystallographic data on 33 may be found in the appendix.

The structure of 33 is best described as a trigonal bipyramidal M_4C cluster in which the metal atoms adopt a butterfly arrangement and the

TABLE 9: Selected Interatomic Distances (Å) and Angles (deg)

Mo-Co(1)	2.620(1)	Mo-Co(2)	2.637(1)	Mo-Fe	2.773(1)
Mo-C(6)	2.091(7)	Co(1)-Fe	2.422(1)	Co(1)-C(6)	1.951(7)
Co(2)-Fe	2.431(1)	Co(2)-C(6)	1.962(7)	Fe-C(6)	2.021(6)
Mo-C(1)	1.967(9)	Mo-C(2)	1.982(9)	Fe-C(3)	1.762(9)
C(1)-O(1)	1.175(9)	C(2)-O(2)	1.16(1)	C(3)-O(3)	1.152(9)
Fe-C(4)	1.787(9)	Fe-C(5)	1.771(9)	C(6)-C(7)	1.500(9)
C(4)-O(4)	1.15(1)	C(5)-O(5)	1.140(9)	C(7)-O(6)	1.198(8)
C(7)-O(7)	1.335(8)	O(7)-C(8)	1.489(9)	C(8)-C(9)	1.53(2)
C(8)-C(10)	1.51(2)	Co(1)-C(11)	2.13(1)	Co(1)-C(12)	2.113(9)
Co(1)-C(13)	2.102(9)	Co(1)-C(14)	2.142(8)	Co(1)-C(15)	2.126(9)
Co(2)-C(21)	2.163(9)	Co(2)-C(22)	2.10(1)	Co(2)-C(23)	2.12(2)
Co(2)-C(24)	2.135(9)	Co(2)-C(25)	2.138(9)	Mo-C(31)	2.320(8)
Mo-C(32)	2.360(7)	Mo-C(33)	2.341(8)	Mo-C(34)	2.322(8)
Mo-C(35)	2.319(8)				
Mo-Co(1)-C(6)	51.9(2)	Fe-Co(1)-C(6)	53.7(2)	Mo-Co(1)-Fe	66.6(1)
Mo-Co(2)-C(6)	51.6(2)	Fe-Co(2)-C(6)	53.5(2)	Mo-Co(2)-Fe	66.2(1)
Co(1)-Mo-Fe	53.3(1)	Co(1)-Mo-C(6)	47.6(2)	Co(1)-Fe-Mo	60.1(1)
Co(2)-Mo-Fe	53.3(1)	Co(2)-Mo-C(6)	47.3(2)	Co(2)-Fe-Mo	60.5(1)
Co(1)-Fe-C(6)	51.4(2)	Co(1)-C(6)-Fe	74.9(2)	Co(1)-C(6)-Mo	84.8(2)
Co(2)-Fe-C(6)	51.3(2)	Co(2)-C(6)-Fe	75.2(2)	Co(2)-C(6)-Mo	81.1(3)
Fe-Mo-C(6)	46.5(2)	Mo-C(6)-Fe	84.8(2)	C(6)-Fe-Mo	48.7(2)
Co(1)-Mo-C(1)	67.0(2)	Co(1)-Mo-C(2)	125.9(3)	Fe-Mo-C(1)	75.5(2)
Co(2)-Mo-C(1)	126.2(3)	Co(2)-Mo-C(2)	65.0(2)	Fe-Mo-C(2)	74.7(3)
C(6)-Mo-C(1)	108.9(3)	Mo-C(1)-O(1)	169.2(7)	C(1)-Mo-C(2)	88.4(3)
C(6)-Mo-C(2)	107.1(3)	Mo-C(2)-O(2)	168.7(8)	Co(1)-C(6)-Co(2)	146.1(4)
Co(1)-Fe-C(3)	79.9(3)	Co(1)-Fe-C(4)	167.7(3)	C(1)-Fe-C(5)	56.3(2)
Co(2)-Fe-C(3)	162.6(3)	Co(2)-Fe-C(4)	95.5(3)	Co(2)-Fe-C(5)	102.0(3)
C(6)-Fe-C(5)	131.1(3)	C(6)-Fe-C(4)	96.2(4)	C(6)-Fe-C(5)	93.8(3)
Mo-Fe-C(3)	106.9(3)	Mo-Fe-C(4)	110.6(3)	Mo-Fe-C(5)	142.3(2)
C(3)-Fe-C(4)	96.2(4)	C(3)-Fe-C(5)	95.1(4)	C(4)-Fe-C(5)	96.5(4)
Fe-C(3)-O(3)	175.4(7)	Fe-C(4)-O(4)	175.0(9)	Fe-C(5)-O(5)	177.0(8)
Co(1)-C(6)-C(7)	80.9(3)	Co(2)-C(6)-C(7)	86.3(3)	Mo-C(6)-C(7)	124.2(3)
C(6)-C(7)-O(6)	124.8(6)	C(6)-C(7)-O(7)	111.2(6)	O(6)-C(7)-O(7)	124.0(6)
C(7)-O(7)-C(8)	116.8(6)	O(7)-C(8)-C(9)	108.4(8)	O(7)-C(8)-C(10)	104.1(8)
C(9)-C(8)-C(10)	111(1)	Fe-C(6)-C(7)	138.6(5)	Co(1)-Fe-Co(2)	101.3(1)
Co(1)-Mo-Co(2)	91.1(1)				

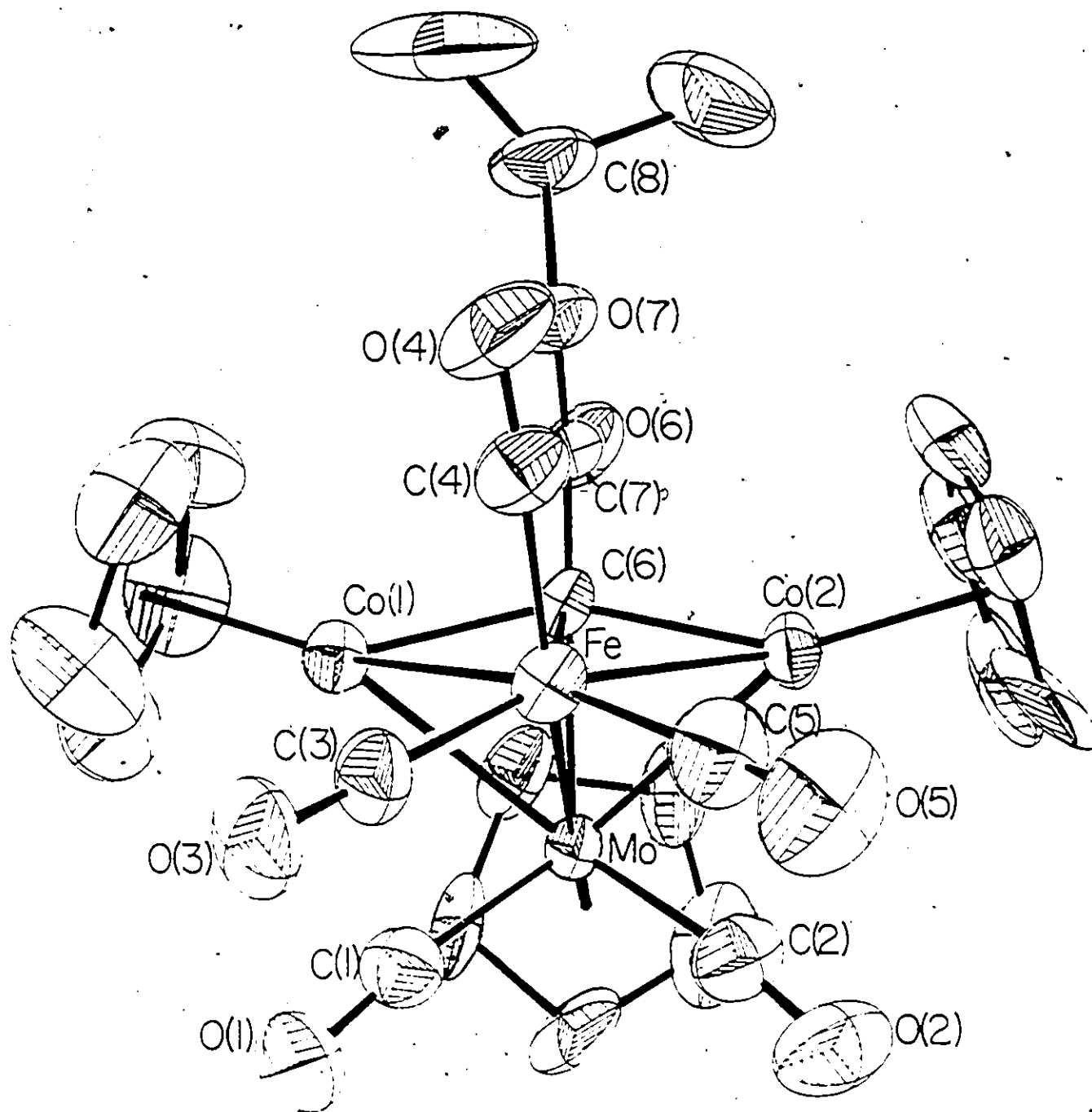


Figure 22:

ORTEP Diagram of $\text{Cp}_3\text{Co}_2\text{MoFe}(\text{CO})_5\text{CCO}_2\text{CMe}_2\text{H}$, $\lambda\lambda$

carbonyl carbon is equatorial. From the structure it can be seen that the CpCo units are found at the wing-tips of the butterfly while the CpMo(CO)₂ and Fe(CO)₃ moieties comprise the hinge. The molecule has approximate C_s symmetry. A formal electron count would assign each of the cobalt atoms 17 electrons while the molybdenum would possess 19. In addition, the alkylidyne carbon could be formally viewed as being 5-coordinate. In the structure it appears that an attempt is made to alleviate the excess electron density on the Mo atom through a weak semi-bridging interaction of each carbonyl on molybdenum with a cobalt atom. This results in Mo-C(1)-O(1) and Mo-C(2)-O(2) angles of 169.2(7) and 168.7(8) respectively. In contrast, all the Fe-C-O angles of the Fe(CO)₃ unit approach linearity. This interaction is also evident from the Co(1)-C(1) and Co(2)-C(2) distances of 2.590(7) and 2.544(7) Å respectively. These are much shorter than the sum of the van der Waals radii (3.25 Å) and 0.2 Å shorter than the Co(1)-C(3) distance of 2.735(7) Å. The weak semi-bridging interaction accounts for weak bands observed at 1840 and 1795 cm⁻¹ in the IR spectrum of 33. Other bond lengths and angles agree well with values found for fragments in similar environments.

4.4 Close Clusters

The synthetic sequence described in Figure 21 represents a rationalized route to mixed-metal M₄CR close clusters. In the only other reported route, a coordinatively unsaturated trimetallic cluster was treated with a metal-carbyne complex to yield an M₄CR close cluster.^{116,175} Prior to these reports the only known close clusters of this type were the Fe₄C systems. These resulted from either the oxidation of an octahedral Fe₆C carbido cluster^{176,177} or synthetic manipulations of

$\text{Fe}_4(\text{CO})_{13}$ ²⁻ 178-180 The route developed in Figure 21 is based on the expansion of a tetrahedral molecule.

The stepwise sequence arriving at $\mathfrak{33}$ can be explained as follows. As previously indicated in Section 4.2, the role of Cp_2Ni in cluster synthesis is two-fold. It can result in substitution of a $\text{Co}(\text{CO})_3$ by an isolobal CpNi fragment as expected. However, upon prolonged thermolysis, it has a tendency to release cyclopentadienyl groups which are capable of displacing the labile carbonyl ligands on cobalt. It was seen in Section 4.2 that treatment of $\mathfrak{23}$ with Cp_2Ni led to cyclopentadienylation at cobalt competitive with replacement of a Co vertex by a CpNi moiety. In order to bring about clean substitution without cyclopentadienylation, it was necessary to employ $[\text{CpNi}(\text{CO})]_2$ as a reagent. As shown in Figure 21, it was possible to prepare the chiral molecule $\mathfrak{29}$ without the by-products $\mathfrak{30}$ and $\mathfrak{31}$. Furthermore, treatment of $\mathfrak{28}$ with cyclopentadiene yielded $\mathfrak{31}$ in which two Cp rings have displaced five carbonyl ligands on the two cobalt atoms, leaving only a single bridging carbonyl functionality between the two. Subsequent reaction of $\mathfrak{31}$ with $\text{Fe}_2(\text{CO})_9$ gave the closo molecule $\mathfrak{33}$. The independent synthesis of $\mathfrak{33}$ in this manner is reminiscent of the approach adopted by Aimè and Osella.¹⁸¹ They found when nido- $\text{HRu}_3(\text{CO})_9\text{C}_5\text{H}_7$ was treated with $[\text{CpNi}(\text{CO})]_2$, the net result was the incorporation of CpNi (a three electron unit) while CO and H were eliminated to yield the closo- $\text{CpNiRu}_3(\text{CO})_8\text{C}_5\text{H}_7$.

There are very few five vertex closo clusters known and molecule $\mathfrak{33}$ is only the third such heterometallic M_4C system known. The other known examples are $\text{CpOs}_3\text{W}(\text{CO})_{11}\text{CR}$ ¹¹⁶ and $\text{CpWRu}_2\text{Co}(\text{CO})_{10}\text{CR}$,¹⁷⁵ where in both cases the R group is a para-tolyl substituent. In both these clusters

a tetrahedral arrangement of the metal atoms with the alkylidyne group capping one of the triangular faces is observed. The most common examples of clusters adopting a closo- M_4C geometry involve the homometallic Fe system. Molecules such as $HFe_4(CO)_{12}CCH_3$,¹⁸² the related anion $Fe_4(CO)_{12}CCH_3^-$ ¹⁸³ and $Fe_4(CO)_{12}COCH_3^-$ ^{178,180} have all been found to exhibit the same geometry as the Os_3WCR and WRu_2CoCR systems. The methoxy- Fe_4 anionic cluster is derived by methylation of $Fe_4(CO)_{13}^{2-}$ which possesses a carbonyl triply bridging a triangular face. In $\mathcal{33}$ a butterfly arrangement of metal atoms with the alkylidyne moiety in an equatorial position of the trigonal bipyramid was found. This structure is remarkably similar to that found by Bradley for $Fe_4(CO)_{12}CCO_2CH_3^-$,¹⁷⁶ the comparison of the two metal frameworks is shown in Figure 23. The most notable feature of the two structures is the $Co_{ax}-C-Co_{ax}$ angle in $\mathcal{33}$ is 146° , while the corresponding Fe-C-Fe angle in $Fe_4(CO)_{12}CCO_2CH_3^-$ is 148° . Two other clusters which adopt a butterfly arrangement of metals show similar angles to the values observed above. In $H CpRu_3Ni(CO)_9^-$ ($\mu_4-C=CHR$)¹⁸⁴ and $CpFeCo_3(\mu-CO)_2(CO)_7(\mu_4-C=CH_2)$ ¹⁷⁴ the Ru-C-Ni and Fe-C-Co angles are 153° and 155° respectively. However, in both these complexes, the μ_4 -carbon is not carbonyl but is part of a vinylidene group.

In terms of the isolobal analogy, $\mathcal{33}$ and the $Fe_4(CO)_{12}CCO_2CH_3^-$ can be related. The axial $Fe(CO)_3$ fragments have been replaced by isolobal CpCo units; one equatorial $Fe(CO)_3$ moiety (which furnishes three frontier orbitals and two electrons to the cluster) has been replaced by a three electron vertex, i.e., $CpMo(CO)_2$. The overall polyhedral electron counts for the two clusters are identical (62 electrons) since the $MoFeCo_2CR$ system is neutral while Bradley's Fe_4CR molecule is

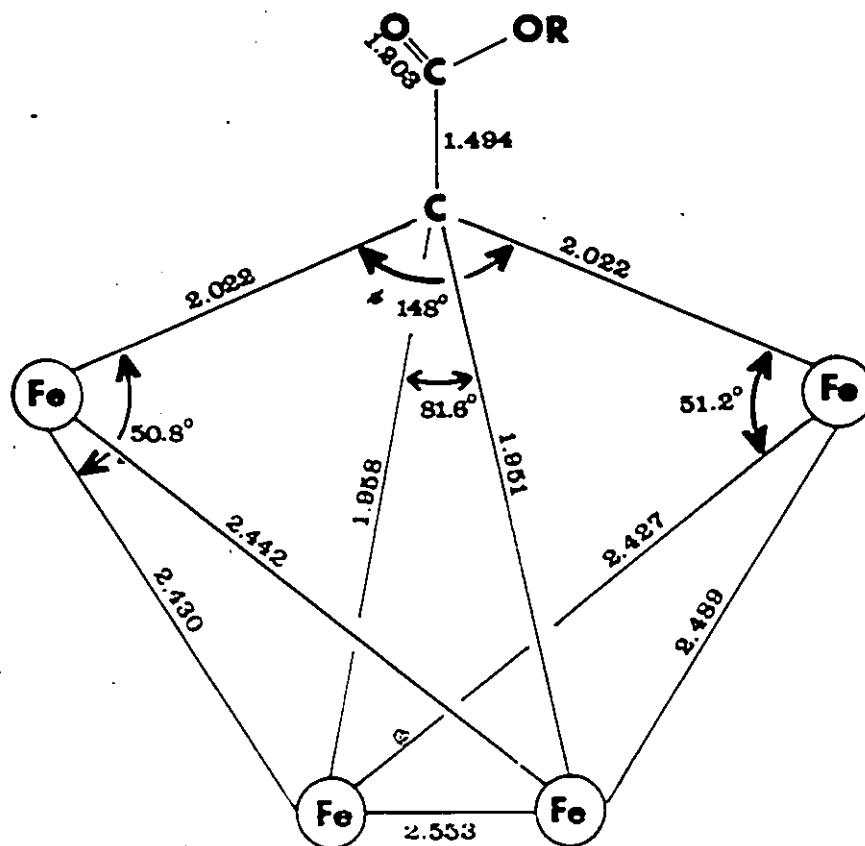
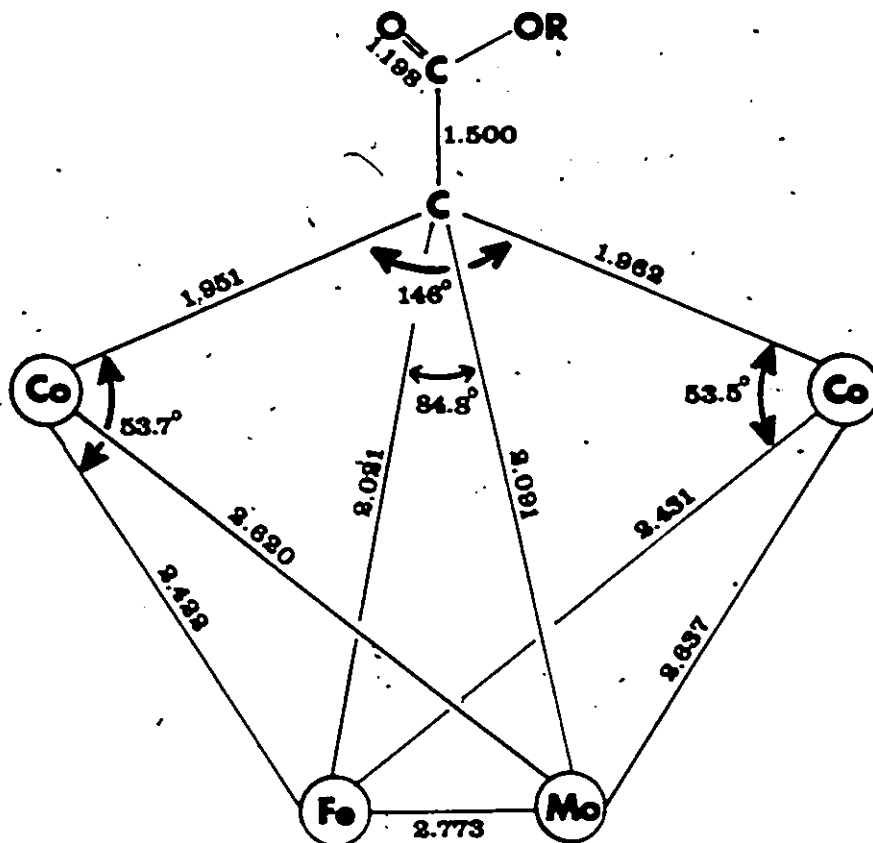


Figure 23:

Comparison of Core Geometries of $\text{Cp}_3\text{Co}_2\text{MoFe}(\text{CO})_5\text{CCO}_2\text{CMe}_2\text{H}$, 33 and $\text{Fe}_4(\text{CO})_{12}\text{CCO}_2\text{CH}_3^-$

anionic. Employing PSEP, the Bradley cluster and also the MoFeCo_2CR molecule, $\mathfrak{33}$, would be viewed as closo trigonal bipyramids since they each possess six skeletal electron pairs. In $\mathfrak{33}$ the two CpCo units and the $\text{Fe}(\text{CO})_3$ each contribute two skeletal electrons each, the remaining six are contributed by the $\text{CpMo}(\text{CO})_2$ unit and the alkylidyne group.

Two other iron systems $\text{HFe}_4(\text{CO})_{12}\text{CH}^{185}$ and $\text{HFe}_4(\text{CO})_{12}\text{COCH}_3^{179,180}$ also show the butterfly structure, however, the angles between the axial Fe's and the equatorial C are considerably larger, i.e., 170.5° and 160.9° , respectively. These latter molecules can be assigned seven skeletal electron pairs and as a result be considered arachno-octahedra. Neutron and X-ray diffraction studies on these molecules have shown that the electron pair associated with the exo-skeletal bond on the carbon atom interacts with the metal skeleton thus providing an extra pair of skeletal electrons. This is similar to that found in butterfly carbide clusters, in which all four electrons associated with the carbon atom participate in cluster bonding and the wingtip-carbon-wingtip angle approaches linearity.¹⁷⁷ Indeed, one can observe the transition from carbide to alkylidyne bonding in these systems by increasing the electron withdrawing power of the exo-skeletal substituent. The measure of this transition being the wing-tip-carbon-wing-tip angle. Thus in terms of the angle, the progression is $\text{Fe}_4(\text{CO})_{12}\text{C}^{2-} > \text{HFe}_4(\text{CO})_{12}\text{CH} > \text{HFe}_4(\text{CO})_{12}\text{COCH}_3 > \text{Fe}_4(\text{CO})_{12}\text{CCO}_2\text{CH}_3^-$ and $\mathfrak{33}$.

It is particularly interesting to note that in the molecules $\text{HFe}_4(\text{CO})_{12}\text{CCH}_3$, the corresponding anion $\text{Fe}_4(\text{CO})_{12}\text{CCH}_3^-$ and $\text{Fe}_4(\text{CO})_{12}\text{COCH}_3^-$, the alkylidyne group is axial while in $\text{Fe}_4(\text{CO})_{12}\text{CCO}_2\text{CH}_3^-$, $\text{HFe}_4(\text{CO})_{12}\text{COCH}_3$, $\text{HFe}_4(\text{CO})_{12}\text{CH}$ and $\mathfrak{33}$ the alkylidyne fragment is located in an equatorial

position. In one regard the difference may be electronic since the axial carbyne bears an electron donating methyl while with an electron withdrawing ester substituent it is found in an equatorial site.

These effects are very subtle since although the methoxy anion is a capped tetrahedron, the corresponding neutral cluster adopts the butterfly configuration. Very recent studies have demonstrated that interconversion between the capped tetrahedral and butterfly isomers of the clusters $\text{HFe}_4(\text{CO})_{13}^-$, $\text{Fe}_4(\text{AuPEt}_3)(\text{CO})_{13}^-$ and $\text{Fe}_4(\text{CuPEt}_3)(\text{CO})_{13}^-$ occurs in solution.^{131,186}

The scheme presented in Figure 21 and work by others has indicated that a simple and straightforward method of synthesizing heteronuclear clusters is by the substitution of one vertex by another. As with other cluster reactions very little mechanistic information is known about these substitution reactions, in which three bonds are broken and then reformed. The only detail which is evident is that the substituting and substituted vertices are isolobal. One could speculate that the initial attack of the incoming metal fragment on the tetrahedral alkylidyne cluster produces a transient five vertex cluster. From the M.O. diagram shown in Figure 24, it can be seen that for the five vertex intermediate at least one electron is found in an orbital of antibonding character with respect to the cluster. The instability which this produces in the cluster results in subsequent elimination of one of the original vertices, generating the final product. Elimination of one of the original vertices rather than the attacking species probably occurs because the homonuclear bonds are weaker than the heteronuclear ones. This proposed addition-elimination

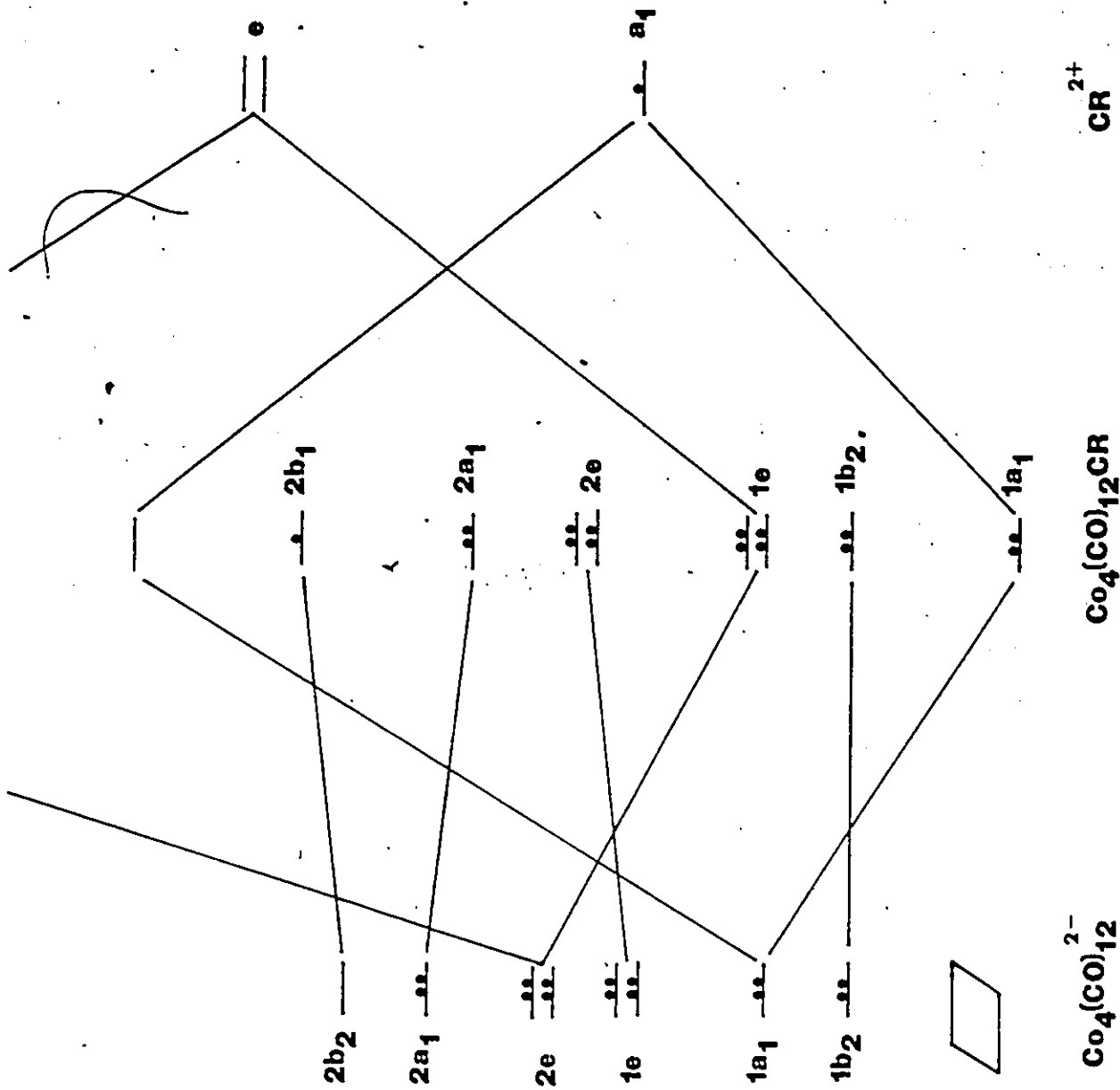
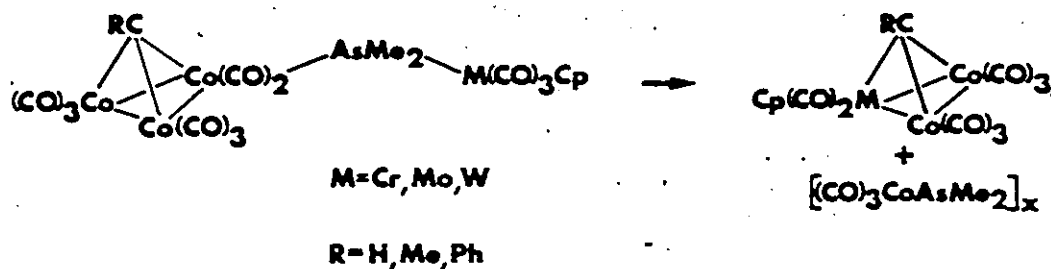


Figure 24:

Qualitative Molecular Orbital Diagram Rationalising Substitution Reactions on Tetrahedral Clusters

mechanism is reminiscent of Vahrenkamp's earlier mixed metal cluster syntheses.¹⁸⁷ These apparently involved attack upon an open face of the metal polyhedron by a pendant metal centre linked to the "leaving group" via a dimethylarsino bridge, as shown below.



In the case of the substituting fragments, CpNi or $\text{CpMo}(\text{CO})_2$ are isolobal with $\text{Co}(\text{CO})_3$ and with CH and bear three electrons in their frontier orbitals. This contrasts the $\text{Fe}(\text{CO})_3$ moiety which furnishes only two electrons to the total involved in skeletal bonding. Therefore, addition of an $\text{Fe}(\text{CO})_3$ fragment would not populate any antibonding orbitals. By invoking the analogy between boranes and metal clusters, it could be said that addition of a vertex with an

extra pair of electrons brings about the change from a tetrahedron (nido-trigonal bipyramid) to the 14 electron square-based pyramid (nido-octahedron). The generality of this reaction is shown by the addition of $\text{Fe}(\text{CO})_3$ to either $\underline{24}$ or $\underline{25}$ giving $\underline{34}$ and $\underline{35}$, respectively. Perhaps the addition of $\text{Fe}(\text{CO})_3$ to $\underline{31}$ initially results in a square pyramidal intermediate which then loses a carbonyl to generate $\underline{33}$. Since NMR evidence indicated that both $\underline{34}$ and $\underline{35}$ possessed C_s symmetry, it could be assumed that such is also the case for the proposed square pyramidal intermediate. This would require the carbonyl bridging the two cobalts effectively to bridge the open face of the square pyramidal cluster. Such an arrangement for a carbonyl ligand is not known and this factor may facilitate loss of the carbonyl leading to $\underline{33}$.

A number of factors still need to be understood in these reactions. All of them have involved replacement of $\text{Co}(\text{CO})_3$ vertices. As reactions have not been attempted with other homometallic alkylidyne systems, it remains to be seen whether other good "leaving groups" can be found. It is also interesting to note that replacement of two cobalt vertices by CpNi (albeit in low yield) occurred when the $\text{CpMo}(\text{CO})_2$ unit was present. However, attempts to synthesize $(\text{CpNi})_2\text{Co}(\text{CO})_3\text{CR}$ from the parent tricobalt cluster failed.

4.5 The Isolobal Nature of CpRh and $\text{Fe}(\text{CO})_3$ Fragments

The addition of an $\text{Fe}(\text{CO})_3$ moiety via the reaction of $\text{Fe}_2(\text{CO})_9$ with various tetrahedral clusters provided a logical and simple route to clusters of increased nuclearity. However, it was not known if this reaction was unique to $\text{Fe}(\text{CO})_3$ or whether it could be extended to include other metal fragments containing two electrons in their frontier

orbitals. In Section 1.4, it had been noted that the fragments BH, $\text{Fe}(\text{CO})_3$ and CpCo were all isolobal. This analogy has been successfully exploited by many workers in the synthesis of metalloboranes. Thus, Group IX metal cyclopentadienyl fragments might behave in a similar manner to the $\text{Fe}(\text{CO})_3$ fragment. The cyclopentadienyl metal units have the advantage of providing another probe by which to study the reaction course. Namely, ^1H and ^{13}C NMR of the cyclopentadienyl ligand bound to the metal. However, the use of CpCo units is not particularly advantageous. First, as the starting point of the cluster syntheses is a tricobalt cluster, addition of another cobalt moiety does not really change the identity of the cluster greatly. Second, as was described earlier in this chapter many of the synthesized tetrahedral clusters already possess CpCo moieties. The fragment chosen to initially probe the generality of the $\text{Fe}(\text{CO})_3$ behaviour was $\text{C}_5\text{Me}_5\text{Rh}$, generated from $\text{C}_5\text{Me}_5\text{Rh}(\text{CO})_2$.¹⁸⁸ Rh allowed for incorporation of a metal not found in the tetrahedral precursors, and also provided a metal atom vertex with a spin quantum number $I = \frac{1}{2}$. This enhanced the possibility of inferring changes in molecular geometry through the use of multinuclear NMR. A substituted cyclopentadienyl group was employed so as not to further complicate the cyclopentadienyl regions in the ^1H and ^{13}C NMR spectra; furthermore, the bulky cyclopentadienyl units would increase the solubility of the resultant products.

The first reaction attempted was that of $\text{C}_5\text{Me}_5\text{Rh}(\text{CO})_2$ with C_2H_4 . It was carried out in cyclohexane so as to prevent the possible coordination of solvent molecules to the Rh centre. The ^1H NMR

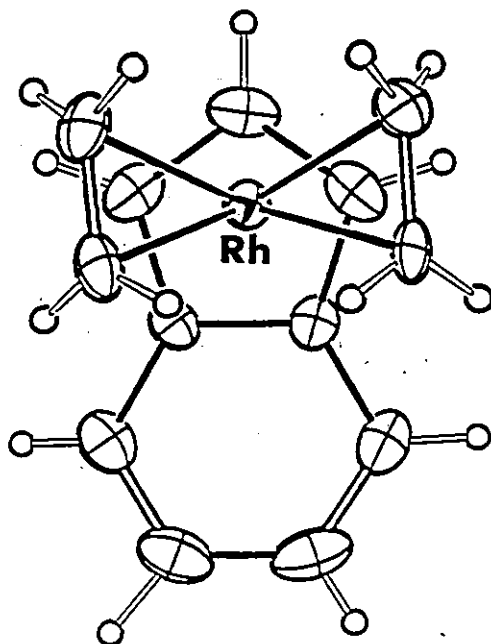
spectrum of the major product $\underline{36}$ exhibited singlets at $\delta 4.80$ and $\delta 1.83$ respectively, in addition to the resonances attributed to the ester isopropyl group. The singlets were assigned to NiCp and RhC₅Me₅ units respectively and integration showed them to be in the ratio of 1:3. Also, both the cyclopentadienyl and isopropyl methyl resonances were found to be in different positions compared to in $\underline{24}$, the former had moved upfield while the latter had shifted downfield. From the infrared spectrum it was found that $\underline{36}$ exhibited a band at 1795 cm^{-1} , possibly due to a bridging carbonyl. ¹³C NMR studies on $\underline{36}$ surprisingly did not change in the same manner as did the proton spectrum. The extremely low yields of $\underline{36}$ and its subsequent decomposition during the NMR studies prevented a mass spectroscopic investigation on it.

Perhaps the most interesting product obtained was $\underline{37}$, from the reaction of $\underline{28}$ with C₅Me₅Rh(CO)₂. The ¹H and ¹³C NMR spectra both gave two resonances in both the cyclopentadienyl and pentamethylcyclopentadienyl regions. In the ¹H NMR they were found at 5.28, 5.15, 1.82 and 1.81 respectively and do not correspond to values attributed to the starting materials. Integration of the peak areas showed them to be in a 1:3 ratio. As with $\underline{36}$, a band in the semi-bridging carbonyl region was observed in the IR spectrum of $\underline{37}$. The pairs of resonances observed could possibly be due to two isomeric forms of the square pyramidal geometry, in which the positions of the C₅Me₅Rh and CpMo(CO)₂ units are interchanged. Attempts to observe coalescence between either the cyclopentadienyl or pentamethylcyclopentadienyl signals failed and resulted only in decomposition of the product.

The most conclusive evidence for the addition of a C_5Me_5Rh fragment, came from the product $\underline{38}$, of the reaction of $\underline{23}$ with $C_5Me_5Rh(CO)_2$. In the 1H NMR spectrum the correct integral ratio of 2:5 was observed for the methyl versus pentamethylcyclopentadienyl protons. Also a semi-bridging carbonyl band was found in the infrared spectrum of $\underline{38}$. More importantly, mass spectroscopic investigation gave a peak at 766 corresponding to the parent ion for $\underline{38}$.

The reactions carried out with $C_5Me_5Rh(CO)_2$ were all plagued with extremely poor yields. This was probably caused by the reaction conditions, in which prolonged thermolysis was required to generate the reactive C_5Me_5Rh unit by loss of two carbonyl ligands from $C_5Me_5Rh(CO)_2$. It was clear in order to incorporate cyclopentadienyl Rh units into tetrahedral clusters, a much more reactive Rh precursor was needed.

The compound chosen was $(C_9H_7)Rh(C_2H_4)_2$, $\underline{39}$,¹⁸⁹ whose structure is shown below. (Indenyl)rhodium units had been successfully incorporated into tetrahedral clusters by Stone and his co-workers in reactions with metal carbynes.¹⁴⁷ In contrast to $C_5Me_5Rh(CO)_2$ in which displacement of both carbonyls was difficult, it had been shown that the ethylenes in $\underline{39}$ were extremely labile, even at room temperature. Basolo had found that the related dicarbonyl complex of $\underline{39}$ underwent phosphine substitution 10^8 times faster than the corresponding cyclopentadienyl derivatives.¹⁹⁰ The mechanism proposed to account for this observation was an associative one, with the driving force of the reaction being slippage of η^5 ring to η^3 with accompanying rearomatization of the six membered ring.



The reactions of 23 and 28 were repeated with $(C_9H_7)Rh(C_2H_4)_2$. The reaction conditions employed were much milder than those employed for $C_5Me_5Rh(CO)_2$. In these studies, the two reactants were simply stirred at room temperature in hexane for a period of a week. From the NMR spectra of the resultant products 40 and 41, the signals due to the ethylene ligands had disappeared. In addition, both the proton and carbon resonances associated with the five membered ring of the indenyl group had moved with respect to the starting material 39. A shift to lower field was seen for the cyclopentadienyl protons in 41, compared to where they were previously found in 28. In contrast to the infrared spectrum of the products resulting from the reaction with $C_5Me_5Rh(CO)_2$, neither 40 or 41 exhibited bands due to semi-bridging carbonyls. Mass spectroscopic results on both 40 and 41 did not yield parent ions for

the compounds. This was not surprising for even in 38 which showed a parent, the first fragment loss corresponded to the C_5Me_5Rh unit.

In an attempt to obtain crystals suitable for X-ray diffraction purposes, 42, the pentamethylcyclopentadienylated derivative of 28 was treated with $(C_9H_7)Rh(C_2H_4)_2$. The product obtained, 43, exhibited NMR and IR spectra similar to those seen for 40 and 41. Furthermore, just as with those products it was not possible to obtain crystals for X-ray diffraction.

The results of this section are summarized in Figure 25. Most of the spectroscopic evidence points to the final products being cyclopentadienyl rhodium adducts of the tetrahedral precursors. The structures of the products presented in Figure 25 are those predicted by PSEP. In all the structures, the eighteen electron rule is satisfied by all the metals but as was seen from some of the NMR data, the possibility of other isomers does exist. In conclusion, the success of incorporating $Fe(CO)_3$ units into tetrahedral clusters has been extended to include other fragments bearing two electrons in their frontier orbitals, namely C_5Me_5Rh and C_9H_7Rh ; however, yields are rather low.

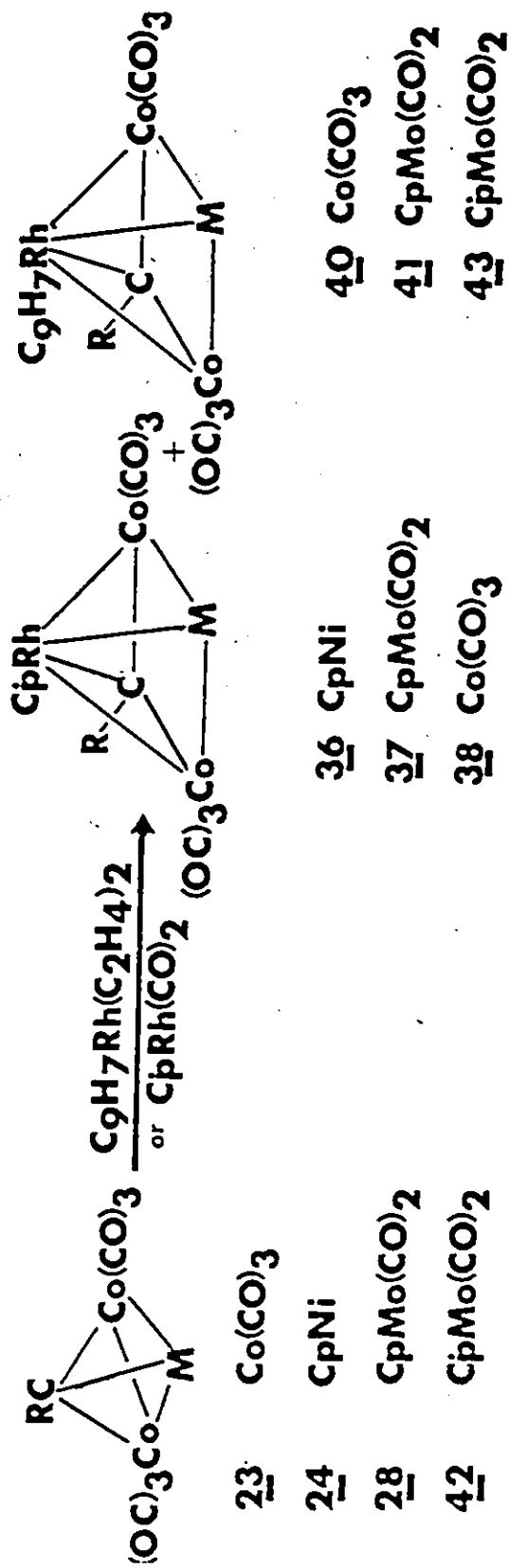


Figure 25:

Synthetic Scheme Involving Cluster Reactions with $\text{C}_5\text{Me}_5\text{Rh}(\text{CO})_2$ and $\text{C}_9\text{H}_7\text{Rh}(\text{C}_2\text{H}_4)_2$

CHAPTER V

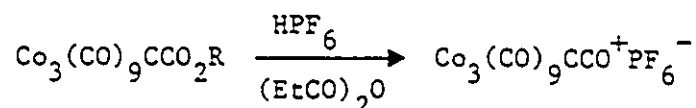
INVESTIGATIONS OF TRIMETALLIC ACYLIUM CATION CLUSTERS

5.1 Introduction

One of the most fascinating heterogeneous transition metal catalyzed processes is the Fischer-Tropsch reaction.¹⁹¹ It involves production of liquid hydrocarbons by hydrogenation of CO. Surface carbon, presumed to result from dissociative adsorption of CO, is thought to play an important role in overall Fischer-Tropsch syntheses. Towards this end, carbides or carbide derivatives are believed to be key intermediates in the catalytic cycle.¹⁹² The butterfly clusters discussed in Chapter IV have been considered models for these intermediates in homogeneous catalysis. All of the homometallic Fe₄ clusters with the exception of Fe₄(CO)₁₂CCO₂Me⁻ involved C₁ ligands. Vinylidene butterfly clusters, such as HCpNiRu₃(CO)₉(μ⁴-η²-C=CR₂), are thought to represent a potential model in Fischer-Tropsch for chain growth steps.¹⁹³

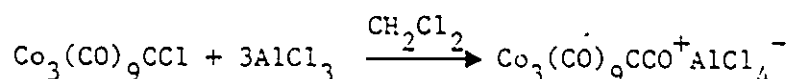
Perhaps the most interesting model clusters are those which involve a carbonyl bonded to a carbon atom which is part of the cluster skeleton. It is this type of ketenediyl cluster which was thought to be an intermediate in the synthesis of Fe₄(CO)₁₂CCO₂Me⁻ from Fe₆(CO)₁₆C²⁻.¹⁷⁷ However, attempts to isolate the presumed intermediate were unsuccessful. The first synthesis of a cluster of this type was reported in 1972.¹⁹⁴

It was reported that treatment of a concentrated H_2SO_4 solution of the cluster $\text{Co}_3(\text{CO})_9\text{CCO}_2\text{H}$ with various alcohols led to formation of the respective ester derivatives. The reaction was believed to proceed via the intermediacy of the acylium cation, $\text{Co}_3(\text{CO})_9\text{CCO}^+$. In the same work, the isolation of the acylium cation as a salt was demonstrated. This occurred from treatment of a propionic anhydride solution of the acid or ester derivative of the cluster with HPF_6 ;



The existence of the acylium cation was attributed to the intervention of the A_{Ac1} ester hydrolysis mechanism, well known for sterically hindered esters of acids. The steric hindrance in the cluster resulted from six of the nine carbonyls bonded to cobalt being displaced upwards towards the apical carbon and its substituent. This prevents protonation at the carbonyl oxygen and results in protonation at the alkoxy oxygen thereby generating the acylium cation. The presence of the acylium cation salt was confirmed by its reaction with various alcohols, amines and thiols giving the appropriate esters, amides and thioesters.¹⁹⁵

A continuing study from the same laboratory showed the acylium cation could be prepared in an alternative manner;^{196,197}



Similar results were reported for $\text{H}_3\text{Ru}_3(\text{CO})_9\text{CX}$, $\text{X} = \text{Cl}, \text{Br}$ and $\text{H}_3\text{Os}_3(\text{CO})_9\text{CBr}$ when they were treated with three equivalents of AlCl_3 .¹⁹⁸ Just

as for the PF_6 salt, the addition of various nucleophiles gave the expected carboxylic acid derivatives.

The first neutral ketenylidene cluster synthesized was $\text{H}_2\text{Os}_3(\text{CO})_9\text{CCO}$. It resulted from the thermal rearrangement of $\text{HOs}_3(\text{CO})_{10}\text{CH}$.¹⁹⁹ Employing similar methods, the Ru analogue has also been prepared.²⁰⁰ The first anionic ketenylidene cluster obtained was $\text{Fe}_3(\text{CO})_9\text{CCO}^{2-}$.¹⁶⁰ It was derived from acylation of a bridging CO in $\text{Fe}_3(\text{CO})_{11}^{2-}$, followed by reductive cleavage. Protonation of the iron ketenylidene cluster did not give the neutral analogue observed for Ru and Os but yielded a methylidyne cluster, $\text{HFe}_3(\text{CO})_{10}\text{CH}$.

This chapter reports a dynamic NMR study on the $\text{Co}_3(\text{CO})_9\text{CCO}^+$ cluster, giving support for a bent configuration of the ketenylidene ligand. In addition, a new route to the $[\text{Co}_3(\text{CO})_9\text{C}]_2$ cluster and the synthesis of the first mixed metal acylium cation are discussed. Finally, some proposals for future research are outlined.

5.2 Dynamic NMR Studies of $\text{Co}_3(\text{CO})_9\text{CCO}^+$

Despite the great deal of chemistry carried out on tricobalt acylium cation, the actual structure of this complex is unknown. Figure 26 illustrates the two structures proposed for the $\text{Co}_3(\text{CO})_9\text{CCO}^+$ complex. In the first, the ketenylidene ligand is bonded in an upright manner relative to the metal triangle while in the other it adopts a tilted configuration.

Many of the other known ketenylidene clusters have had their structures determined. $\text{H}_2\text{Os}_3(\text{CO})_9\text{CCO}$ was shown to have an upright configuration.²⁰¹ The anionic ketenylidene clusters $\text{Fe}_3(\text{CO})_9\text{CCO}^{2-}$ and $\text{CoFe}_2(\text{CO})_9\text{CCO}^-$ have both been found to assume a tilted

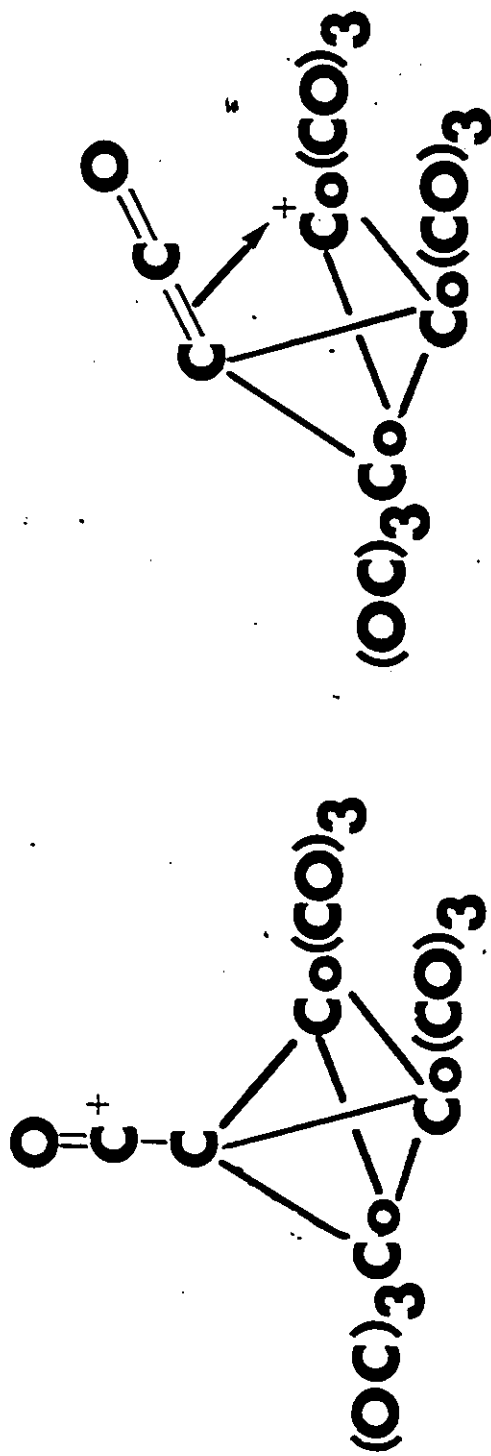


Figure 26:

Proposed Structures for the $Co_3(CO)_9CCO^+$ Complex

configuration.^{160,202} The CCO tilt angles relative to a plane vertical to the plane of the metal triangle were found to be 33° and 24° respectively. If the replacement of Fe(CO)₃ units from the parent Fe₃(CO)₉CCO²⁻ cluster is extended, one would expect the tilt angle would decrease as one went to Co₂Fe(CO)₉CCO and Co₃(CO)₉CCO⁺ respectively.

In contrast with the structural information establishing an upright configuration for the CCO ligand in H₂Os₃(CO)₉CCO, experimental evidence on the isoelectronic complexes H₂Os₃(CO)₉(C=CH₂),²⁰³ H₃Os₃(CO)₉(C=CH₂)⁺²⁰⁴ and Co₃(CO)₉(C=CHR)⁺²⁰⁵ points to a tilted configuration in these cases.

A molecular orbital analysis on Co₃(CO)₉CCH₂⁺ had predicted the preferred conformation to be a tilted one.¹⁰⁸ This was believed to be due to interaction between a vacant orbital on the methylene carbon and a filled metal orbital, a situation only possible for the tilted configuration. The CCO ligand with its p-π* orbitals in e pairs was thought to have no incentive to point away from a perpendicular conformation.

In order to determine a preferred conformation for the CCO ligand in Co₃(CO)₉CCO⁺, a dynamic ¹³C NMR study of the molecule was carried out. It was hoped any asymmetry in the molecule could be observed by monitoring the resonances attributed to the carbonyl ligands bonded to the cobalt atoms. The experiment first involved synthesis of the Co₃(CO)₉CCl cluster and its subsequent enrichment with ¹³CO, in order to aid in the acquisition of spectra. The acylium cation was then generated by addition of 3 equivalents of AlCl₃ and filtered under N₂ into an NMR

tube. In order to prevent the possibility of the acylium cation being hydrolyzed to the acid, the tube was sealed in vacuo. Generation of the cation employing this method rather than the one involving HPF_6 and a tricobalt ester derivative was chosen as it ensured that the CO bonded to the apical carbon would be enriched.

From the room temperature ^{13}C NMR spectrum the signal corresponding to the carbonyl ligands was found to occur at 191.2 ppm, similar to that observed for the same ligands in the $\text{Co}_3(\text{CO})_9\text{CCH}_2^+$ system.²⁰⁶ The resonance attributed to the CO of the ketenylidene ligand which had never been previously reported was found at 168.2 ppm. A comparison of the ^{13}C chemical shifts of the $\text{Co}_3(\text{CO})_9\text{CCO}^+$ cluster with shifts in other ketenylidene clusters is found in Table 9. Attempts to observe a signal for the quaternary carbon in the enriched sample of $\text{Co}_3(\text{CO})_9\text{CCO}^+$ proved unsuccessful. This failure could have been due to two factors. First, the quaternary carbon is bonded to three quadrupolar cobalt atoms ($I = 7/2$), this would serve to broaden the signal associated with it. Secondly, with the apical CO being enriched to approximately 33%, the quaternary carbon would display ^{13}C satellites from coupling to the CO ligand. This would have resulted in the signal of the quaternary carbon being only two-thirds as intense as it would be if an unenriched sample had been employed. Subsequently, an overnight run on an unenriched sample gave a broad resonance at 108.4 ppm for the quaternary carbon.

Table 10- Comparison of ^{13}C Shifts in Ketenylidene Clusters

Compound	Temp.	^{13}C NMR(ppm)	Ref.
$\text{Co}_3(\text{CO})_9\text{CCO}^+$	$25^\circ\text{C}^{\text{a}}$	191.2(9CO);168.2(CCO);108.4(CCO)	this work
	$-110^\circ\text{C}^{\text{a}}$	197.8(3CO);188.4(6CO)	
$\text{H}_2\text{Os}_3(\text{CO})_9\text{CCO}$	$25^\circ\text{C}^{\text{b}}$	175.6(3CO);165.8(6CO);160.3(CCO); 8.6(CCO)	199
	$-60^\circ\text{C}^{\text{a}}$	179.6(2CO);173.0(2CO);169.9(1CO); 168.0(2CO);158.3(2CO)	
$\text{CoFe}_2(\text{CO})_9\text{CCO}^-$	$-90^\circ\text{C}^{\text{a}}$	213.5(9CO);172.5(CCO);82.8(CCO)	202
$\text{Fe}_3(\text{CO})_9\text{CCO}^{2-}$	$-40^\circ\text{C}^{\text{c}}$	222.3(9CO);182.2(CCO);90.1(CCO)	160

a. CD_2Cl_2 , b. CDCl_3 , c. CD_3CN

The signal observed at room temperature for the metal carbonyls was a rather broad one. It was considerably broader than that observed for the carbonyls in $\text{Co}_3(\text{CO})_9\text{CCl}$. This indicated that this was due to more than bonding to the quadrupolar cobalt atoms. It suggested some type of exchange process may have been occurring. Upon cooling a sample of the $\text{Co}_3(\text{CO})_9\text{CCO}^+$ to -110°C , the 125MHz ^{13}C NMR spectrum revealed the signal associated with the metal carbonyls had split into two resonances at 197.8 ppm and 188.4 ppm in a ratio of 3:6. As seen in Figure 27, the signal due to the ketenylidene CO remained sharp at low temperatures. Attempts to observe exchange at high temperature between the ketenylidene CO and the metal carbonyls was precluded due to the low boiling point of CH_2Cl_2 .

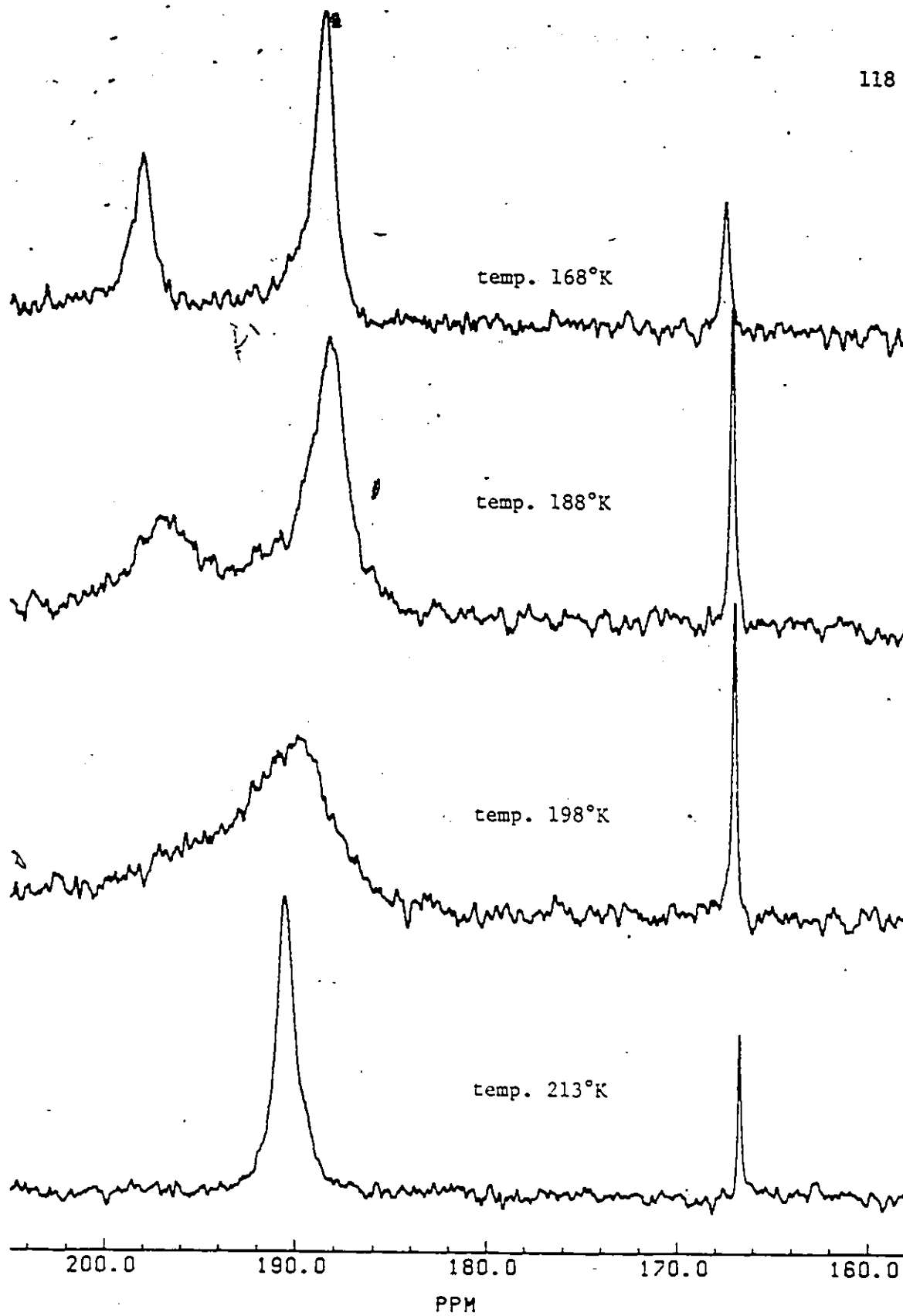


Figure 27:

Experimental 125 MHz Variable-Temperature ^{13}C NMR Spectra of
 $\text{Co}_3(\text{CO})_9\text{CCO}^+$

There are two possible explanations for the splitting of the metal carbonyl resonance of $\text{Co}_3(\text{CO})_9\text{CCO}^+$ at low temperature. The first is that exchange between the axial and equatorial carbonyls has been stopped on the NMR time scale. This has never been previously observed for Co clusters. In the ^{13}C NMR spectrum of $\text{Co}_3(\text{CO})_9\text{CCO}_2\text{CHMe}_2$ at -90°C on a 400 MHz spectrometer, the carbonyl resonance was found to be a sharp singlet.

Alternatively, it could be envisaged that if the ground state conformation of $\text{Co}_3(\text{CO})_9\text{CCO}^+$ was bent, this would lead to the observation of two different signals for the metal carbonyls at low temperature. At higher temperatures, the upright geometry could be thought to represent the excited state of the complex as demonstrated by the carbonyls appearing as a single peak. In contrast to $\text{H}_2\text{Os}_3(\text{CO})_9\text{CCO}$, where two different Os environments result from positioning of the hydrides, two different types of Co atoms in $\text{Co}_3(\text{CO})_9\text{CCO}^+$ are only possible with a bent arrangement of the CCO ligand. Unfortunately, further splitting of the carbonyl resonances into a 2:2:2:2:1 ratio was not observed. This pattern would have provided unequivocal evidence for the tilted structure of $\text{Co}_3(\text{CO})_9\text{CCO}^+$. The resonance for the quaternary carbon is found in the same area as that found for the bent anionic ketenylidene clusters. This too, lends support for the acylium cation adopting a tilted arrangement of the CCO ligand.

5.3 A Novel Route to $[\text{Co}_3(\text{CO})_9\text{C}]_2$

Early studies on the tricobalt systems had shown that when the apical substituent was a halogen, the carbon-halogen bond was very susceptible to nucleophilic attack and heterolytic fission.^{154,165}

Complexes with direct carbon-carbon linkages were the products of these transformations. The first report of this chemistry involved the refluxing of the $\text{Co}_3(\text{CO})_9\text{CBr}$ cluster in toluene. Products obtained from the reaction were identified as $[\text{Co}_3(\text{CO})_9\text{C}]_2$ and $[\text{Co}_3(\text{CO})_9\text{C}]_2\text{CO}$.²⁰⁷ When methanol was employed as a solvent, the reaction yielded the ester derivative, $\text{Co}_3(\text{CO})_9\text{CCO}_2\text{CH}_3$.²⁰⁸ It was later shown that the reaction of Ph_3As with $\text{Co}_3(\text{CO})_9\text{CCl}$ gave only small amounts of Ph_3As substituted product, the major product being $[\text{Co}_3(\text{CO})_9\text{C}]_2$.²⁰⁹ When Ph_3As is replaced with Ph_3Sb , the latter being a poorer Lewis base than the former, the only product obtained in high yield is the dimeric product.²¹⁰

In an attempt to prepare an NMR sample of $\text{Co}_3(\text{CO})_9\text{CCO}^+\text{PF}_6^-$, a small scale reaction of $\text{Co}_3(\text{CO})_9\text{CCO}_2\text{CHMe}_2$ and HPF_6 was carried out. No immediate precipitation of the black acylium salt was observed. In the hope of precipitating the cation out of solution, anhydrous Et_2O was added to the reaction mixture. This resulted in a small amount of black crystals dropping out of solution. In the expectation they were the acylium cation, an X-ray structure of the product was obtained. This revealed the product not to be an acylium cation but that of the neutral dimer, $[\text{Co}_3(\text{CO})_9\text{C}]_2$, the ORTEP of which is seen in Figure 28. The structure of the compound had been previously determined by Penfold and co-workers.²¹¹ The values obtained from this study agreed with those presented by the previous authors.

As outlined earlier, the dimer had been synthesized before. However, the reaction conditions employed in its synthesis were much more vigorous than the ones presented above. The mechanism of formation in these other routes was believed to involve free radical species. In

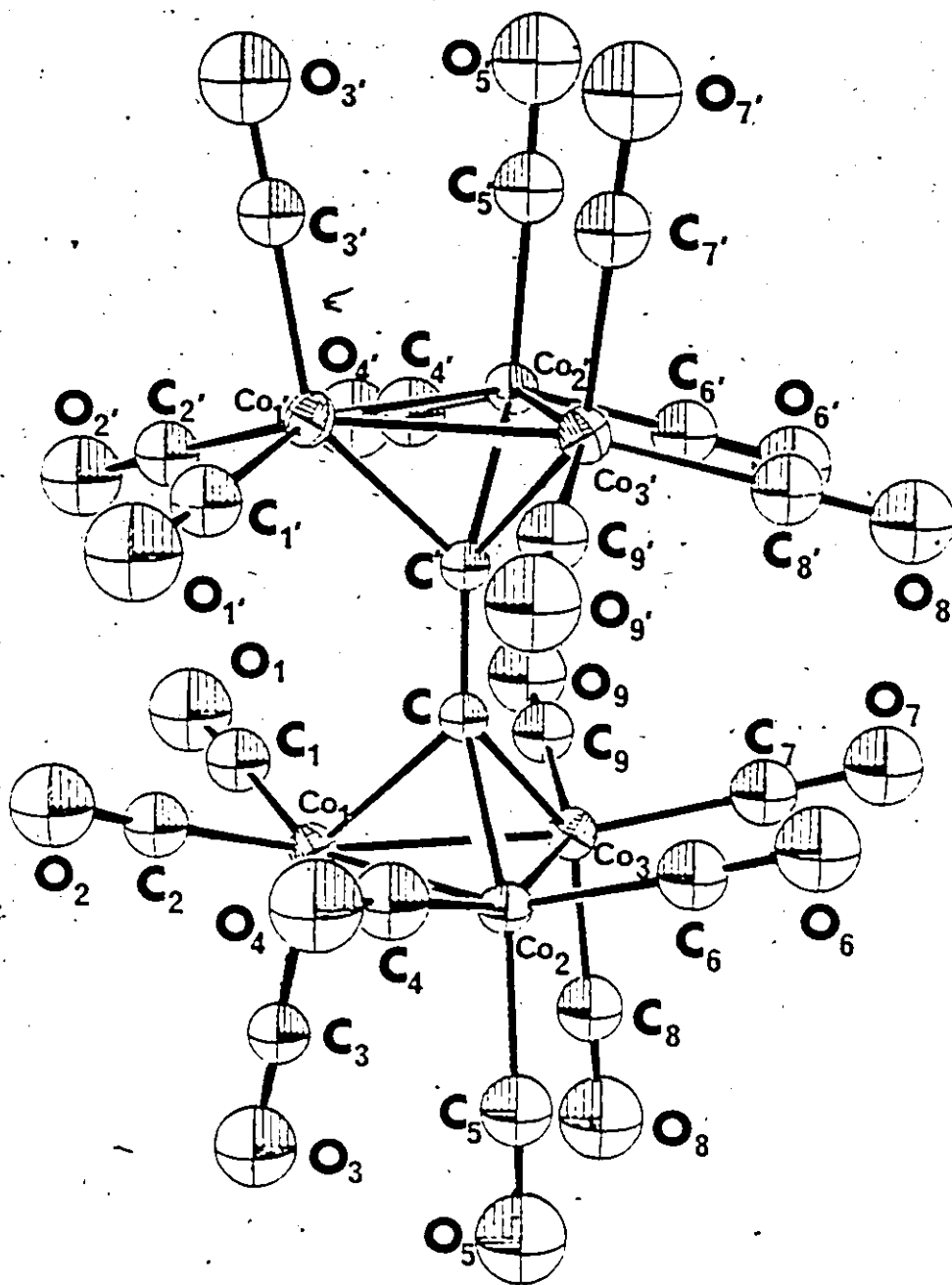


Figure 28:

ORTEP Diagram of $[\text{Co}_3(\text{CO})_9\text{C}]_2$

contrast, the use of aqueous HPF_6 in propionic anhydride is not suggestive of free radical formation. A possible mechanism for formation of the dimer is proposed in Figure 29. It is believed to proceed initially via formation of the acid derivative of the starting cluster. This could result from the presence of trace quantities of water not destroyed by the propionic anhydride. The acid derivative could then act as a nucleophile, attacking any additional acylium cation which had been formed. This results in formation of an anhydride derivative of two cluster molecules, which is then thought to undergo decarbonylation followed by decarboxylation. The last sequence is believed to proceed in that order because other studies had shown the ketone bridged dimer to be more stable than the carbon dimer.²⁰⁷

The same dimeric products were previously observed to result from the attempted alkylations of $\text{Co}_3(\text{CO})_9\text{CCO}^+\text{PF}_6^-$ with alkyl-lithium or magnesium Grignard reagents.¹⁹⁵ Their formation was attributed to complex electron transfer processes. However, trace quantities of moisture which are difficult to remove in reagents of this type, could have led to formation of dimeric products in the same manner as proposed above. In addition, it was reported that treatment of primary amides with the acylium cation, led to a product believed to be the corresponding imide. The product was observed to decompose at 0°C even under an inert atmosphere.¹⁹⁵ The instability of the imide is reminiscent of that proposed for the anhydride derivative in Figure 29. Attempts to synthesize an anhydride derivative of the cobalt cluster by treatment of the acylium cation with the salt of an acid yielded no isolable products.

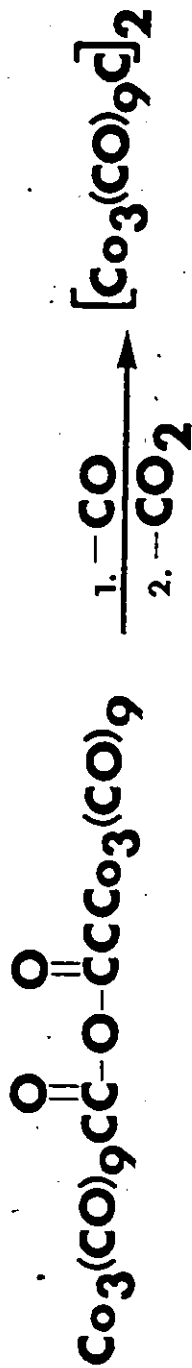
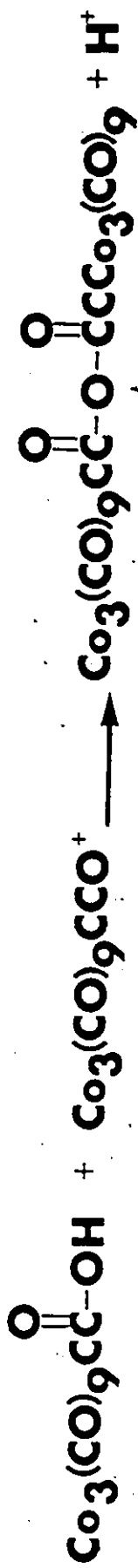
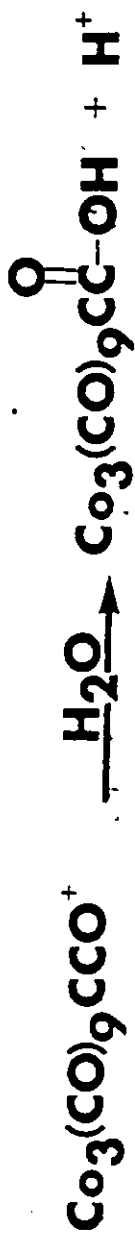


Figure 29:

Proposed Mechanism for $[\text{Co}_3(\text{CO})_9\text{C}]_2$ Formation

5.4 Synthesis and Characterization of a Mixed Metal Acylium Cation

The only report of a mixed metal cluster containing a ketenylidene linkage is $\text{Fe}_2\text{Co}(\text{CO})_9\text{CCO}^-$,²⁰² No neutral or cationic mixed species are known. The mixed systems might provide both different stability and reactivity from that observed for the homometallic systems. The tilt angle of the CCO ligand in the CoFe_2 system is smaller than that for the Fe_3 system. Also the mixed system was described as being significantly less reactive than the Fe_3 cluster. The relatively facile synthesis of the mixed metal clusters discussed in Chapter 4 suggested that the isolation of a mixed metal acylium cation might be possible.

The cluster system chosen for initial study was $\text{CpMoCo}_2(\text{CO})_8\text{CCO}_2\text{CHMe}_2$. From previous work on this complex it seemed to be the best behaved of the clusters described in the preceding chapter. The method of synthesis was similar to that employed in the preparation of the tricobalt acylium cation. Upon dissolving the cluster in propionic anhydride, a dark green solution was obtained, addition of HPF_6 resulted in a color change from dark green to brown. A brown-black microcrystalline solid dropped out of solution, complete precipitation was ensured through addition of Et_2O to the brown solution. Just as for the cobalt system, the solid cation in the form of a PF_6^- salt was found to be insoluble and unaffected by ethers and saturated hydrocarbons. In contrast to $\text{Co}_3(\text{CO})_9\text{CCO}^+\text{PF}_6^-$, which is soluble only in CH_3NO_2 , $\text{CpMoCo}_2(\text{CO})_8\text{CCO}^+\text{PF}_6^-$ was found to be sparingly soluble in CH_2Cl_2 and soluble in both CH_3CN and acetone. A solution infrared spectrum of the MoCo_2 cation in CH_2Cl_2 gave bands at 2090(m), 2080(m), 2035(s), 2010(s) and 1680(w), cm^{-1} , the bands being shifted 10 - 15 cm^{-1} higher than the neutral cluster.

In order to confirm the presence of the mixed metal cation, a CH_2Cl_2 slurry of $\text{CpMoCo}_2(\text{CO})_8\text{CCO}^+\text{PF}_6^-$ was treated with various nucleophiles. Treatment with methanol resulted in the immediate appearance of a dark green homogeneous solution, the product of the reaction being the expected methyl ester derivative. Reaction of the MoCo_2 cation with diethylamine once again occurred instantaneously. However, the resulting amide proved to be extremely unstable. Attempts to purify the compound by column chromatography under a N_2 atmosphere proved impossible. The compound was stable if the solvent was removed immediately after completion of the reaction and the resulting solid was stored under an inert atmosphere. As with the cobalt system, the reaction of the mixed metal cation with *N,N*-dimethylaniline gave a Friedel-Crafts product. From the ^1H NMR spectrum, acylation was found to occur only at the para position. The reaction with thiophenol did not occur instantaneously as was reported for the cobalt cation. After three days of stirring, the corresponding thioester was obtained. The slow reactivity in this case compared to that of $\text{Co}_3(\text{CO})_9\text{CCO}^+$ may have possibly been due to steric problems posed by the cyclopentadienyl ring bonded to Mo.

If the structure of $\text{CpMoCo}_2(\text{CO})_8\text{CCO}_2\text{CHMe}_2$ is similar to that when the apical group is C_6H_5 ,¹⁸⁷ the cyclopentadienyl ring would be located below the plane containing the triangle of metals. This would mean the two carbonyl ligands bound to Mo would be disposed towards the apical carbon. Therefore, just as is the case with $\text{Co}_3(\text{CO})_9\text{CCO}_2\text{R}$, a sterically hindered environment for the ester group is provided. Should the cyclopentadienyl group be located above the plane containing

the three metal atoms; the steric hindrance would be even more pronounced. In addition to the steric effects of the cyclopentadienyl group, it is also most likely responsible for the increased solubility of the $\text{CpMoCo}_2(\text{CO})_8\text{CCO}^+\text{PF}_6^-$ complex in comparison to the cobalt complex.

5.5 Proposals for Future Work

Despite the great activity in the field of metal clusters, many areas remain unexplored. Much insight has been gained in both logical synthetic routes to clusters and their structure from work of the past ten years. However, the subjects of reaction mechanism in the synthesis of many clusters and reactivity of metal clusters offer opportunities in supplying a greater understanding of clusters. Outlined below are a few suggestions for further study in areas involving the work described previously.

The mechanism of formation of $\text{Co}_3(\text{CO})_9\text{CR}$ clusters from the reaction of $\text{Co}_2(\text{CO})_8$ and RCCl_3 has yet to be elucidated. In Chapter 4, it was suggested that this might occur via cobalt carbyne formation. In order to test this hypothesis, a bulky R group such as adamantyl on the trichlorocompound should be utilized. This may prevent the presumed addition of the $\text{Co}_2(\text{CO})_6$ unit and allow for isolation of the proposed reactive carbyne unit. The reaction of $(\text{RC}\equiv\text{CH})\text{Co}_2(\text{CO})_6$ complexes with dilute aqueous methanolic H_2SO_4 was the first route to clusters of the type $\text{RCH}_2\text{CCo}_3(\text{CO})_9$.¹⁶² With the availability of many other homo- and hetero- dimetallic alkyne clusters, a similar reaction with these complexes has the possibility of providing a new route to mixed metal alkylidyne clusters.

Without a crystal structure of the $\text{Co}_3(\text{CO})_9\text{CCO}^+$ complex, the controversy as to whether the CCO moiety is bent or upright will continue. The dynamic NMR studies presented earlier in this chapter lent some credence for the bent configuration. Further evidence could be obtained if the $(\text{dppe})\text{Co}_3(\text{CO})_7\text{CCO}^+$ complex could be generated. In principle, for the bent configuration; the phosphorus atoms being better donors than the carbonyls, one would expect that one of them would be bonded to the cobalt bearing the positive charge. Therefore, if two phosphorus resonances are observed in the ^{31}P NMR spectrum, the CCO moiety would have to be bent not upright. Earlier, it was mentioned that the action of HPF_6 on $\text{Co}_3(\text{CO})_9\text{CCO}_2\text{CHMe}_2$ led to formation of the dimer, $[\text{Co}_3(\text{CO})_9\text{C}]_2$. This reaction was believed to proceed via a dicluster anhydride intermediate. Anhydride derivatives of tricobalt clusters are not known. A possible route to them could involve the reaction of the acylium cation with a solid acid. If, instead of anhydride derivatives, alkyl or aryl substituted compounds are obtained, this observation would support the proposed mechanism of formation of the dimer. In addition to regular organic acids, this reaction could be carried out with $\text{Co}_3(\text{CO})_9\text{CCO}_2\text{H}$ in order to see if the dimer is obtained.

The solubility of the MoCo_2 cation might allow for crystals to be grown which are suitable for X-ray diffraction purposes, in order to determine the orientation of the CCO ligand relative to the metal triangle. In addition, dynamic NMR studies similar to those described for the cobalt system might yield information regarding the structure of the mixed cation. A comparison of the reactivity of the mixed cation

against that of $\text{Co}_3(\text{CO})_9\text{CCO}^+$ would be beneficial as it would give a measure of the electrophilic character of each. Finally, attempts could be made to generate cations from other clusters in which the existing cobalt vertices have been replaced or modified. The method of generation for the ester derivatives could be extended to include HBF_4 , $\text{CF}_3\text{CO}_2\text{H}$, FSO_3H and $\text{R}_3\text{O}^+\text{X}^-$ (where R = alkyl groups, X = BF_4 , PF_6 , SbCl_6).

CHAPTER VI

EXPERIMENTAL

6.1 General Spectroscopic Techniques

^1H and ^{13}C NMR spectra were recorded using Bruker WM500, WM400, WM250 and WP80 spectrometers. Chemical shifts are referenced to tetramethylsilane. Infrared spectra were recorded on a Perkin-Elmer 283 instrument using KBr solution cells. Mass spectrometry was performed on a VG micromass 7070F spectrometer equipped with a VG 2035 data system.

6.2 General Procedures

All reactions were performed under a dry nitrogen atmosphere employing conventional benchtop and glovebag techniques. Solvents were dried according to standard procedures before use.²¹² Silica gel (60-200 mesh, Baker Analyzed) was employed for column chromatography. Isopropyl phenylpropiolate and isopropyl trichloroacetate were prepared by the method described in Vogel.²¹³ The following compounds were prepared by literature methods: $\text{C}_5\text{Me}_5\text{Rh}(\text{CO})_2$ ¹⁸⁸, $\text{C}_9\text{H}_7\text{Rh}(\text{C}_2\text{H}_4)_2$ ¹⁸⁹, $[\text{C}_5\text{Me}_5\text{Mo}(\text{CO})_3]_2$ ²¹⁴, $\text{Co}_3(\text{CO})_9\text{CCl}$ ²¹⁵ and $\text{Co}_3(\text{CO})_9\text{CCO}^+\text{AlCl}_4^-$ ¹⁹⁷.

6.3 Experimental Procedures of Chapter 2

Preparation of $(\text{C}_5\text{H}_5)_2\text{Ni}_2(\text{PhC}_2\text{CO}_2\text{CHMe}_2)$, 13

Cp_2Ni (1 g, 5.3 mmoles) and $\text{PhC}_2\text{CO}_2\text{CHMe}_2$ (0.500 g, 2.7 mmoles) were heated in toluene (30 cm³) at 105°C for 10 h. under an atmosphere of nitrogen. After removal of solvent, the products were

separated by thin layer chromatography on silica gel using as eluent a 9:1 mixture of petroleum ether/ether. The product was a green oil showing ν_{CO} at 1712 cm^{-1} in heptane solution. $^1\text{H NMR}$ (CDCl_3), δ 7.19-7.62(m, 5H, Ph), 5.26(s, 5H, Cp), 5.15(septet, 1H, CHMe_2), 1.25(d, 6H, Me's, $J = 6.2 \text{ Hz}$).

Preparation of $(\text{C}_5\text{H}_5)_2\text{NiMo}(\text{CO})_2(\text{PhC}_2\text{CO}_2\text{CHMe}_2)$, $\underline{14}$

Cp_2Ni (1 g, 5.3 mmol), $\text{Cp}_2\text{Mo}_2(\text{CO})_6$ (1.3 g, 2.7 mmol) and $\text{PhC}_2\text{CO}_2\text{CHMe}_2$ (1 g; 5.3 mmol) were heated at 105°C in 35 cm^3 toluene for 7 h. under N_2 . T.l.c. as before afforded 1.19 g (40%) of $\underline{14}$ as a red-brown crystalline solid, m.p. $90-91^\circ\text{C}$, $m/z = 529.9922$, calc: 529.99254, [I.R. (heptane), ν_{CO} 2030(w), 1978(sh), 1968(vs), 1930(s), 1902(m), 1875(s) and 1682(m) cm^{-1} ; $^1\text{H NMR}$ (CDCl_3); δ 7.25-7.54(m, 5H, Ph), 5.24(s, 5H, Cp), 5.14(s, 5H, Cp), 1.35(d, 6H, CH_3 , $J = 6.4 \text{ Hz}$)] together with $\text{Ni}_2\text{Cp}_2(\text{CO})_2$, $\text{Ni}_2\text{Cp}_2(\text{PhC}_2\text{CO}_2\text{CHMe}_2)$ and unreacted $\text{Mo}_2\text{Cp}_2(\text{CO})_6$.

Preparation of $(\text{C}_5\text{H}_5)\text{NiCo}(\text{CO})_3(\text{PhC}_2\text{CO}_2\text{CHMe}_2)$, $\underline{15}$

$\text{Co}_2(\text{CO})_8$ (1 g, 2.9 mmol), Cp_2Ni (1 g, 5.3 mmol) and $\text{PhC}_2\text{CO}_2\text{CHMe}_2$ (1 g, 5.3 mmol) were heated at 100°C in heptane under N_2 for 6 h. and gave rise to the heterobimetallic-acetylene complex $\underline{15}$ [25% yield; oil, $m/z = 453.9756$, calc $m/z = 453.9761$; $^1\text{H NMR}$ (CD_2Cl_2), δ 7.35-7.66 (m, 5H, Ph), 5.31(s, 5H, C_5H_5), 1.29(d, 6H, CH_3 , $J = 6.6 \text{ Hz}$)] [I.R. (neat liquid), ν_{CO} 2055(s), 2000(vs), 1700(s) cm^{-1}] as the main product together with, inter alia, $\text{Ni}_2\text{Cp}_2(\text{CO})_2$, $\text{Co}_2(\text{CO})_6(\text{PhC}_2\text{CO}_2\text{CHMe}_2)$, $\text{Ni}_2\text{Cp}_2(\text{PhC}_2\text{CO}_2\text{CHMe}_2)$, separated on silica gel using petroleum ether/ether (9:1).

Preparation of $(C_5H_5)NiFeCo(CO)_6(PhC_2CO_2CHMe_2)$, 17

$Fe_2(CO)_9$ (0.920 g, 2.5 mmol) and 15 (1 g, 2.3 mmol) were heated at 40°C in heptane for 6 h. under an atmosphere of nitrogen. After removal of solvent, the product was chromatographed on silica gel and eluted with petroleum ether/ether (80/20) to give 17 (85%) as a green solid which was recrystallised from heptane/ $CHCl_3$; 17, m.p. 120°C, showed 1H NMR ($CDCl_3$), δ 7.14-7.26(m, 5H, Ph), 4.88(s, 5H, Cp), 1.02(d, J = 6.4 Hz, 3H, Me), 0.90(d, J = 6.3 Hz, 3H, Me); IR ($CHCl_3$), ν_{CO} 2060(s), 2015(vs), 2000(s), 1970(m), 1960(m), 1950(m) cm^{-1} ; m/z 593.9001; calcd. 593.896.

Preparation of 16 and 18

$Fe_2(CO)_9$ (0.920 g, 2.5 mmol) and 14 (1.2 g, 2.8 mmol) were heated at 40°C in heptane for 4 h. under an atmosphere of nitrogen. Chromatography on silica gel and elution with petroleum ether/ether (90/10) yielded 18 (70%) as a grey solid, m.p. 145°C, showing 1H NMR ($CDCl_3$), δ 7.17-7.24(m, 5H, Ph), 4.85(m, 1H, $\underline{CHMe_2}$), 5.14(s, 5H, Cp), 4.70(s, 5H, Cp), 1.02(d, J = 6.3 Hz, 3H, Me), 0.90(d, J = 6.3 Hz, 3H, Me); I.R. (heptane), ν_{CO} 2028(vs), 1970(vs), 1876(w), 1830(w) cm^{-1} ; m/z 585.929 (M-3CO); calcd., 585.9274.

Similarly, $Fe_2(CO)_9$ and 13 gave 16, m.p. 125°C, m/z 573.9528, calcd. 573.9522 ν_{CO} at 1955(m) and 1915(s) cm^{-1} ; 1H NMR ($CDCl_3$) δ 7.15-7.35(m, 5H, Ph), 5.28(s, 5H, Cp), 4.99(s, 5H, Cp), 4.39(m, 1H, $\underline{CHMe_2}$), 0.78(pseudo triplet, 6H, Me). 16, 17 and 18 were all characterized by X-ray crystallography.

Structural Determinations of 16, 17 and 18

The experimental data for the X-ray diffraction studies of 16, 17 and 18 are summarised in Tables A1 through A6. All the crystallographic data were obtained on small single crystals at room temperature using Enraf-Nonius CAD 4 diffractometers equipped with a graphite monochromator. The unit cell dimensions were determined by least squares refinement of the best angular positions for 25 independent reflections. During the collection of intensity data, the intensities of three standard reflections were monitored periodically; only statistical fluctuations were noted in each case. Data were corrected for Lorentz and polarisation effects and anomalous scattering corrections were included in all structure factor calculations. Atomic scattering factors were taken from ref. 216.

The three structures were solved by the heavy atom method and refined by full-matrix least squares treatment. For 16 and 18 the hydrogen atoms were located at the end of the refinement. Their positional parameters were kept constant for 16 but refined for 17. All the non-hydrogen atoms were refined anisotropically except the 11 peripheral atoms in 17 and the 24 peripheral atoms in 18. In each case the residual electron density peaks after the last Fourier synthesis were less than $0.5 \text{ electrons/\AA}^2$ near the heavy atoms.

6.4 Experimental Procedures for Chapter 4

Preparation of $\text{Co}_3(\text{CO})_9\text{CCO}_2\text{CHMe}_2$, 23

Following the general procedure of Seyferth,²¹⁵ $\text{Co}_2(\text{CO})_8$ and $\text{CCl}_3\text{CO}_2\text{CHMe}_2$ reacted to give 23 in 40% yield. The crude product was

recrystallized from petroleum-ether/ether. The ^1H NMR (C_6D_6), spectrum showed a doublet at $\delta 1.34$ (6H) and a septet at $\delta 5.27$ (1H), ($J_{\text{HH}} = 6.3$ Hz). The ^{13}C NMR (C_6D_6), spectrum showed peaks at $\delta 69.7$ (CH) and $\delta 21.7$ (CH_3). The infrared spectrum (cyclohexane), exhibited ν_{CO} at 2105(m), 2075(s), 2045(s), 2025(s), 1980(w) and 1690(ester) cm^{-1} . Major mass spectral peaks occurred at m/z (%): 500, $\text{C}_{13}\text{H}_7\text{Co}_3\text{O}_{10}^+$, (2); 388, $\text{C}_9\text{H}_7\text{Co}_3\text{O}_6^+$, (2); 360, $\text{C}_8\text{H}_7\text{Co}_3\text{O}_5^+$, (4); 332, $\text{C}_7\text{H}_7\text{Co}_3\text{O}_4^+$, (2); 304, $\text{C}_6\text{H}_7\text{Co}_3\text{O}_3^+$, (1); 248, $\text{C}_4\text{H}_7\text{Co}_3\text{O}^+$, (2); 190, CHCo_3^+ , (1); 59, Co^+ , (100).

Reaction of $\text{Co}_3(\text{CO})_9\text{CCO}_2\text{CHMe}_2$ with Cp_2Ni

(a) At room temperature. To a solution containing 0.68 g (1.29 mmol) of $\underline{23}$ in THF (50 cm^3) was added 0.55 g (2.91 mmol) of Cp_2Ni , and the solution was stirred at room temperature for one week. Progress of the reaction was monitored by t.l.c. (eluent, ether/pet. ether, 15:85; yellow spot Cp_2Ni , $R_f = 0.86$; greyish-purple spot $\underline{23}$, $R_f = 0.80$; dark brown spot $\underline{24}$, $R_f = 0.65$; black spot $\underline{25}$, $R_f = 0.50$). The solvent was removed in vacuo to yield a dark brown solid which was chromatographed on silica gel with ether/pet. ether (15:85) to give deep brown crystals of $\underline{24}$ (0.63 g, 1.24 mmol; 96%). The ^1H NMR (C_6D_6), spectrum showed a doublet at $\delta 1.30$ (6H), a singlet at $\delta 4.99$ (5H) and a septet at $\delta 5.27$ (1H), ($J_{\text{HH}} = 6.1$ Hz). The ^{13}C NMR (C_6D_6), spectrum showed peaks at $\delta 22.5$ (CH_3), $\delta 68.0$ (CH) and $\delta 91.7$ (C_5H_5). The infrared spectrum (cyclohexane), exhibited ν_{CO} at 2075(m), 2040(s), 2015(s), 2000(s) and 1675 (ester) cm^{-1} . Major mass spectral peaks occurred at m/z (%): 508/510, $\text{C}_{16}\text{H}_{12}\text{Co}_2\text{NiO}_8^+$, (1); 480/482, $\text{C}_{15}\text{H}_{12}\text{Co}_2\text{NiO}_7^+$ (7); 452/454,

$C_{14}H_{12}Co_2NiO_6^+$, (17); 424/426, $C_{13}H_{12}Co_2NiO_5^+$, (3); 396/398,
 $C_{12}H_{12}Co_2NiO_4^+$, (4); 368/370, $C_{11}H_{12}Co_2NiO_3^+$, (36); 340/342, $C_{10}H_{12}Co_2NiO_2^+$,
 (28); 312/314, $C_9H_{12}Co_2NiO^+$, (53); 254/256, $C_6H_6Co_2Ni^+$, (46); 189/191,
 $CHCo_2Ni^+$, (38); 188/190, CCo_2Ni^+ , (100); 173/175, $C_2CoNiO_2^+$, (16); 123/125,
 C_5H_5Ni , (100).

In addition to $\underline{24}$, a trace amount of $\underline{25}$ was recovered. The 1H NMR (C_6D_6), showed a doublet at δ 1.41(6H), a singlet at δ 4.82(10H) and a septet at δ 5.54(1H), ($J_{HH} = 6.4$ Hz). The ^{13}C NMR (C_6D_6), spectrum showed peaks at δ 22.3(CH_3), δ 68.5(CH) and δ 88.1(C_5H_5). The infrared spectrum (cyclohexane), exhibited ν_{CO} at 2080(m), 2045(s), 2010(s), 1975(w), 1810(s) and 1680(ester) cm^{-1} .

(b) In refluxing THF. To a solution of $\underline{23}$ (1.48 g, 2.80 mmol) in THF (50 cm^3) was added 1.90 g (10 mmol) of Cp_2Ni . The resulting solution was heated under reflux overnight. Progress of the reaction was monitored by t.l.c. and indicated the formation of five products. The solution was allowed to cool to room temperature, the solvent removed in vacuo and the residue chromatographed on silica gel. The first two bands were eluted with pet. ether, the next two with ether-pet. ether (15:85) and the final band with ether. Recrystallisation of the third band gave purple-black crystals of $\underline{26}$ (0.46 g., 0.92 mmol; 33%), and recrystallisation of the fourth band gave dark brown crystals (0.69 g., 1.39 mmol; 49%) of $\underline{27}$.

The first, second and fifth bands were obtained only in minor amounts and could not be identified. The first band gave a light brown powder which gave no assignable IR or 1H NMR peaks. The second band yielded a yellow-brown powder showing IR absorptions at 1900, 1860

and 1855 cm^{-1} , but no ester carbonyl. ^1H NMR gave only a broad singlet centred at $\delta 5$. The final band to be eluted gave a brown-black solid exhibiting IR absorptions at 1790 , 1765 and 1680 cm^{-1} . The ^1H NMR spectrum showed Cp resonances at $\delta 4.8$, 4.9 , 5.2 and 5.3 and was certainly a mixture of several compounds. Presumably these complexes and others which could not be eluted from the column account for the remainder of the nickel from the starting material.

The ^1H NMR (C_6D_6), spectrum of 26 showed a broad singlet at $\delta 9.4(1\text{H})$, a doublet at $\delta 1.41(6\text{H})$, a singlet at $\delta 4.82(15\text{H})$ and a septet at $\delta 5.55(1\text{H})$ ($J_{\text{HH}} = 6.2\text{ Hz}$). The ^{13}C NMR (C_6D_6), spectrum showed peaks at $\delta 22.7(\text{CH}_3)$, $\delta 67.8(\text{CH})$ and $\delta 88.7(\text{C}_5\text{H}_5)$. The infrared spectrum (cyclohexane), exhibited ν_{CO} at $1820(\text{m})$ and $1680(\text{ester})\text{ cm}^{-1}$.

Major mass spectral peaks at m/z (%): 500 , $\text{C}_{21}\text{H}_{23}\text{Co}_3\text{O}_3^+$, (4); 499 , $\text{C}_{21}\text{H}_{22}\text{Co}_2\text{O}_3^+$, (8); 472 , $\text{C}_{20}\text{H}_{23}\text{Co}_3\text{O}_2^+$, (2); 471 , $\text{C}_{20}\text{H}_{22}\text{Co}_3\text{O}_2^+$, (3); 414 , $\text{C}_{17}\text{H}_{17}\text{Co}_3\text{O}^+$, (2); 413 , $\text{C}_{17}\text{H}_{16}\text{Co}_3\text{O}^+$, (4); 386 , $\text{C}_{16}\text{H}_{17}\text{Co}_3^+$, (4); 385 , $\text{C}_{16}\text{H}_{16}\text{Co}_3^+$, (14); 370 , $\text{C}_{11}\text{H}_{13}\text{Co}_3\text{O}_3^+$, (8); 369 , $\text{C}_{11}\text{H}_{12}\text{Co}_3\text{O}_3^+$, (3); 305 , $\text{C}_6\text{H}_8\text{Co}_3\text{O}_3^+$, (7); 304 , $\text{C}_6\text{H}_7\text{Co}_3\text{O}_3^+$, (4); 246 , $\text{C}_3\text{HCo}_3\text{O}_2^+$, (8); 190 , $\text{C}_{10}\text{H}_{11}\text{Co}^+$, (10); 189 , $\text{C}_{10}\text{H}_{10}\text{Co}^+$, (100); 125 , $\text{C}_5\text{H}_6\text{Co}^+$, (5); 124 , $\text{C}_5\text{H}_5\text{Co}^+$, (78); 66 , C_5H_6^+ , (25); 65 , C_5H_5^+ , (15); 59 , Co^+ , (24).

The ^1H NMR (C_6D_6), spectrum of 27 showed a doublet at $\delta 1.46(6\text{H})$, singlets at $\delta 4.89(10\text{H})$ and $\delta 5.09(5\text{H})$ and a septet at $\delta 5.55(1\text{H})$ ($J_{\text{HH}} = 6.2\text{ Hz}$). The ^{13}C NMR (C_6D_6), spectrum showed peaks at $\delta 23.1(\text{CH}_3)$, $\delta 68.2(\text{CH})$, $\delta 86.7(\text{C}_5\text{H}_5\text{Co})$ and $\delta 91.0(\text{C}_5\text{H}_5\text{Ni})$. The infrared spectrum (cyclohexane), exhibited ν_{CO} at $1810(\text{m})$ and $1680(\text{ester})\text{ cm}^{-1}$. Major mass spectral peaks occurred at m/z (%): $498/500$, $\text{C}_{21}\text{H}_{22}\text{Co}_2\text{NiO}_3^+$, (25); $470/472$, $\text{C}_{20}\text{H}_{22}\text{Co}_2\text{NiO}_2^+$, (9); $412/414$, $\text{C}_{17}\text{H}_{16}\text{Co}_2\text{NiO}^+$, (5); $384/386$,

$C_{16}H_{16}Co_2Ni^+$, (41); 371/373; $C_{15}H_{15}Co_2Ni^+$, (8); 190, $C_{10}H_{11}Co^+$, (11); 189, $C_{10}H_{10}Co^+$, (100); 124, $C_5H_5Co^+$, (10); 123/125, $C_5H_5Ni^+$, (4).

Preparation of $CpMo(CO)_2Co_2(CO)_6CCO_2CHMe_2$, $\overset{28}{\sim}$

To a solution containing $\overset{23}{\sim}$ (1.23 g., 2.33 mmol) in THF (50 cm³) was added $[CpMo(CO)_3]_2$ (0.59 g., 1.21 mmol). The reaction mixture was heated under reflux to completion (~ 10 h). The progress of the reaction was monitored by t.l.c. (eluent, ether/pet. ether, 15:85; greyish-purple spot, $\overset{23}{\sim}$, $R_f = 0.80$ and dark green spot, $\overset{28}{\sim}$, $R_f = 0.69$). The solution was allowed to cool to room temperature, the solvent removed in vacuo and the residue chromatographed on silica gel. Elution first with pet. ether and then a mixture of ether/pet. ether, 10:90 allowed separation of the two bands. Recrystallization of the dark green band from ether/pet. ether gave black crystals of $\overset{28}{\sim}$ (0.46 g., 0.76 mmol; 33%): ¹H NMR (C_6D_6), δ 1.31(d, 6H), 4.75(s, 5H) and 5.19 (septet, 1H, J = 6.2 Hz). ¹³C NMR (C_6D_6), δ 92.4(C_5H_5), 67.9(CH) and 22.1(CH_3). IR (Cyclohexane) ν_{CO} at 2080(m), 2075(sh), 2050(s), 2030(s), 2000(s), 1945(w), 1900(w), 1670(ester) cm⁻¹. Major mass spectral peaks occurred at m/z (%): 576, $C_{17}H_{12}O_9Co_2Mo^+$ (1); 548, $C_{16}H_{12}O_8Co_2Mo^+$ (2); 520, $C_{15}H_{12}O_7Co_2Mo^+$ (1); 492, $C_{14}H_{12}O_6Co_2Mo^+$ (2); 464, $C_{13}H_{12}O_5Co_2Mo^+$ (2); 436, $C_{12}H_{12}O_4Co_2Mo^+$ (7); 408, $C_{11}H_{12}O_3Co_2Mo^+$ (2); 380, $C_{10}H_{12}O_2Co_2Mo^+$ (2); 322, $C_7H_6OC_2Mo^+$ (1); 294, $C_6H_6Co_2Mo^+$ (3); 229, $CHCo_2Mo^+$ (2); 219, $C_7H_5O_2Mo^+$ (2); 180, $C_7H_5O_2Co^+$ (43); 152, $C_6H_5Co^+$ (42); 124, $C_5H_5Co^+$ (100). Molybdenum-containing ions exhibited the correct isotope abundance patterns but the only ones listed are for the ⁹⁸Mo contributors.

Reactions of $\underline{28}$ with Cp_2Ni

To a solution of $\underline{28}$ (0.60 g., 1.00 mmol) in THF (30 cm³) was added Cp_2Ni (0.80 g., 4.23 mmol). The reaction mixture was stirred overnight at room temperature. The reaction was monitored by t.l.c. (eluent, ether/pet. ether, 10:90) and indicated the formation of a major and a minor component. Removal of solvent left a brownish-black solid which was chromatographed on silica gel. Separation was effected using ether/pet. ether/benzene, 5:75:20, to give the major component (subsequently shown to be a mixture of $\underline{29}$, $\underline{30}$ and $\underline{31}$) and the minor component which could not be identified due to extensive decomposition. Spectroscopic data indicated that the major component was a mixture of $\underline{29}$, $\underline{30}$ and $\underline{31}$ and this material was together treated with $\text{Fe}_2(\text{CO})_9$.

Reaction of $\underline{29}$, $\underline{30}$ and $\underline{31}$ with $\text{Fe}_2(\text{CO})_9$

To a solution containing 0.20 g of the mixture of $\underline{29}$, $\underline{30}$ and $\underline{31}$ in toluene (10 cm³) was added $\text{Fe}_2(\text{CO})_9$ (0.22 g., 0.60 mmol). The suspension was stirred at 50° for 2 hours; the progress of the reaction was monitored by t.l.c. (eluent, ether/pet. ether, 25:75) and indicated three products. The solution was allowed to cool to room temperature, the solvent removed in vacuo and the residue was chromatographed on silica gel. The first band was eluted with ether/pet. ether to give dark brown crystals of $\underline{29}$ (0.046 g., 0.08 mmol). ¹H NMR (C_6D_6), δ 1.29(d,3H), 1.33(d,3H), 4.99(s,5H), 5.17(s,5H) and 5.25 (septet; 1H, J = 6.2 Hz). ¹³C NMR (C_6D_6), δ 93.7(C_5H_5), 92.0(C_5H_5), 67.9(CH) and 22.1(CH_3). IR (cyclohexane), ν_{CO} at 2060(s), 2040(m),

2005(s), 1990(sh), 1925(m) and 1665(ester) cm^{-1} . Major mass spectral peaks occurred at m/z (%): 569, $\text{C}_{19}\text{H}_{14}\text{O}_7\text{CoMoNi}^+$ (1); 500, $\text{C}_{17}\text{H}_{17}\text{O}_4\text{CoMoNi}^+$ (3); 472, $\text{C}_{16}\text{H}_{17}\text{O}_3\text{CoMoNi}^+$ (3); 444, $\text{C}_{15}\text{H}_{17}\text{O}_2\text{CoMoNi}^+$ (3); 386, $\text{C}_{12}\text{H}_{11}\text{OCMoNi}^+$ (5); 358, $\text{C}_{11}\text{H}_{11}\text{CoMoNi}^+$ (5); 293, $\text{C}_6\text{H}_6\text{CoMoNi}^+$ (5); 228, CHCoMoNi^+ (5); 219, $\text{C}_7\text{H}_5\text{O}_2\text{Mo}^+$ (5); 189, $\text{C}_{10}\text{H}_{10}\text{Co}^+$ (50); 180, $\text{C}_7\text{H}_5\text{O}_2\text{Co}^+$ (30); 163, $\text{C}_5\text{H}_5\text{Mo}^+$ (5); 152, $\text{C}_6\text{H}_5\text{OCO}^+$ (30); 124, $\text{C}_5\text{H}_5\text{Co}^+$ (100); 123, $\text{C}_5\text{H}_5\text{Ni}^+$ (15).

The second band gave black crystals of 33 (0.15 g., 0.22 mmol). ^1H NMR (C_6D_6), δ 1.42(d, 6H), 4.80(s, 10H), 5.04(s, 5H) and 5.57(septet, 1H, $J = 6.3$ Hz). ^{13}C NMR (C_6D_6), δ 89.9(CoC_5H_5), 92.3(MoC_5H_5) and 22.5(CH_3). IR (cyclohexane), ν_{CO} at 2180(s), 2160(sh), 2080(s), 1955(w), 1910(m), 1840(w), 1795(w) and 1660(ester) cm^{-1} . This compound was also characterized by an X-ray crystallographic structure determination.

The final band gave a trace amount of 32 which was characterized mass spectrometrically. Major mass spectral peaks occurred at m/z (%): 564, $\text{C}_{22}\text{H}_{22}\text{O}_4\text{MoNi}_2^+$ or $\text{C}_{20}\text{H}_{22}\text{O}_2\text{FeMoNi}_2^+$ (4); 508, $\text{C}_{20}\text{H}_{22}\text{O}_2\text{MoNi}_2^+$ (1); 450, $\text{C}_{17}\text{H}_{16}\text{OMoNi}_2^+$ (1); 422, $\text{C}_{16}\text{H}_{16}\text{MoNi}_2^+$ (14); 357, $\text{C}_{11}\text{H}_{11}\text{MoNi}_2^+$ (2); 292, $\text{C}_6\text{H}_6\text{MoNi}_2^+$ (1); 226, CMoNi_2^+ (1); 186, $\text{C}_{10}\text{H}_{10}\text{Fe}^+$ (100); 121, $\text{C}_5\text{H}_5\text{Fe}^+$ (38).

Preparation of $\text{CpMo}(\text{CO})_2\text{Cp}_2\text{Co}(\text{CO})\text{CCO}_2\text{CHMe}_2$, 31

To a solution containing 28 (0.24 g, 0.41 mmol) in THF (40 cm^3) was added 2 cm^3 of C_5H_6 . The reaction mixture was heated under reflux overnight. The progress of the reaction was monitored by t.l.c. (eluent, benzene-pet. ether 90:10; yellow-orange spot, C_5H_6 , $R_f = 0.85$, dark green spot, 28, $R_f = 0.56$ and yellow-brown spot, 31, $R_f = 0.37$). The solution was cooled to room temp., the solvent removed in vacuo and the residue chromatographed on silica gel. Elution with pet. ether/benzene 10:90

allowed for separation of the three bands. Recrystallization of the yellow-brown band from the eluent mixture gave brown crystals of 31 (0.055 g., 0.092 mmol, 22%). ^1H NMR (C_6D_6), δ 1.44(d,6H), 4.79(s,10H), 5.04(s,5H) and 5.36(septet,1H, $J = 6.3$ Hz). ^{13}C NMR (C_6D_6), δ 92.9 (MoC_5H_5), δ 90.5(CoC_5H_5), δ 68.4(CH) and δ 23.2(CH_3). IR (cyclohexane), ν_{CO} at 1990(w), 1910(s), 1845(m), 1795(w), 1655(ester) cm^{-1} . Major mass spectral peaks occurred at 594, $\text{C}_{23}\text{H}_{22}\text{O}_5\text{Co}_2\text{Mo}^+$ (1); 566, $\text{C}_{22}\text{H}_{22}\text{O}_4\text{Co}_2\text{Mo}^+$ (2); 538, $\text{C}_{21}\text{H}_{22}\text{O}_3\text{Co}_2\text{Mo}^+$ (2); 452, $\text{C}_{17}\text{H}_{16}\text{OCo}_2\text{Mo}^+$ (5); 424, $\text{C}_{16}\text{H}_{16}\text{Co}_2\text{Mo}^+$ (9); 359, $\text{C}_{11}\text{H}_{11}\text{Co}_2\text{Mo}^+$ (5), 294, $\text{C}_6\text{H}_6\text{Co}_2\text{Mo}^+$ (3); 228, CCo_2Mo^+ (3); 219, $\text{C}_7\text{H}_5\text{O}_2\text{Mo}^+$ (2); 191, $\text{C}_6\text{H}_5\text{OMo}^+$ (2); 189, $\text{C}_{10}\text{H}_{10}\text{Co}^+$ (100); 180, $\text{C}_7\text{H}_5\text{O}_2\text{Co}^+$ (2); 163, $\text{C}_5\text{H}_5\text{Mo}^+$ (1); 152, $\text{C}_6\text{H}_5\text{OC}^+$ (2); 124, $\text{C}_5\text{H}_5\text{Co}^+$ (50).

Preparation of $\text{CpMo}(\text{CO})_2\text{CpNiCo}(\text{CO})_3\text{CCO}_2\text{CHMe}_2$, 29

To a solution containing 28 (0.61 g, 1.00 mmol) in benzene (40 cm^3) was added $[\text{CpNi}(\text{CO})]_2$ (0.31 g, 1.00 mmol). The reaction mixture was heated at 60°C for 5 days. The progress of the reaction was monitored by t.l.c. (eluent, benzene/pet. ether, 90:10); red spot, $[\text{CpNi}(\text{CO})]_2$, $R_f = 0.91$, green spot, 28, $R_f = 0.56$, and brown spot, 29, $R_f = 0.37$. The solution was allowed to cool to room temperature, the solvent removed in vacuo and the residue chromatographed on silica gel. Elution with benzene/pet. ether, 90:10 allowed separation of the 3 bands. Recrystallization of the brown band gave dark brown crystals of 29 (0.095 g, 0.16 mmol, 16%). Spectroscopic data for the compound matched those obtained when the product was isolated from the reaction of 28 and Cp_2Ni .

Reaction of 24 with $\text{Fe}_2(\text{CO})_9$

When 24 was treated with $\text{Fe}_2(\text{CO})_9$ the product 34 was obtained.

^1H NMR (C_6D_6), δ 1.45(d,6H), 5.09(septet,1H, $J = 6.3$ Hz), 5.63(s,5H).

^{13}C NMR (C_6D_6), δ 91.7(C_5H_5), 70.7(CH) and 22.3(CH_3). IR (cyclohexane),

ν_{CO} at 2040(m), 1995(w), 1985(s), 1965(s) and 1680(ester). Major mass

spectral peaks occurred at m/z : 592, $\text{C}_{17}\text{H}_{12}\text{O}_9\text{Co}_2\text{FeNi}^+$; 536, $\text{C}_{15}\text{H}_{12}\text{O}_7\text{Co}_2\text{FeNi}^+$;

480, $\text{C}_{13}\text{H}_{12}\text{O}_5\text{Co}_2\text{FeNi}^+$; 452, $\text{C}_{12}\text{H}_{12}\text{O}_4\text{Co}_2\text{FeNi}^+$; 424, $\text{C}_{11}\text{H}_{12}\text{O}_3\text{Co}_2\text{FeNi}^+$;

331; $\text{C}_5\text{H}_7\text{O}_2\text{FeCo}_2\text{Ni}^+$; 273, $\text{C}_2\text{HOC}_2\text{FeNi}^+$; 254, $\text{C}_6\text{H}_6\text{Co}_2\text{Ni}^+$; 188, CCO_2Ni^+ ;

140, $\text{C}_3\text{O}_3\text{Fe}^+$; 123, $\text{C}_5\text{H}_5\text{Ni}^+$; 66, C_5H_6^+ ; 59, Co^+ ; 58, Ni^+ ; 56, Fe^+ .

Reaction of 28, with $\text{Fe}_2(\text{CO})_9$

Similarly, 28 and $\text{Fe}_2(\text{CO})_9$ gave 35. ^1H NMR (C_6D_6), δ 1.34(d,6H),

5.09(septet,1H, $J = 6.3$ Hz) and 5.21(s,5H). ^{13}C NMR (C_6D_6), δ 91.4(C_5H_5),

δ 67.9(CH) and 21.4(CH_3). IR (cyclohexane), ν_{CO} at 2015(s), 1985(s),

1975(s), 1920(m), 1890(w) and 1655(ester) cm^{-1} . Major mass spectral

peaks occurred at m/z : 744, $\text{C}_{21}\text{H}_{12}\text{O}_{13}\text{Co}_2\text{FeMo}^+$; 688, $\text{C}_{19}\text{H}_{12}\text{O}_{11}\text{Co}_2\text{FeMo}^+$;

576, $\text{C}_{15}\text{H}_{12}\text{O}_7\text{Co}_2\text{FeMo}^+$; 520, $\text{C}_{13}\text{H}_{12}\text{O}_5\text{Co}_2\text{FeMo}^+$; 511, $\text{C}_{10}\text{H}_7\text{O}_7\text{Co}_2\text{FeMo}^+$;

483, $\text{C}_9\text{H}_7\text{O}_6\text{Co}_2\text{FeMo}^+$; 455, $\text{C}_8\text{H}_7\text{O}_5\text{Co}_2\text{FeMo}^+$; 436, $\text{C}_{10}\text{H}_{12}\text{O}_2\text{Co}_2\text{FeMo}^+$;

371, $\text{C}_5\text{H}_7\text{O}_2\text{Co}_2\text{FeMo}^+$; 322, $\text{C}_7\text{H}_6\text{OCo}_2\text{Mo}^+$; 315, $\text{C}_5\text{H}_7\text{O}_2\text{Co}_2\text{Mo}^+$; 292, $\text{C}_6\text{H}_6\text{Co}_2\text{Mo}^+$;

257, $\text{C}_2\text{HOC}_2\text{Mo}^+$; 219, $\text{C}_7\text{H}_5\text{O}_2\text{Mo}^+$; 163, $\text{C}_5\text{H}_5\text{Mo}^+$; 98, Mo^+ ; 59, Co^+ ; 56, Fe^+ .

Collection of the X-ray data on 33

An acicular crystal, sealed in a Lindemann capillary, was used for X-ray studies. Precession photographs showed the crystal was monoclinic and unit cell parameters were obtained from a least squares fit of χ , ϕ , and 2θ for 15 reflections in the range $19.4^\circ < 2\theta < 29.7^\circ$.

All measurements were made on a Syntex P2₁ diffractometer with use of MoK α radiation (λ 0.71069Å). Crystal data and other numbers related to data collection are summarised in Table A7.

Intensities were measured with use of a coupled θ (crystal)- 2θ counter scan. The methods of selection of scan rates and initial data treatment have been described.^{217,218} Corrections were made by Lorentz and polarization effects and absorption.

Solution of the Structure

The phases were determined by direct methods; 50 reflections were used with $|E| > 1.6$ and 12 sets of starting phases. The metal atoms were easily located in the E map and subsequent refinement and electron density difference syntheses revealed all the non-hydrogen atoms. Further refinement with anisotropic temperature factors for all atoms minimized $\sum_w (|F_o| - |F_c|)^2$ and was terminated when the maximum shift/error fell below 0.2. No attempt was made to locate the hydrogen atoms. Corrections were made for secondary extinction by the method in SHELX.²¹⁹ Scattering curves were from Cromer and Waber²¹⁶ and anomalous dispersion corrections²¹⁶ were applied to the curves for Mo, Fe, and Co. The atom parameters are listed in Table A8.

Reaction of $\overset{24}{\text{C}}_5\text{Me}_5\text{Rh}(\text{CO})_2$ with $\text{C}_5\text{Me}_5\text{Rh}(\text{CO})_2$

To a solution containing $\overset{24}{\text{C}}_5\text{Me}_5\text{Rh}(\text{CO})_2$ (0.16 g, 0.31 μmoles) in cyclohexane (35 cm^3) was added $\text{C}_5\text{Me}_5\text{Rh}(\text{CO})_2$ (0.10 g, 0.34 μmoles). The reaction mixture was stirred at room temperature for two days. The progress of the reaction was monitored by t.l.c. (eluent, ether-pet. ether, 15:85; dark brown spot, $\overset{24}{\text{C}}_5\text{Me}_5\text{Rh}(\text{CO})_2$, $R_f = 0.65$, brown spot, $\overset{36}{\text{C}}_5\text{Me}_5\text{Rh}(\text{CO})_2$, $R_f = 0.39$ and

red spot, $C_5Me_5Rh(CO)_2$, $R_f = 0$). The solvent was removed in vacuo and the residue chromatographed on silica gel. Elution with same eluent composition as t.l.c. allowed for separation of the three bands. Recrystallization of the second band gave dark brown crystals of $\underline{36}$ (0.025 g, 0.03 mmoles, 11%). 1H NMR (C_6D_6), δ 1.29(d,6H), 155(s,15H), 5.02(s,5H) and 5.33(septet,1H, $J = 6.2$ Hz). ^{13}C NMR (C_6D_6), 10.7(C_{5Me_5}), 21.4(CH_3), 68.6(CH) and 90.9(C_5H_5). IR (cyclohexane, ν_{CO} at 2080(w), 2030(s), 1995(s), 1795(m), 1670(ester) cm^{-1}).

Reaction of $\underline{28}$ with $C_5Me_5Rh(CO)_2$

To a solution containing $\underline{28}$ (0.07 g, 0.12 mmoles) in cyclohexane (20 cm^3) was added $C_5Me_5Rh(CO)_2$ (0.03 g, 0.11 mmoles). The reaction mixture was stirred for 3 days at room temperature with no evidence of new product formation. Subsequent reflux of the solution for 15 hours led to the appearance of new products according to t.l.c. (eluent, ether-pet. ether, 15:85; green spot, $\underline{28}$, $R_f = 0.28$, black spot, $\underline{37}$, $R_f = 0.19$ and red spot, $C_5Me_5Rh(CO)_2$, $R_f = 0$). The solution was cooled to room temperature, the solvent removed in vacuo and the residue chromatographed on silica gel. Elution with ether-pet. ether 15:85 allowed for separation of the three bands. Recrystallization of the black band gave shiny black crystals of $\underline{37}$ (0.01 g, 0.014 mmol, 12%). 1H NMR (C_6D_6), δ 1.45(d,6H), 1.81(s,15H) and 5.15(s,5H). ^{13}C NMR (C_6D_6), δ 8.9(C_{5Me_5}), δ 22.7(CH_3), δ 67.4(CH), δ 89.8(C_5H_5) and δ 102.2(C_{5Me_5}). IR (cyclohexane) ν_{CO} at 1890(m) semi-bridging and 1660(ester) cm^{-1} .

Reaction of 28 with $C_5Me_5Rh(CO)_2$

To a solution containing 23 (0.22 g, 0.41 mmol) in benzene (25 cm³) was added $C_5Me_5Rh(CO)_2$ (0.12 g, 0.42 mmol). The reaction mixture was stirred for 1 week at room temperature. T.l.c. indicated formation of a product (eluent, ether-pet. ether, 15:85, purplish-black spot, 23, $R_f = 0.86$, black spot, 38, $R_f = 0.48$ and red spot, $C_5Me_5Rh(CO)_2$, $R_f = 0$). Removal of the solvent in vacuo left a crude mixture which was chromatographed on silica gel. Elution with isopropyl alcohol-hexane, 25:75 allowed for separation of the product 38 (0.045 g, 0.06 mmol, 15%). ¹H NMR (C_6D_6), δ 1.46(d,6H), 1.85(s,15H) and 5.41 (septet,1H, J = 6.1 Hz). IR (cyclohexane) ν_{CO} at 2110(w), 2060(s), 2040(s), 2020(s), 1980(m), 1790(m), 1660(ester) cm⁻¹. Major mass spectral peaks occurred at m/z (%): 766, $C_{24}H_{22}O_{11}Co_3Rh^+$ (1); 738, $C_{23}H_{22}O_{10}Co_3Rh^+$ (2); 710, $C_{22}H_{22}O_9Co_3Rh^+$ (3); 570, $C_{17}H_{22}O_4Co_3Rh^+$ (1); 542, $C_{16}H_{22}O_3Co_3Rh^+$ (1); 528, $C_{14}H_7O_{11}Co_3^+$ (12); 514, $C_{15}H_{22}O_2Co_3Rh^+$ (1); 500, $C_{13}H_7O_{10}Co_3^+$ (2); 472, $C_{12}H_7O_9Co_3^+$ (15); 444, $C_{11}H_7O_8Co_3^+$ (3); 294, $C_{12}H_{15}O_2Rh^+$ (4); 238, $C_{11}H_{15}ORh^+$ (2); 194, $C_{10}H_{15}Rh^+$ (20); 189, CCo_3^+ (20).

Reaction of 23 with $(C_9H_7)Rh(C_2H_4)_2$

To a solution containing 23 (0.20 g, 0.38 mmol) in hexane (50 cm³) was added $(C_9H_7)Rh(C_2H_4)_2$ (0.10 g, 0.36 mmol). The reaction mixture was stirred for 2 days at room temperature. T.l.c. indicated appearance of a product (eluent, pet.-ether, purplish-black spot, 23, $R_f = 0.85$, yellow spot, $C_9H_7Rh(C_2H_4)_2$, $R_f = 0.81$ and black spot, 40, $R_f = 0.27$). The solvent was removed in vacuo and the crude mixture

was chromatographed on silica gel. This allowed for isolation of 40 (0.032 g, 0.043 mmol, 11%). ^1H NMR (d_6 -acetone) δ 1.46(d,6H), 5.18(septet,1H, $J = 6.2$ Hz), 6.17(d,2H), 6.30(q,1H) and 7.29-7.43(m,4H). ^{13}C NMR (d_6 -acetone), δ 21.9(CH_3), 69.7(CH), 76.8($\text{C}^{1,3}$), 98.6(C^2) and 119.9, 125.7(C^{4-7}). IR (cyclohexane), ν_{CO} at 2105(m), 2075(s), 2045(s), 2025(s), 1980(w), 1690(ester) cm^{-1} .

Reaction of 28 with $\text{C}_9\text{H}_7\text{Rh}(\text{C}_2\text{H}_4)_2$

To a solution of 28 (0.22 g, 0.37 mmol) in hexane (25 cm^3) was added $\text{C}_9\text{H}_7\text{Rh}(\text{C}_2\text{H}_4)_2$ (0.10 g, 0.37 mmol). The reaction mixture was stirred for 1 week at room temperature. T.l.c. indicated formation of a product (eluent, ether-pet. ether, 15:85, yellow spot, $\text{C}_9\text{H}_7\text{Rh}(\text{C}_2\text{H}_4)_2$, $R_f = 0.82$, green spot, 28, $R_f = 0.34$ and green spot, 41, $R_f = 0.17$). Removal of the solvent in vacuo left a crude mixture which was chromatographed on silica gel. This allowed for isolation of 41 (0.038 g, 0.046 mmol, 12%). ^1H NMR (d_6 -acetone), δ 1.31(d,6H), 5.07(septet,1H, $J = 6.3$ Hz), 5.73(s,5H), 6.04(d,2H), 6.15(q,1H), 7.19-7.32(m,4H). ^{13}C NMR (d_6 -acetone), δ 22.0(CH_3), 669.2(CH), 676.7($\text{C}^{1,3}$), 693.1(C_5H_5), 698.6(C^2) and 119.9, 125.7(C^{4-7}). IR (cyclohexane), ν_{CO} at 2075(w), 2030(s), 2000(s), 1950(w) and 1725(ester) cm^{-1} .

Preparation of $\text{C}_5\text{Me}_5\text{MoCo}_2(\text{CO})_8\text{CCO}_2\text{CHMe}_2$, 42

To a solution of 23 (0.60 g, 1.14 mmol) in THF (35 cm^3) was added $[\text{C}_5\text{Me}_5\text{Mo}(\text{CO})_3]_2$ (0.34 g, 0.54 mmol). The reaction mixture was refluxed overnight. The progress of the reaction was monitored by t.l.c. (eluent, ether-pet. ether, 15:85; purple-black spot, 23,

$R_f = 0.86$, red spot, $[\text{C}_5\text{Me}_5\text{Mo}(\text{CO})_3]_2$, $R_f = 0.46$ and dark green spot, 42 , $R_f = 0.29$). The solution was allowed to cool to room temperature, the solvent removed in vacuo and the residue chromatographed on silica gel. Elution with ether-pet. ether, 30:70 allowed for isolation of the product 42 (0.19 g, 0.28 mmol, 25%). ^1H NMR (C_6D_6), δ 1.34(d, 6H), 1.81(s, 15H) and 5.22(septet, 1H, $J = 6.1$ Hz). ^{13}C NMR (C_6D_6), δ 9.8(C_5Me_5), 21.9(CH_3), 68.6(CH) and 105.7(C_5Me_5). IR (cyclohexane), ν_{CO} at 2070(s), 2030(s), 2000(s), 1930(m), 1875(m) and 1655(ester) cm^{-1} .

Reaction of 42 with $\text{C}_9\text{H}_7\text{Rh}(\text{C}_2\text{H}_4)_2$

To a solution of 42 (0.14 g, 0.21 mmol) in hexane (20 cm^3) was added $\text{C}_9\text{H}_7\text{Rh}(\text{C}_2\text{H}_4)_2$ (0.057 g, 0.21 mmol). The reaction mixture was stirred for 1 week at room temperature. T.l.c. indicated formation of a product (eluent, ether-pet. ether, 15:85; yellow spot, $\text{C}_9\text{H}_7\text{Rh}(\text{C}_2\text{H}_4)_2$, $R_f = 0.80$, green spot, 43 , $R_f = 0.46$ and green spot, 42 , $R_f = 0.32$). The solvent was removed in vacuo and the residue chromatographed on silica gel. This allowed for isolation of 43 (0.024g, 0.027 mmol, 13%). ^1H NMR (d_6 -acetone), δ 1.40(d, 6H), 2.09(s, 15H), 5.15(septet, 1H, $J = 6.1$ Hz), 6.13(d, 2H), 6.25(q, 1H) and 7.27-7.39(m, 4H). ^{13}C NMR (d_6 -acetone) δ 10.2(C_5Me_5), 22.1(CH_3), 69.2(CH), 76.8($\text{C}^{1,3}$), 98.6(C^2) and 119.9, 125.7 (C^{4-7}). IR(CH_2Cl_2), ν_{CO} at 2075(w), 2065(w), 2020(s), 1995(sh), 1985(s) and 1665(ester) cm^{-1} .

6.5 Experimental Procedures for Chapter 5

Preparation of $[\text{Co}_3(\text{CO})_9\text{Cl}]_2$

To a solution containing 23 (0.24 g, 0.46 mmol) in propionic anhydride (3.4 cm^3) was added 65% aqueous HPF_6 (0.1 ml, 1.13 mmol). The reaction mixture was stirred for 30 minutes at room temperature. Addition of 5 cm^3 of anhydrous Et_2O resulted in the precipitation of small shiny black crystals. An X-ray diffraction study on the product revealed it to be $[\text{Co}_3(\text{CO})_9\text{Cl}]_2$. Subsequently, an IR spectrum of the black crystals was in agreement with that reported for $[\text{Co}_3(\text{CO})_9\text{Cl}]_2$ in the literature.²⁰⁹

^{13}C Enrichment of $\text{Co}_3(\text{CO})_9\text{Cl}$

A 1.0 g sample of $\text{Co}_3(\text{CO})_9\text{Cl}$ was dissolved in 15 cm^3 CH_2Cl_2 . The solution was degassed, and 760 torr of ^{13}CO was placed over the solution, which was then stirred for 1 week at 25°C . The exchanged CO was removed, the solution exposed to fresh ^{13}CO , and the process repeated. After filtration to remove any decomposed cluster, the CH_2Cl_2 was removed under vacuum. This procedure resulted in $\sim 33\%$ enrichment of all carbonyls in $\text{Co}_3(\text{CO})_9\text{Cl}$, and treatment with AlCl_3 in CH_2Cl_2 resulted in the production of $\text{Co}_3(\text{CO})_9\text{CCO}^+$ that had been enriched at all carbon atoms with the exception of the apical one.

Preparation of $\text{CpMoCo}_2(\text{CO})_8\text{CCO}^+\text{PF}_6^-$

To a solution containing 28 (0.17 g, 0.28 mmol) in propionic anhydride (2.1 cm^3) was added 65% aqueous HPF_6 (32 μl , 0.36 mmol).

Upon addition of the acid, the color of the solution was transformed from green to dark brown. During stirring of the mixture, a dark brown precipitate began to form. After 30 minutes of stirring, 5 cm³ of anhydrous Et₂O was added to the reaction mixture to ensure complete precipitation of the solid. The mixture was then filtered under nitrogen pressure. The product CpMoCo₂(CO)₈CCO⁺PF₆⁻ (0.14 g, 0.20 mmol, 71%) was washed with anhydrous Et₂O and dried in vacuo at room temperature for 30 minutes. IR (CH₂Cl₂), ν_{CO} at 2090(m), 2080(m), 2035(s), 2010(s) and 1680(w) cm⁻¹.

Treatment of CpMoCo₂(CO)₈CCO⁺PF₆⁻ with Nucleophiles

a) MeOH - To a slurry of CpMoCo₂(CO)₈CCO⁺PF₆⁻ in 10 cm³ of dried CH₂Cl₂ was added 1 cm³ of MeOH. The reaction mixture was stirred for 30 minutes and then was poured into 10 cm³ of water. Extraction with 10 cm³ of Et₂O followed. The ether layer was washed with three 10 cm³ portions of 10% aqueous HCl, dried over Na₂SO₄ and evaporated under reduced pressure. The product obtained was CpMoCo₂(CO)₈CCO₂Me. ¹H NMR (C₆D₆), δ 3.67(s, 3H) and 4.71(s, 5H). IR (cyclohexane), ν_{CO} at 2090(m), 2080(sh), 2045(sh), 2040(s), 2005(s), 1950(w), 1905(w) and 1685(ester) cm⁻¹.

b) Et₂NH - The procedure followed was the same as that employed in (a) with the work up differing. The reaction mixture was poured into 10 cm³ water to remove any unreacted amine. The organic layer was separated, dried over Na₂SO₄ and evaporated under pressure. The product obtained was CpMoCo₂(CO)₈CCONEt₂. ¹H NMR (C₆D₆), δ 0.97(t, 6H), 3.26(q, 4H) and 4.71(s, 5H). IR (C₆H₆), ν_{CO} at

2080(s), 2030(sh), 2020(s), 1995(sh), 1940(w), 1890(w) and 1580(amide) cm^{-1} .

c) PhNMe₂ - The procedure followed was the same as that employed in (a) with the work up differing. The solvent was removed in vacuo and the residue was chromatographed on neutral alumina. Elution with ether-pet. ether, 30:70 allowed for isolation of the product, $(\text{CpMoCo}_2(\text{CO})_8\text{CCOPhNMe}_2)$. $^1\text{H NMR}$ (CD_2Cl_2), δ 3.05(s, 6H), 5.42(s, 5H) and 6.61-7.90(m, 4H, AA'BB'). IR (CH_2Cl_2), ν_{CO} at 2065(s), 2025(sh) 2010(s), 1950(w), 1895(w) and 1605(ketone) cm^{-1} .

d) PhSH - The procedure followed was the same as that employed in (a) but the reaction mixture was stirred for three days. The solvent was removed in vacuo and the residue was chromatographed on silica gel. Elution with ether-pet. ether, 50:50 allowed for isolation of the product, $\text{CpMoCo}_2(\text{CO})_8\text{CCOSPh}$. $^1\text{H NMR}$ (CD_2Cl_2), δ 5.11(s, 5H) and 7.20-7.59(m, 5H). IR (CH_2Cl_2), ν_{CO} at 2000(sh), 1995(s), 1990(sh), 1760(w) and 1575(thioester) cm^{-1} .

APPENDIX



TABLE A1: $C_{25}H_{22}FeNi_2O_5$, 16

Mol. wt.	575.7
Temp, °C	18
Space Group	Triclinic $\bar{P}1$
a (Å)	8.312(2)
b (Å)	9.648(3)
c (Å)	16.149(3)
α (deg)	104.97(2)
β (deg)	102.84(1)
γ (deg)	93.94(2)
V (Å ³)	1208.9
Z	2
ρ calcd (g/cm ³)	1.58
Crystal dimensions, (mm)	0.20 x 0.25 x 0.30
Radiation	Mo - K α
Linear absorption coefficient (cm ⁻¹)	21.8
Scan Type	ω -2 θ
Scan Range (deg.)	1.15 + 0.35 tan θ
θ limits (deg.)	2-25
Data collected	5231
Unique data used	3122 [I > 3 σ (I)]
$R = \Sigma(F_o - F_c) / \Sigma F_o $	0.041
$R_w = (\Sigma w(F_o - F_c)^2 / \Sigma w F_o^2)^{1/2}$	0.047

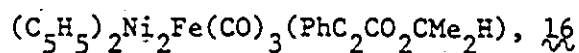
TABLE A2: $C_{23}H_{17}CoFeNiO_8$, 17

Mol. wt.	594.9
Temp, °C	18
Space Group	$P\bar{1}$
a (Å)	8.179(1)
b (Å)	11.910(2)
c (Å)	12.512(4)
α (deg)	94.02(2)
β (deg)	106.73(2)
γ (deg)	90.33(2)
V (Å ³)	1163.9
Z	2
ρ calcd (g/cm ³)	1.70
Crystal dimensions, (mm)	0.45 x 0.20 x 0.15
Radiation	Mo - K α
Linear absorption coefficient (cm ⁻¹)	21.7
Scan Type	ω -2 θ
Scan Range (deg.)	1.40 + 1.0 tan θ
θ limits (deg.)	1-30
Data collected	5455
Unique data used	3312[F > 3 σ (F)]
$R = \Sigma(F_o - F_c) / \Sigma F_o $	0.046
$R_w = (\Sigma w(F_o - F_c)^2 / \Sigma w F_o^2)^{1/2}$	0.059

TABLE A3: $C_{27}H_{22}FeMoNiO_7$, 18

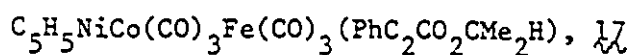
Mol. wt.	669.0
Temp, °C	18
Space Group	$P\bar{1}$
a (Å)	8.634(3)
b (Å)	9.879(2)
c (Å)	15.471(5)
α (deg)	90.71(2)
β (deg)	100.32(3)
γ (deg)	99.16(2)
V (Å ³)	1280.5
Z	2
ρ calcd (g/cm ³)	1.73
Crystal dimensions, (mm)	0.50 x 0.25 x 0.15
Radiations	Ag-K α
Linear absorption coefficient (cm ⁻¹)	14
Scan Type	ω -2 θ
Scan Range (deg.)	2.4 + 1.0 tan θ
θ limits (deg.)	1-21
Data collected	4603
Unique data used	2608[I > 3 σ (I)]
$R = \Sigma(F_o - F_c) / \Sigma F_o $	0.053
$R_w = (\Sigma w(F_o - F_c)^2 / \Sigma w F_o^2)^{1/2}$	0.055

TABLE A4: Positional Parameters for Non-Hydrogen Atoms of



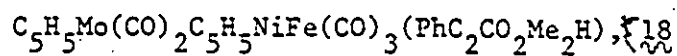
Atom	x/a	y/b	z/c
Ni1	0.17381(6)	0.33205(5)	0.25636(3)
Ni2	0.23613(6)	0.13777(5)	0.32507(3)
Fe	0.02418(7)	0.28205(6)	0.35830(4)
O1	- 0.0816(5)	0.1755(5)	0.4937(2)
O2	0.3027(5)	0.4842(6)	0.4823(3)
O3	- 0.2170(5)	0.4853(4)	0.3494(3)
O4	- 0.3118(4)	0.2022(4)	0.1676(2)
O5	- 0.1437(3)	0.1993(4)	0.0793(2)
C1	- 0.0435(6)	0.2143(6)	0.4393(3)
C2	0.1946(6)	0.4036(7)	0.4322(3)
C3	- 0.1243(6)	0.4061(5)	0.3524(3)
C4	- 0.0229(4)	0.2010(4)	0.2247(2)
C5	0.0075(5)	0.0909(4)	0.2622(2)
C6	- 0.1760(5)	0.2028(4)	0.1563(2)
C7	- 0.2826(6)	0.1967(7)	0.0049(3)
C8	- 0.3171(10)	0.0503(8)	- 0.0541(4)
C9	- 0.2341(9)	0.3055(7)	- 0.0368(4)
C10	- 0.0922(5)	- 0.0541(4)	0.2357(3)
C11	- 0.1454(6)	- 0.1296(5)	0.1476(3)
C12	- 0.2434(8)	- 0.2627(6)	0.1214(4)
C13	- 0.2908(7)	- 0.3206(5)	0.1822(5)
C14	- 0.2428(8)	- 0.2462(6)	0.2675(4)
C15	- 0.1382(8)	- 0.1152(5)	0.2963(4)
CP11	0.3761(6)	0.3877(5)	0.2094(3)
CP12	0.2264(7)	0.3902(6)	0.1497(3)
CP13	0.1445(7)	0.4934(5)	0.1918(4)
CP14	0.2371(8)	0.5552(6)	0.2745(5)
CP15	0.3780(6)	0.4924(6)	0.2866(4)
CP21	0.3693(6)	- 0.0412(5)	0.3069(3)
CP22	0.3250(6)	- 0.0189(5)	0.3865(3)
CP23	0.4021(7)	0.1177(7)	0.4399(3)
CP24	0.4897(6)	0.1786(6)	0.3918(4)
CP25	0.4699(6)	0.0813(5)	0.3106(3)

TABLE A5: Positional Parameters for Non-Hydrogen Atoms of



Atom	x/a	y/b	z/c
Ni	0.14418(9)	0.18392(6)	0.32095(6)
Co	0.09269(10)	0.27127(6)	0.14377(6)
Fe	0.30206(10)	0.11899(6)	0.19270(6)
C1	0.3361(7)	0.2879(4)	0.2204(4)
C2	0.3605(7)	0.2405(4)	0.3208(4)
C3	0.4600(8)	0.3642(4)	0.1924(4)
O1	0.5922(6)	0.3374(4)	0.1780(4)
O2	0.3995(5)	0.4683(3)	0.1845(4)
C4	0.5081(9)	0.5563(5)	0.1596(5)
C5	0.626(1)	0.6070(7)	0.2689(7)
C6	0.381(1)	0.6401(6)	0.0969(7)
C30	0.0229(8)	0.3960(5)	0.2050(6)
O30	- 0.0190(7)	0.4740(4)	0.2438(5)
C31	- 0.1024(9)	0.1869(5)	0.0932(5)
O31	- 0.2241(6)	0.1330(4)	0.0595(5)
C32	0.1040(9)	0.3181(6)	0.0121(6)
O32	0.1134(9)	0.3465(6)	- 0.0699(5)
C40	0.1444(8)	0.0085(5)	0.1585(5)
O40	0.0463(6)	- 0.0650(4)	0.1355(4)
C41	0.3514(8)	0.1170(5)	0.0623(5)
O41	0.3790(7)	0.1180(5)	- 0.0218(4)
C42	0.4695(8)	0.0286(5)	0.2557(5)
O42	0.5723(7)	- 0.0332(4)	0.2926(5)
C21	0.5042(7)	0.2620(4)	0.4246(4)
C22	0.5636(8)	0.1774(5)	0.4959(5)
C23	0.6974(9)	0.2006(6)	0.5938(6)
C24	0.7727(9)	0.3068(6)	0.6198(6)
C25	0.7116(9)	0.3914(6)	0.5500(6)
C26	0.5769(8)	0.3688(5)	0.4537(5)
CP1	- 0.039(1)	0.0752(7)	0.3560(7)
CP2	0.113(1)	0.0788(7)	0.4433(7)
CP3	0.147(1)	0.1857(7)	0.4908(7)
CP4	0.023(1)	0.2560(8)	0.4349(7)
CP5	- 0.099(1)	0.1859(7)	0.3481(7)

TABLE A6: Positional Parameters for Non-Hydrogen Atoms of



Atom	x/a	y/b	z/c
Mo	0.1267(1)	0.2237(1)	0.15065(8)
Ni	0.1225(2)	0.1424(1)	0.3106(1)
Fe	0.3461(2)	0.0832(2)	0.2421(1)
C1	0.363(1)	0.282(1)	0.2415(9)
C2	0.242(1)	0.312(1)	0.2822(9)
C3	0.502(1)	0.381(1)	0.224(1)
O1	0.639(1)	0.364(1)	0.2492(9)
O2	0.463(1)	0.4894(8)	0.1845(7)
C4	0.590(2)	0.595(2)	0.167(1)
C5	0.517(2)	0.674(2)	0.094(1)
C6	0.657(3)	0.684(2)	0.254(2)
C20	0.243(1)	0.123(1)	0.0803(9)
O20	0.292(1)	0.068(1)	0.0289(8)
C21	0.001(1)	0.044(1)	0.167(1)
O21	- 0.081(1)	- 0.062(1)	0.1563(7)
C30	0.456(2)	0.082(1)	0.3473(9)
O30	0.534(2)	0.085(1)	0.4161(9)
C31	0.263(2)	- 0.097(1)	0.227(1)
O31	0.213(1)	- 0.211(1)	0.2188(7)
C32	0.510(2)	0.072(1)	0.189(1)
O32	0.617(1)	0.064(1)	0.1582(8)
CP1	0.128(2)	0.395(1)	0.050(1)
CP2	0.016(2)	0.279(2)	0.009(1)
CP3	- 0.109(2)	0.257(2)	0.060(1)
CP4	- 0.081(2)	0.354(2)	0.125(1)
CP5	0.067(2)	0.440(1)	0.119(1)
C11	0.240(1)	0.438(1)	0.3352(9)
C12	0.094(2)	0.482(1)	0.3415(9)
C13	0.092(2)	0.595(2)	0.395(1)
C14	0.233(2)	0.664(2)	0.439(1)
C15	0.378(2)	0.624(2)	0.436(1)
C16	0.378(2)	0.510(1)	0.380(1)
CP6	0.034(2)	- 0.033(2)	0.377(1)
CP7	- 0.093(2)	0.036(2)	0.345(1)
CP8	- 0.055(2)	0.169(2)	0.389(1)
CP9	0.089(2)	0.182(2)	0.439(1)
CP10	0.150(2)	0.054(2)	0.432(1)

TABLE A7: Crystal Data For $\text{C}_{25}\text{H}_{22}\text{Co}_2\text{FeMoO}_7$

Compound	$\text{C}_{25}\text{H}_{22}\text{Co}_2\text{FeMoO}_7$
f.w. (Daltons)	704.0
crystal size (mm)	0.075 0.10 0.35
systematic absences	0k0, k = 2n+1, h0l, l = 2n+1
space group	P2 ₁ /c (No. 14)
unit cell (Å, deg)	a = 12.309(5) b = 14.731(6) c = 17.298(7) β = 124.63(6)
volume (Å ³)	2581(1)
Z	4
ρ_{calc} (g/cm ³)	1.812
temp °C	22
linear absorp. coeff. μ (cm ⁻¹)	23.9
Absorption limits	1.647 - 1.354
Standard reflection (e.s.d.%)	2 3 -1 (1.48) 1 4 -2 (1.44)
Max. 2θ reflections measured	45°, h, k, ±l
No. of independent reflections	3376
No. with I > 0 (used)	3133
Final R ₁ , R ₂ ^a	0.0522, 0.0571
Final shift/error, max. (ave)	0.181 (0.049)
x (secondary extinction)	0.00014
Final diff. map. max peak (valley) eÅ ⁻³	0.67, -0.47
Weighting scheme	$(\sigma_F^2 + 0.000921F_o^2)^{-1}$
Error in an observation of unit wt.	1.18

$$^a R_1 = \sum ||F_o| - |F_c|| / \sum |F_o|; R_2 = \{ \sum w(|F_o| - |F_c|)^2 / \sum w F_o^2 \}^{1/2}$$

TABLE A8: Atomic Positional Coordinates and Temperature Factors (\AA^2) For 33.

	x	y	z	Ueq*
Co(1)	2127(1)	706(1)	7546(1)	32.5(5)
Co(2)	1904(1)	3000(1)	6522(1)	37.4(6)
Mo	3307(1)	1515.1(4)	6864.3(4)	24.6(4)
Fe	2651(1)	2282(1)	8012(1)	28.4(6)
C(1)	4551(8)	967(6)	8105(6)	38(5)
O(1)	5411(6)	606(5)	8789(4)	58(5)
C(2)	4348(9)	2652(6)	7346(6)	43(5)
O(2)	5104(7)	3244(5)	7608(5)	63(5)
C(3)	3645(8)	1752(6)	9117(6)	38(5)
O(3)	4295(7)	1459(4)	9866(4)	57(4)
C(4)	1298(8)	2476(6)	8093(5)	47(6)
O(4)	456(6)	2578(5)	8180(4)	70(6)
C(5)	4551(8)	967(6)	8105(6)	39(5)
O(5)	5411(6)	606(5)	8789(4)	60(5)
C(6)	1514(7)	1757(5)	6702(5)	24(4)
C(7)	78(7)	1598(5)	5958(5)	27(4)
O(6)	- 348(5)	1271(4)	5202(4)	44(3)
O(7)	- 674(5)	1868(4)	6245(3)	38(3)
C(8)	-2116(8)	1689(7)	5599(7)	54(6)
C(9)	-2767(10)	2504(9)	4948(9)	86(7)
C(10)	-2565(12)	1589(13)	6247(11)	128(11)
C(11)	2600(13)	- 693(7)	7856(11)	64(6)
C(12)	2525(13)	- 295(8)	8550(7)	65(6)
C(13)	1238(14)	68(7)	8140(9)	61(6)
C(14)	514(9)	- 169(7)	7187(8)	54(6)
C(15)	1319(13)	- 599(6)	6996(7)	54(6)
C(21)	449(13)	3511(7)	5128(7)	64(7)
C(22)	1746(17)	3769(9)	5442(11)	81(10)
C(23)	2275(12)	4337(7)	6277(11)	72(8)
C(24)	1328(12)	4376(6)	6478(8)	56(7)
C(25)	227(10)	3876(7)	5770(9)	93(8)
C(31)	3597(11)	220(6)	6238(6)	46(6)
C(32)	2283(9)	494(6)	5586(6)	45(6)
C(33)	2324(11)	1354(7)	5250(6)	51(6)
C(34)	3655(14)	1615(7)	5681(8)	58(7)
C(35)	4473(10)	896(8)	6310(7)	57(7)

$$*U_{eq} = 1/3 (U_{11} + U_{22} + U_{33} + 2U_{13} \cos \beta)$$

REFERENCES

1. B. F. G. Johnson, Ed. "Transition Metal Clusters", Wiley-Interscience, New York, 1980.
2. W. L. Gladfelter and G. L. Geoffroy, Adv. Organomet. Chem. (1980), 18, 207.
3. J. Lewis and B. F. G. Johnson, Adv. Inorg. Chem. Radiochem. (1981), 24, 255.
4. F. G. A. Stone, Acc. Chem. Res. (1981), 14, 318.
5. E. L. Muetterties, Chem. Eng. News., August 30, 1982, 60, 28.
6. J. Lewis and M. L. H. Green (Eds.), "Metal Clusters in Chemistry", Phil. Trans. Roy. Soc. Lond. (1982), A308, 1-166.
7. D. A. Roberts and G. L. Geoffroy in "Comprehensive Organometallic Chemistry", Eds. G. Wilkinson, F. G. A. Stone and E. W. Abel, Pergamon Press, Oxford, 1982, Vol. 6, pp 763-877.
8. E. Sappa, A. Tiripicchio and P. Braunstein, Chem. Rev. (1983), 83, 203.
9. H. Vahrenkamp, Adv. Organomet. Chem. (1983), 22, 169.
10. F. G. A. Stone, "Inorganic Chemistry Towards the 21st Century", ACS Symp. Ser. (1983), 211, p 383-397.
11. F. G. A. Stone, Angew. Chem. Int. Ed. Engl. (1984), 23, 89.
12. F. A. Cotton and G. Wilkinson, "Advanced Inorganic Chemistry", Wiley-Interscience, New York, 1980, p 1080-81.
13. F. A. Cotton and M. Chisholm, Chem. Eng. News, June 28, 1982, 60, 40.

14. E. L. Muetterties, *Science*, (1977), 196, 839.
15. J. D. Corbett and P. A. Edwards, *J. Am. Chem. Soc.*, (1977), 99, 3313.
16. R. M. Friedman and J. D. Corbett, *Inorg. Chem.* (1973), 12, 1134.
17. C. R. Eady, P. F. Jackson, B. F. G. Johnson, J. Lewis, M. C. Malatesta, M. McPartlin and W. J. H. Nelson, *J. Chem. Soc. Dalton. Trans.* (1980), 383.
18. C. R. Eady, B. F. G. Johnson and J. Lewis, *J. Chem. Soc. Dalton Trans.* (1975), 2606.
19. J. Knight and M. J. Mays, *Chem. Ind. (London)*, (1968), 1159.
20. D. B. W. Yawney and F. G. A. Stone, *J. Chem. Soc. A* (1968), 502.
21. P. Chini, L. Colli and M. Peraldo, *Gazz. Chim. Ital.* (1960), 90, 1005.
22. A. T. T. Hsieh and J. Knight, *J. Organomet. Chem.* (1971), 26, 125.
23. P. C. Steinhardt, W. L. Gladfelter, A. D. Harley, J. R. Fox and G. L. Geoffroy, *Inorg. Chem.* (1980), 19, 332.
24. G. L. Geoffroy and W. L. Gladfelter, *J. Am. Chem. Soc.* (1977), 99, 7565.
25. L. J. Farrugia, J. A. K. Howard, P. Mitrprachachon, J. L. Spencer, F. G. A. Stone and P. Woodward, *J. Chem. Soc. Chem. Commun.* (1978), 260.
26. M. D. Curtis and R. J. Klingler, *J. Organomet. Chem.* (1978), 161, 23.
27. M. Green, R. M. Mills, G. N. Pain, F. G. A. Stone and P. Woodward, *J. Chem. Soc. Dalton Trans.* (1982), 1309.
28. G. Maier, S. Pfriem, U. Schäfer and R. Matusch, *Angew. Chem. Int. Ed. Engl.* (1978), 17, 520.
29. H. W. Sternberg, H. Greenfield, R. A. Friedel, J. Wotiz, R. Markby and I. Wender, *J. Am. Chem. Soc.* (1954), 76, 1457.

30. W. I. Bailey Jr., M. H. Chisholm, F. A. Cotton and L. A. Rankel, J. Am. Chem. Soc. (1978), 100, 5764.
31. D. S. Ginley, C. R. Brock and M. S. Wrighton, Inorg. Chim. Acta. (1977), 23, 85.
32. R. J. Gillespie, "Molecular Geometry", Van Nostrand Reinhold, London 1972.
33. G. E. Coates, M. L. H. Green and K. Wade, "Organometallic Compounds", 3rd Ed. Vol. 2 "Transition Metals", Methuen, 1968.
34. C. A. Tolman, Chem. Soc. Rev. (1972), 1, 337.
35. R. F. Heck, "Organotransition Metal Chemistry: A Mechanistic Approach", Academic Press, New York, 1974.
36. E. L. Muetterties, W. R. Pretzer, M. G. Thomas, B. F. Beier, D. L. Thorn, V. W. Day and A. B. Anderson, J. Am. Chem. Soc. (1978), 101, 2090.
37. G. N. Lewis, J. Am. Chem. Soc. (1916), 38, 762.
38. K. Wade, "Electron Deficient Compounds", Nelson, London 1971.
39. H. C. Longuet-Higgins, Quart. Rev. Chem. Soc. (1957), 11, 121.
40. R. B. King and D. H. Rouvray, J. Am. Chem. Soc. (1977), 99, 7834.
41. D. M. P. Mingos, J. Chem. Soc. Dalton Trans. (1974), 133.
42. K. Wade, Adv. Inorg. Chem. Radiochem. (1976), 18, 1.
43. R. E. Williams, Adv. Inorg. Chem. Radiochem. (1976), 18, 67.
44. R. W. Rudolph, Acc. Chem. Res. (1976), 9, 446.
45. D. M. P. Mingos, Adv. Organomet. Chem. (1977), 15, 1.
46. D. M. P. Mingos, Acc. Chem. Res. (1984), 17, 311.
47. R. F. W. Bader, T. T. Nguyen-Dang and Y. Tal, Reports on Progress in Physics (1981), 44, 893.

48. C. E. Housecroft and K. Wade, *Gazz. Chim. Ital.* (1980), 110, 87.
49. K. Wade in "Transition Metal Clusters", Ed. B. F. G. Johnson, Wiley-Interscience, New York 1980, pp 193-264.
50. P. Chini, *J. Organomet. Chem.* (1980), 200, 37.
51. J. L. Vidal, W. E. Walker, R. L. Pruett and R. C. Shoening, *Inorg. Chem.* (1979), 18, 129.
52. J. W. Lauher *J. Am. Chem. Soc.* (1978); 100, 5305.
53. M. Mannassero, M. Sansoni and G. Longoni, *J. Chem. Soc. Chem. Commun.* (1976), 919.
54. B. K. Teo, *Inorg. Chem.* (1984), 23, 1251.
55. D. E. Sherwood Jr. and M. B. Hall, *Organometallics* (1982), 1, 1519.
56. J. W. Lauher, *J. Organomet. Chem.* (1981), 213, 25.
57. P. F. Jackson, B. F. G. Johnson, J. Lewis, W. J. H. Nelson and M. McPartlin, *J. Chem. Soc. Dalton Trans.* (1982), 2099.
58. K. J. Haller, E. L. Anderson and T. P. Fehlner, *Inorg. Chem.* (1981), 20, 309.
59. C. E. Housecroft and T. P. Fehlner, *Inorg. Chem.* (1982), 21, 1739.
60. N. N. Greenwood, C. G. Savory, R. N. Grimes, L. G. Sneddon, A. Davison and S. S. Wreford, *J. Chem. Soc. Chem. Commun.* (1974), 718.
61. W. J. Evans, G. B. Dunks and M. F. Hawthorne, *J. Am. Chem. Soc.* (1973), 95, 4565.
62. V. R. Miller, L. G. Sneddon, D. C. Beer and R. N. Grimes, *J. Am. Chem. Soc.* (1974), 96, 3090.
63. C. E. Housecroft and T. P. Fehlner, *Adv. Organomet. Chem.* (1982), 21, 57.

64. M. Elian and R. Hoffmann, *Inorg. Chem.* (1975), 14, 1058.
65. M. Elian, M. M. L. Chen, D. M. P. Mingos and R. Hoffmann, *Inorg. Chem.* (1976), 15, 1148.
66. R. Hoffmann, *Science* (1981), 211, 995.
67. R. Hoffmann, *Angew. Chem. Int. Ed. Engl.* (1982), 21, 711.
68. T. A. Albright, *Tetrahedron* (1982), 38, 1339.
69. A. H. Cowley, *Polyhedron* (1984), 3, 389.
70. J. P. Collman and L. S. Hegecius, "Principles and Applications of Organotransition Metal Chemistry", University Science Books, Mill Valley, Ca. 1980.
71. V. W. Day, M. F. Fredrich, G. S. Reddy, A. J. Sivak, W. R. Pretzer and E. L. Muetterties, *J. Am. Chem. Soc.* (1977), 99, 8091.
72. E. L. Muetterties, T. N. Rhodin, E. Band, C. F. Brucker and W. R. Pretzer, *Chem. Rev.* (1979), 79, 91.
73. E. L. Muetterties and M. J. Krause, *Angew. Chem. Int. Ed. Engl.* (1983), 22, 135.
74. R. Whyman in "Transition Metal Clusters", B. F. G. Johnson (Ed.) Wiley-Interscience, New York 1980.
75. K. M. Nicholas and R. Pettit, *Tetrahedron Letters* (1971) 3475.
76. F. R. Hartley in "Comprehensive Organometallic Chemistry", Eds. G. Wilkinson, F. G. A. Stone and E. W. Abel, Volume 6 Pergamon Press, Oxford, 1982.
77. A. J. Carty, S. A. MacLaughlin and N. J. Taylor, *J. Organomet. Chem.* (1981), 204, C27.
78. W. J. Sly, *J. Amer. Chem. Soc.* (1959), 81, 18.

79. R. F. Gerlach, D. N. Duffy and M. D. Curtis, *Organometallics* (1983), 2, 1172.
80. J. R. Fox, W. L. Gladfelter, G. L. Geoffroy, I. Tavanaiepour, S. Abdel-Mequid and V. W. Day, *Inorg. Chem.* (1981), 20, 3230.
81. S. Aime, L. Milone, E. Sappa, E. Rosenberg, A. M. Manotti-Lanfredi and A. Tiripicchio, *J. Chem. Soc. Dalton Trans.* (1981), 2023.
82. A. J. Deeming, S. Hasso and M. Underhill, *J. Chem. Soc. Dalton Trans.* (1975), 1614.
83. A. J. Carty, *Pure Appl. Chem.* (1982), 54, 113.
84. K. P. C. Vollhardt, *Angew. Chem. Int. Ed. Engl.* (1984), 23, 539.
85. S. A. R. Knox, R. F. D. Stansfield, F. G. A. Stone, M. J. Winter and P. Woodward, *J. Chem. Soc. Dalton Trans.* (1982), 173.
86. W. Hübel in "Organic Synthesis via Metal Carbonyls", Vol. 1 Interscience, New York, 1968, pp. 273-342.
87. S. A. Gardner, P. S. Andrews and M. D. Rausch, *Inorg. Chem.* (1973), 12, 2396.
88. M. Tachikawa, J. R. Shapley and C. G. Pierpont, *J. Am. Chem. Soc.* (1975), 97, 7172.
89. L. Busetto, M. Green, J. A. K. Howard, B. Hessner, J. C. Jeffery, R. M. Mills, F. G. A. Stone and P. Woodward, *J. Chem. Soc. Chem. Commun.* (1981), 1101.
90. J. F. Tilney-Bassett and O. S. Mills, *J. Am. Chem. Soc.* (1959), 81, 4757.
91. S. R. Finnimore, S. A. R. Knox and G. E. Taylor, *J. Chem. Soc. Dalton Trans.* (1982), 1783.
92. T. Madach and H. Vahrenkamp, *Chem. Ber.* (1980), 113, 2675.

93. B. H. Freeland, J. E. Hux, N. C. Payne and K. G. Tyers, *Inorg. Chem.* (1980), 19, 693.
94. D. C. Miller and T. B. Brill, *Inorg. Chem.* (1978), 17, 240.
95. S. F. Xiang, A. A. Bakke, H. W. Chen, C. J. Eyerman, J. L. Haskins, T. H. Lee, D. Seyferth, H. P. Withers and W. L. Jolly, *Organometallics* (1982), 1, 699.
96. R. J. Doedens and L. F. Dahl, *J. Am. Chem. Soc.* (1966), 88, 4847.
97. M. J. McGlinchey, M. Mlekuz, P. Bougeard, B. G. Sayer, A. Marinetti, J.-Y. Saillard and G. Jaouen, *Can. J. Chem.* (1983), 61, 1319.
98. J. F. Tilney-Bassett, *J. Chem. Soc.* (1963), 4784.
99. M. I. Bruce, J. R. Rodgers, M. R. Snow and F. S. Wong, *J. Organomet. Chem.* (1982), 240, 299.
100. F. A. Cotton and G. Wilkinson in "Advanced Inorganic Chemistry", Wiley-Interscience, New York, 1980. pp. 1272-74.
101. E. Sappa, A. Tiripicchio and M. Tiripicchio-Camellini, *J. Organomet. Chem.* (1980), 199, 243.
102. N. E. Kobolova, L. L. Ivanov, O. S. Zvanko, A. S. Batsanov and Yu. T. Struchkov, *J. Organomet. Chem.* (1982), 231, 37.
103. P. Bougeard, S. Peng, M. Mlekuz and M. J. McGlinchey, *J. Organomet. Chem.*, submitted for publication.
104. J. F. Blount, L. F. Dahl, C. Hoogzand and W. Hübel, *J. Am. Chem. Soc.* (1966), 88, 292.
105. J. R. Fritch and K. P. C. Vollhardt, *Angew. Chem. Int. Ed. Engl.* (1980), 19, 559.
106. L. Busetto, J. C. Jeffery, R. M. Mills, F. G. A. Stone, M. J. Went and P. Woodward, *J. Chem. Soc. Dalton Trans.* (1983), 101.

107. B. H. Freeland, N. C. Payne, M. A. Stalteri and H. Van Leeuwen, *Acta. Cryst.* (1983), C39, 1533.
108. B. E. R. Schilling and R. Hoffmann, *J. Am. Chem. Soc.* (1979), 101, 3456.
109. J.-F. Halet, J.-Y. Saillard, R. Lissillour, M. J. McGlinchey and G. Jaouen, *Inorg. Chem.* (1985) } 24, 218.
110. E. Sappa, A. M. Manotti-Lanfredi and A. Tiripicchio, *J. Organomet. Chem.* (1981), 221, 93.
111. F. W. B. Einstein, B. H. Freeland, K. G. Tyers, D. Sutton and J. M. Waterous, *J. Chem. Soc. Chem. Commun.* (1982), 371.
112. C. G. Pierpont, *Inorg. Chem.* (1977), 16, 636.
113. P. Braunstein, J. Rose and O. Bars, *J. Organomet. Chem.* (1983), 252, C101.
114. E. Sappa, A. Tiripicchio and M. Tiripicchio-Camellini, *J. Organomet. Chem.* (1981), 213, 175.
115. Trinh-Toan, R. W. Broach, S. A. Gardner, M. D. Rausch and L. F. Dahl, *Inorg. Chem.* (1977), 16, 279.
116. L. Busetto, M. Green, B. Hessner, J. A. K. Howard, J. C. Jeffery and F. G. A. Stone, *J. Chem. Soc. Dalton Trans.* (1983), 519.
117. M. R. Churchill, C. Bueno and H. J. Wasserman, *Inorg. Chem.* (1982), 21, 640.
118. A. Bondi, *J. Phys. Chem.* (1964), 68, 441.
119. J. E. Huheey, "Inorganic Chemistry, Principles of Structure and Reactivity", 2nd Ed. Harper and Row, New York, 1978, pp. 579.
120. L. M. Jackman and F. A. Cotton, "Dynamic Nuclear Magnetic Resonance", Academic Press, New York, 1975.

121. G. Schroder, J. F. M. Oth and R. Merenyi, *Angew. Chem. Int. Ed. Engl.* (1965), 4, 752.
122. F. A. Cotton and G. Wilkinson, "Advanced Inorganic Chemistry", 4th Ed., Wiley-Interscience, New York, 1980, pp. 1219 - 1221.
123. F. A. Cotton, *J. Organomet. Chem.* (1975), 100, 29.
124. E. Band and E. L. Muetterties, *Chem. Rev.* (1978), 78, 639.
125. J. Evans, *Adv. Organomet. Chem.* (1977), 16, 319.
126. B. F. G. Johnson and R. E. Benfield in "Transition Metal Clusters", B. F. G. Johnson (Ed.), Wiley-Interscience, New York, 1980, pp. 471 - 543.
127. C. Brown, B. T. Heaton, P. Chini, A. Fungalli and G. Longoni, *J. Chem. Soc. Chem. Commun.* (1977), 309.
128. B. F. G. Johnson and R. E. Benfield, *J. Chem. Soc. Dalton Trans.* (1978), 1554.
129. H. Dorn, B. E. Hanson and E. Motell, *Inorg. Chim. Acta.* (1981), 54, L71.
130. O. A. Gansow, D. S. Gill, F. J. Bennis, J. R. Hutchinson, J. L. Vidal and R. C. Shoening, *J. Am. Chem. Soc.* (1980), 102, 2449.
131. C. P. Horwitz and D. F. Shriver, *Organometallics* (1984), 3, 756.
132. M. Rosenblum, B. North, D. Wells and W. P. Giering, *J. Am. Chem. Soc.* (1972), 94, 1239.
133. R. Case, E. R. H. Jones, N. V. Schwartz and M. C. Whiting, *Proc. Chem. Soc.* (1962), 256.
134. W. N. Lipscomb, *Science* (1966), 153, 373.
135. V. R. Miller and R. N. Grimes, *J. Am. Chem. Soc.* (1975), 97, 4213.

136. T. Yamamoto, A. R. Garber, G. M. Bodner, L. J. Todd, M. D. Rausch and S. A. Gardner, *J. Organomet. Chem.* (1973), 56, C23.
137. A. J. Deeming, R. E. Kimber and M. Underhill, *J. Chem. Soc. Dalton Trans.* (1973), 2589.
138. L. J. Todd, J. R. Wilkinson, M. D. Rausch, S. A. Gardner and R. S. Dickson, *J. Organomet. Chem.* (1975), 101, 133.
139. A. J. Deeming, I. P. Rothwell, M. B. Hursthouse and J. D. J. Backer-Dirks, *J. Chem. Soc. Dalton Trans.* (1981), 1879.
140. A. J. Deeming, *J. Organomet. Chem.* (1978), 150, 123.
141. J. Evans and G. J. McNulty, *J. Chem. Soc. Dalton Trans.* (1981), 2017.
142. R. D. Adams, D. A. Katahira and L-W. Yang, *Organometallics* (1982), 1, 235.
143. R. D. Barr, M. Green, J. A. K. Howard, T. B. Marder, A. G. Orpen and F. G. A. Stone, *J. Chem. Soc. Dalton Trans.* (1984), 2757.
144. D. A. Kleir and G. Binsch, Q.C.P.E. No. 165, Indiana University, 1969.
145. B. E. R. Schilling and R. Hoffmann, *Acta. Chem. Scand. Ser. B.* (1979), 33, 231.
146. W. D. Stohrer and R. Hoffmann, *J. Am. Chem. Soc.* (1972), 94, 1661.
147. M. Green, J. C. Jeffery, S. J. Porter, H. Razay and F. G. A. Stone, *J. Chem. Soc. Dalton Trans.* (1982), 2475.
148. M. J. Chetcuti, P. A. M. Chetcuti, J. C. Jeffery, R. M. Mills, P. Mitprachachon, S. J. Pickering, F. G. A. Stone and P. Woodward, *J. Chem. Soc. Dalton Trans.* (1982), 699.

149. M. Green, S. J. Porter and F. G. A. Stone, *J. Chem. Soc. Dalton Trans.* (1983), 513.
150. G. A. Carriedo, J. C. Jeffery and F. G. A. Stone, *J. Chem. Soc. Dalton Trans.* (1984), 1597.
151. M. J. Chetcuti, J. A. K. Howard, R. M. Mills, F. G. A. Stone and P. Woodward, *J. Chem. Soc. Dalton Trans.* (1982), 1757.
152. M. J. Chetcuti, K. Marsden, I. Moore, F. G. A. Stone and P. Woodward, *J. Chem. Soc. Dalton Trans.* (1982), 1749.
153. J. A. Connor in "Transition Metal Clusters", Ed. B. F. G. Johnson, Wiley-Interscience, New York 1980, pp. 345-391.
154. D. Seyferth, *Adv. Organomet. Chem.* (1976), 14, 97.
155. T. V. Voyevodskya, I. M. Pribytkova and Yu. A. Ustynyuk, *J. Organomet. Chem.* (1972), 37, 187.
156. B. L. Booth and G. C. Casey, *J. Organomet. Chem.* (1979), 178, 371.
157. A. J. Canty, B. F. G. Johnson, J. Lewis and J. R. Norton, *J. Chem. Soc. Chem. Commun.* (1972), 1331.
158. R. B. Calvert and J. R. Shapley, *J. Am. Chem. Soc.* (1977), 99, 5225.
159. J. B. Keister, *J. Chem. Soc. Chem. Commun.* (1979), 214.
160. J. W. Kolis, E. M. Holt and D. F. Shriver, *J. Am. Chem. Soc.* (1983), 105, 7307.
161. W. A. Herrmann, J. Plank, D. Riedel, M. L. Ziegler, K. Weidenhammer, E. Guggolz and B. Balbach, *J. Am. Chem. Soc.* (1981), 103, 63.
162. R. Markby, I. Wender, R. A. Friedel, F. A. Cotton and H. W. Sternberg, *J. Am. Chem. Soc.* (1958), 80, 6529.

163. W. T. Dent, L. A. Duncanson, R. G. Guy, H. W. B. Reed and B. L. Shaw, Proc. Chem. Soc. (1961), 169.
164. G. Palyi, F. Piacenti and L. Marko, Inorg. Chim. Acta. Rev. (1970), 4, 109.
165. B. R. Penfold and B. H. Robinson, Acc. Chem. Res. (1973), 6, 73.
166. H. Beurich and H. Vahrenkamp, Angew. Chem. Int. Ed. Engl. (1981), 20, 98.
167. S. Jensen, B. H. Robinson and J. Simpson, J. Chem. Soc. Chem. Commun. (1983), 1081.
168. R. A. Epstein, H. W. Withers and G. L. Geoffroy, Inorg. Chem. (1979), 18, 942.
169. P. A. Elder, B. H. Robinson and J. Simpson, J. Chem. Soc. Dalton Trans. (1975), 1771.
170. W. I. Bailey Jr., F. A. Cotton and J. D. Jamerson, J. Organomet. Chem. (1979), 173, 317.
171. E. O. Fischer and C. Palm, Chem. Ber. (1958), 91, 1725.
172. J. F. Tilney-Basset, Proc. Chem. Soc. (1960), 419.
173. K. Sutin, M. Mlekuz, P. Bougeard, J. W. Kolis, B. G. Sayer, M. A. Quilliam, R. Faggiani, C. J. L. Lock, M. J. McGlinchey and G. Jaouen, Organometallics, to be submitted.
174. P. Brun, G. M. Dawkins, M. Green, R. M. Mills, J.-Y. Salaün, F. G. A. Stone and P. Woodward, J. Chem. Soc. Dalton Trans. (1983), 1357.
175. E. Roland and H. Vahrenkamp, Organometallics (1983), 2, 1048.
176. J. S. Bradley, G. B. Ansell and E. W. Hill, J. Am. Chem. Soc. (1979), 101, 7417.

177. J. S. Bradley, G. B. Ansell, M. E. Leonowicz and E. W. Hill, J. Am. Chem. Soc. (1981), 103, 4968.
178. E. M. Holt, K. Whitmire and D. F. Shriver, J. Chem. Soc. Chem. Commun. (1980), 778.
179. K. H. Whitmire, D. F. Shriver and E. M. Holt, J. Chem. Soc. Chem. Commun. (1980), 780.
180. P. A. Dawson, B. F. G. Johnson, J. Lewis and P. R. Raithby, J. Chem. Soc. Chem. Commun. (1980), 781.
181. S. Aime and D. Osella, Inorg. Chim. Acta (1982), 52, 207.
182. P. L. Bogdan, E. M. Holt, K. H. Whitmire, J. W. Kolis and D. F. Shriver, J. Organomet. Chem. (1984), 272, 169.
183. E. M. Holt, K. H. Whitmire and D. F. Shriver, J. Am. Chem. Soc. (1982), 104, 5621.
184. A. J. Carty, N. J. Taylor, E. Sappa and A. Tiripicchio, Inorg. Chem. (1983), 22, 1871.
185. M. A. Beno, J. M. Williams, M. Tachikawa and E. L. Muetterties, J. Am. Chem. Soc. (1981), 103, 1485.
186. C. P. Horwitz, E. M. Holt and D. F. Shriver, J. Am. Chem. Soc. (1985), 107, 281.
187. H. Beurich and H. Vahrenkamp, Angew. Chem. Int. Ed. Engl. (1978), 17, 863.
188. J. W. Kang and P. M. Maitlis, J. Organomet. Chem. (1971), 26, 393.
189. P. Caddy, M. Green, E. O'Brien, L. E. Smart and P. Woodward, J. Chem. Soc. Dalton Trans. (1980), 962.

190. M. E. Rerek, L.-N. Ji and F. Basolo, J. Chem. Soc. Chem. Commun. (1983), 1208.
191. W. Keim, (Ed.) "Catalysis in C₁ Chemistry", D. Reidel Publishing Co., Boston, 1983.
192. W. Herrmann, Angew. Chem. Int. Ed. Engl. (1982), 21, 117.
193. M. Castiglioni, R. Giordano and E. Sappa, J. Organomet. Chem. (1984), 275, 119.
194. J. E. Hallgren, C. S. Eschbach and D. Seyferth, J. Am. Chem. Soc. (1972), 94, 2547.
195. D. Seyferth, J. E. Hallgren and C. S. Eschbach, J. Am. Chem. Soc. (1974), 96, 1730.
196. D. Seyferth and G. H. Williams, J. Organomet. Chem. (1972), 38, C11.
197. D. Seyferth, G. H. Williams and C. L. Nivert, Inorg. Chem. (1977), 16, 758.
198. J. B. Keister and T. L. Horling, Inorg. Chem. (1980), 19, 2304.
199. A. C. Sievert, D. S. Strickland, J. R. Shapley, G. R. Steinmetz and G. L. Geoffroy, Organometallics (1982), 1, 214.
200. J. S. Holmgren and J. R. Shapley, Organometallics (1984), 3, 1522.
201. J. R. Shapley, D. S. Strickland, G. M. St. George, M. R. Churchill and C. Bueno, Organometallics (1983), 2, 185.
202. J. W. Kolis, E. M. Holt, J. A. Hriljac and D. F. Shriver, Organometallics (1984), 3, 496.

203. A. J. Deeming and M. Underhill, *J. Chem. Soc. Dalton Trans.* (1974), 1415.
204. A. J. Deeming, S. Hasso, M. Underhill, A. J. Canry, B. F. G. Johnson, W. G. Jackson, J. Lewis and T. W. Matheson, *J. Chem. Soc. Chem. Commun.* (1974), 807.
205. R. T. Eddin, J. R. Norton and K. Mislow, *Organometallics* (1982), 1, 561.
206. D. Seyferth, G. H. Williams and D. D. Traficante, *J. Am. Chem. Soc.* (1974), 96, 604.
207. G. Allegra, E. M. Peronaci and R. Ercoli, *J. Chem. Soc. Chem. Commun.* (1966), 549.
208. R. Ercoli, *Chim. Ind. (Mil.)*, (1962), 44, 565.
209. T. W. Matheson and B. H. Robinson, *J. Chem. Soc. A* (1971), 1457.
210. K. Sutin, personal communication.
211. M. D. Brice and B. R. Penfold, *Inorg. Chem.* (1972), 11, 1381.
212. D. D. Perrin and D. R. Perrin, "Purification of Laboratory Chemicals", Pergamon Press, New York, 1980.
213. A. I. Vogel, "A Textbook of Practical Organic Chemistry", Longman, London, 1948.
214. R. B. King, M. Z. Iqbal and A. D. King, *J. Organomet. Chem.* (1979), 171, 53.
215. D. Seyferth, J. E. Hallgren and P. L. K. Hung, *J. Organomet. Chem.* (1973), 50, 265.
216. D. T. Cromer and J. T. Waber, in J. A. Ibers, W. C. Hamilton (Eds.) "International Tables for X-ray Crystallography", Kynoch

Press, Birmingham, England, 1974, Vol. IV.

217. R. P. Hughes, N. Krischnamachari, C. J. L. Lock, J. Powell and G. Turner, *Inorg. Chem.* (1977), 16, 314.
218. B. Lippert, C. J. L. Lock, B. Rosenberg and M. Zvagulis, *Inorg. Chem.* (1977), 16, 1525.
219. Initial data used programs from the XRAY 76 package. (J. M. Stewart (1976) - The XRAY 76 system. Tech. Report TR-446, Computer Science Centre, University of Maryland, Maryland) and the structure was solved with the use of SHELX (G. M. Sheldrick (1976) SHELX-Programme for Crystal Structure determination, Cambridge University, England). The least squares plane program NRC-22 (M. E. Pippy, F. R. Ahmed (1978) Mean Plane and Torsion Angles, National Research Council of Canada, Ottawa, Canada) and ORTEP-II (C. K. Johnson (1976) ORTEP-II Report ORNL-5138, Oak Ridge National Laboratory, Tennessee) were also used. All calculations were carried out on CYBER 170/730 and 815 computers.